

T-Pos75 MATHEMATICAL ANALYSIS OF NON-LINEAR RADIATION INACTIVATION DATA WITH APPLICATION TO VASOPRESSIN SENSITIVE KIDNEY ADENYLATE CYCLASE. A.S. Verkman, K.L. Skorecki, C.Y. Jung, and D.A. Ausiello, Renal Divisions, Brigham and Women's Hospital & Massachusetts General Hospital, Boston, MA 02115 and S.U.N.Y. Buffalo, NY 14215

Radiation inactivation has been used as a tool to explore the size and structural arrangement of soluble and membrane bound enzymes. Linear dependence of $\ln(\text{Activity})$, $\ln(A)$, on radiation dose, D , suggests a single functional enzyme with M.W. proportional to the slope of a $\ln(A)$ vs D plot. A concave upward $\ln(A)$ vs D plot suggests multiple independent functional units of distinct size and activity which do not interact with each other. Inactivation of a multimeric enzyme, composed of subunits of different M.W., gives complex $\ln(A)$ vs D curves which depend upon subunit total stoichiometry, equilibrium affinities and energy transfer. For an oligomeric enzyme composed of n identical subunits, $A \leftrightarrow nA$ ($K = [A]^n/[A]$), it is possible to systematically evaluate $\ln(A)$ vs D curve shape in terms of well-defined models. Concave downward $\ln(A)$ vs D curves are consistent with A inactivation with full $A \leftrightarrow nA$ equilibration prior to activity assay, whereas an activation hump at low D suggests incomplete equilibration or the presence of a high M.W. inhibitor. Detailed curve shape depends on n , K , A/A activity ratio, energy transfer and kinetics of equilibration. Radiation inactivation of cultured pig kidney LLC-PK₁ cells gives a concave downward $\ln(\text{adenylate cyclase activity})$ vs D relation; addition of $2 \mu\text{M}$ vasopressin results in a linear relation with M.W. ~ 180 kdaltons. Curve shape analysis suggests the presence of a native tetrameric enzyme complex which dissociates into active monomers following vasopressin addition.

T-Pos76 AN EFFECT OF TETRAHYDROISQUINOLINES AND TETRAHYDRO- β -CARBOLINES ON THE NICOTINIC ACETYLCHOLINE RECEPTOR OF TORPEDO CALIFORNICA AND THE PHEOCHROMOCYTOMA CELL LINE (PC12). D. R. Pratt, R. D. Davis, Daniel Lang, M. J. Hawkes, A. K. Ritchie and S. L. Hamilton. Department of Physiology and Biophysics, University of Texas Medical Branch, Galveston, Texas 77550.

Recent interest in β -carbolines and tetrahydroisquinolines has been stimulated by increasing amount of evidence for their existence in mammalian tissues. These compounds have been implicated in the etiology of chronic alcoholism and schizophrenia and have been shown in vitro to affect a number of neurotransmitter systems suggesting the possibility that they may function as neuromodulators. We demonstrate a pronounced inhibition of both α -neurotoxin and bromoacetylcholine binding to reduced nicotinic acetylcholine receptor-rich membranes of *Torpedo californica* by low concentrations of certain tetrahydroisquinolines and tetrahydro- β -carbolines. We are examining the effect of these compounds on both toxin on-rate and off-rate and on carbamylcholine induced ^{22}Na flux into receptor-rich membranes. Using single electrode voltage clamp techniques we have found that some of these compounds reversibly block carbamylcholine responses in PC12 cells. The compounds do not, however, block α -neurotoxin binding to PC12 membranes.

To determine the structural characteristics of these compounds which are important for their interactions with the receptor, a number of different analogs have been screened for ability to block α -neurotoxin binding and carbamylcholine induced ^{22}Na flux. One of the most potent tetrahydroisquinolines is salsolinol. Conversion of the 6- or 7-OH of salsolinol to a methoxy derivative results in substantial loss of activity. The possibility that some of these compounds may function as modulators of nicotinic acetylcholine receptors in mammalian tissues is discussed.

T-Pos77 EFFECTOR-INDUCED CHANGES IN THE SECONDARY STRUCTURE OF THE NICOTINIC ACETYLCHOLINE RECEPTOR. Mielke, D. L., Kaldany, R.-R., Karlin, A., and Wallace, B. A., Department of Biochemistry, Columbia University, New York, New York, 10032.

Acetylcholine receptor (AChR) was extracted from *Torpedo californica* electric tissue and purified by affinity chromatography in a cholate/asolectin solution. Membrane vesicles containing AChR were prepared by removal of the cholate by dialysis. Circular dichroism (CD) spectroscopy was used to determine the secondary structure of AChR both in the reconstituted vesicles and in the cholate solution. The spectra obtained for the protein in these two environments are very similar and indicate that AChR contains approximately 50% β -structure (sheet plus turn), 30% random coil, and 20% α -helix.

The CD spectrum of the AChR changes significantly following the addition of either an agonist, $20 \mu\text{M}$ carbamylcholine, or a competitive antagonist, $200 \mu\text{M}$ hexamethonium. These changes correspond to a reversible increase in the fraction of β -structure with agonist and a larger increase in β -structure with a significant decrease in α -helix with antagonist. The changes are similar for AChR in cholate solution and in reconstituted vesicles. Over the time period of the CD measurements (several hours), both carbamylcholine and hexamethonium put the AChR into either a desensitized or a blocked state; therefore, the above conformational changes represent equilibrium differences between the resting and the desensitized or blocked states of the AChR.

Supported by research grants from the NIH (NS07065, GM27292), MDA, NSF (PCM82-15109), and by a fellowship from the NY Heart Association to R.-R. K.

T-Pos78 LOCALIZATION AND SOLUBILIZATION OF NITRENDIPINE BINDING SITES IN SKELETAL MUSCLE.

Richard Kawamoto, Neil Brandt and Anthony Caswell, Dept. of Pharmacology, Univ. of Miami School of Medicine, Miami, Florida 33101.

Putative calcium channels in skeletal muscle were identified with an isothiocyanate derivative of nitrendipine (DHP-NCS, dihydro-2,6-dimethyl-4-(2-isothiocyanatophenyl)-3,5-pyridinecarboxylic acid dimethyl ester). Binding sites were identified either by injection of intact muscle prior to homogenization or by specific binding to isolated membrane vesicles. DHP-NCS, nitrendipine and ouabain (a marker for transverse tubules) were all associated with triads when crude microsomes were fractionated on continuous sucrose gradients and T-tubules when the triad junctions were mechanically disrupted. DHP-NCS and nitrendipine binding sites were absent from the longitudinal reticulum and terminal cisternae of the SR. Specific binding of DHP-NCS to isolated T-tubules ($K_{1/2, \max} = 10$ nM after 1 hr at 20°) was similar to nitrendipine specific binding ($K_d = 2$ nM, $B_{\max} = 65$ pmol/mg) and displaceable by nisoldipine. DHP-NCS bound to intact T-tubule membranes was released by SDS but the receptor-ligand complex was stable at neutral pH after membrane solubilization with Triton-X100 or Lubrol PX. The solubilized DHP-NCS-receptor complex chromatographed on Sephacryl S-300 with an apparent M_w of 130,000-150,000 in the presence or absence of 0.1 M NaCl. The enriched complex was stable at room temperature at neutral pH but the ligand was rapidly released at 37° or in alkaline medium indicating a non-covalent attachment of DHP-NCS to the receptor. (Supported by NIH grants HL28804, AM2160 and HL07188).

T-Pos79 LATERAL MOBILITY OF ENDOTOXIN IN MAMMALIAN CELLS. L. Kilpatrick-Smith, G. Maniara, J. Vanderkooi, and M. Erecinska (Intro. by D.F. Wilson) Depts. of Biochemistry & Biophysics and Pharmacology, University of Pennsylvania, Philadelphia, PA 19104.

Fluorescein isothiocyanate-labeled endotoxin was used as a fluorescent probe to measure endotoxin mobility in both primary cells (isolated rat hepatocytes) and transformed cells (neuroblastoma NB41A3) by the fluorescence recovery after photobleaching (FRAP) method. A mobile fraction of between 60-75% of the FITC-labeled endotoxin was found on rat hepatocytes at 25°C with a lateral diffusion coefficient (D) of 4.0×10^{-9} cm²/sec. (The immobilized fraction had a $D < 10^{-12}$ cm²/sec.) In neuroblastoma cells, under the same experimental conditions, a lateral diffusion coefficient of 1.0×10^{-8} cm²/sec was measured with a mobile fraction of between 85-90%. In both cell types, the mobile fraction and D were time independent over a 10-120 min. incubation period. As the incubation temperature was increased from 10° to 37°C, the lateral diffusion rate increased from 1.5×10^{-9} to 4.07×10^{-9} cm²/sec and 3.3×10^{-9} to 1.17×10^{-8} cm²/sec in hepatocytes and neuroblastoma cells, respectively. There was, however, no difference in the mobile fraction. Dead cells as compared with viable cells showed different recovery patterns: the diffusion coefficient was larger and 100% of the probe molecules were mobile. These results suggest: 1) endotoxin binding to mammalian cells consists of two different subpopulations with different mobilities; 2) binding of the immobile fraction may be energy dependent and possibly involve interaction with the cytoskeleton; and 3) the differences in mobility and size of the immobile fraction in transformed cells and primary cells may be due to variations in membrane composition, number of binding sites and/or degree of internalization. (Supported by NIH HL-18708.)

T-Pos80 KINETIC DETERMINATION OF NONCOOPERATIVE INTERACTIONS OF GLUCAGON WITH A HOMOGENEOUS RECEPTOR POPULATION IN ISOLATED RAT HEPATOCYTES. Edwin M. Horwitz, W. Terry Jenkins, Naseema M. Hoosein, and Ruth S. Gurd. (Medical Sciences Program and Department of Chemistry, Indiana University, Bloomington, Indiana 47405.

Hepatocytes, isolated from adult, male Wistar rats by perfusion with collagenase, were purified and enriched in viability by centrifugation (30,000g x 20 min) through a continuous Percoll® (50%, v/v) gradient. Purified mono[¹²⁵I]iodoglucagon, prepared by the chloroglycoluril method (England et al., (1982) *Biochemistry* 21, 940-950) was used throughout.

Assays of binding as a function of time define the kinetic rate constants, $k_1 = 2.23 \times 10^8 \text{ M}^{-1} \text{ min}^{-1}$, and $k_{-1} = 2.40 \times 10^{-2} \text{ min}^{-1}$, yielding a $K_D = 1.08 \times 10^{-10} \text{ M}$.

The Hill coefficient of the dose-response curve of competition binding assays was found to be 0.94, indicating lack of cooperativity in the glucagon receptor binding reaction. Association kinetic assays in the absence and presence of unlabeled glucagon demonstrate no dependence of k_1 on fractional receptor occupancy. Dissociation rate constants determined in the absence and presence of unlabelled glucagon were indistinguishable, and, therefore k_{-1} is also independent of occupancy. Also, k_{-1} is independent of the age of the HR complex prior to dissociation.

The Hill slope of the competition assays indicates a homogeneous receptor population. A linear relationship was found when $\ln[B_{eq}/(B_{eq} - B_t)]$, obtained from the association binding data, was graphed versus time. Dissociation curves were found to be monophasic in every case. These two observations denote receptor homogeneity and do not support a two-stage sequential binding reaction in which binding is followed by a rearrangement to produce an alternative HR complex. (Supported by USPHS Research Grant AM 21121.)

T-Pos81 EFFECT OF N-ETHYLMALIMIDE ON BINDING OF LOCAL ANESTHETICS TO RECONSTITUTED ACETYLCHOLINE RECEPTOR. J.P. Earnest, Department of Biology, University of California, Santa Cruz, Ca. 95064.

Interactions of a spin-labeled local anesthetic with reconstituted acetylcholine receptor membranes have been examined. The membrane vesicles were prepared from acetylcholine receptor isolated from *Torpedo californica*, reconstituted with dioleoylphosphatidylcholine (DOPC) at lipid-to-protein ratios ranging from 100:1 to 700:1. The local anesthetic spin label is an analog of intracaine, with a pK of 7.2 to 7.4. The interactions of the spin-labeled local anesthetic with membrane lipids have been studied previously (H.H. Wang, J.P. Earnest, and H.P. Limbacher, *Proc. Natl. Acad. Sci. USA*, 80:5297-5301, 1983), where it was shown that in its positively-charged form (below pH 7) the spin label is motionally-restricted by negatively-charged groups in the membrane. The electron-spin-resonance spectrum of the local anesthetic spin label in the reconstituted acetylcholine receptor membranes at pH 6 shows an even more strongly-immobilized component which is not present at pH 10. It is suggested that this component represents a population of local anesthetic spin labels which are restricted through electrostatic interactions with the acetylcholine receptor. The size of this restricted component is proportional to the protein:lipid ratio in the membrane. When the membranes are treated with a sulfhydryl-blocking agent such as n-ethyl maleimide, the protein-associated component is partially removed in a dose-dependent fashion. The role of acetylcholine receptor sulfhydryl groups on the binding of the spin-labeled local anesthetic is being studied.

T-Pos82 ADHESIVITY AND RIGIDITY OF RBC MEMBRANE IN RELATION TO WHEAT GERM AGGLUTININ BINDING. E. Evans, Pathology, Univ. of British Columbia, Vancouver, B.C. Canada V6T 1W5

Binding of wheat germ agglutinin (WGA) to red blood cell membranes causes membrane rigidification. Our objectives have been to measure the effects of WGA binding on membrane rigidity and to relate rigidification to the kinetics and levels of WGA binding. Another objective has been to measure the strength of adhesion and mechanics of cell separation for red cells bound together by WGA. Red cell membrane rigidity was measured on single cells by micropipet aspiration. Red cell-red cell adherence properties were studied by micropipet separation of two-cell aggregates. The binding and release of fluorescently labelled WGA to single red blood cells was measured with a laser microfluorometry system. Cells were equilibrated with WGA solutions in the range of concentrations of 0.01 $\mu\text{g/ml}$ to 10 $\mu\text{g/ml}$. The results showed that the stiffening of the cell membrane and binding of fluorescently labelled WGA to the membrane surface followed the same concentration and time dependencies. The threshold concentration for membrane stiffening was at about 0.1 $\mu\text{g/ml}$ where the time course to reach equilibrium was close to an hour. The maximal stiffening (almost 30 fold over the normal membrane elastic modulus) occurred in concentrations above 2 $\mu\text{g/ml}$ where the time to reach equilibrium took less than a minute. WGA binding also altered the normal elastic membrane behavior; the inelastic response indicated that mechanical extension of the membrane caused an increase in cross-linking within the surface plane. Similarly, membrane adhesivity of cells equilibrated with WGA solutions greatly increased with concentration above 0.1 $\mu\text{g/ml}$. The work of separation per unit change in contact area correlated well with a parameter that represented accumulation of WGA cross bridges as the cells were separated; values as large as 1 erg/cm^2 were measured for cells equilibrated with 0.4 $\mu\text{g/ml}$ WGA.

T-Pos83 MEMBRANE FLUIDITY CHANGES DURING MIXED LYMPHOCYTE REACTIONS (MLR). Sudha Agarwal* and Peter L. Gutierrez. Department of Pediatrics and University of Maryland Cancer Center, University of Maryland Medical School, Baltimore, Maryland

Mixed lymphocyte reactions are conventionally monitored by the stimulation of DNA synthesis in responder lymphocytes due to the presence of immunogenetically different cells. Because antigen recognition is a phenomenon closely related to cell membranes, we studied membrane fluidity changes by electron spin resonance spectroscopy (ESR) during MLR of congenic mice having minor H-2 region differences. B10.D₂/nSnN mouse splenic lymphocytes were labeled with 5-doxyl stearic acid. The labeled cells were reacted with unlabeled lymphocytes from B10.BR/SGsN, B10.D₂/nSnJ, B10.RIII/nSnN, B10.Sm/70Ns and autologous cells. The order parameter obtained for B10.D₂/nSnN reacted with or without autologous cells was 0.69 ± 0.01 . When the spin labeled B10.D₂/nSnN cells were reacted with the afore mentioned congenic lymphocytes, the order parameter increased to 0.74 ± 0.01 . Similarly, a mean S value change of at least 0.5 was observed when B10.BR/SGsN splenic lymphocytes were spin labeled and reacted with lymphocytes from B10.D₂/nSnN, B10.RIII/nSnN or B10.D₂/nSnJ splenic cells. The membrane fluidity changes could be detected as early as 3 minutes after the onset of the MLR, followed by a decrease and final disappearance of the ESR signal. This drastic decrease was not observed in control experiments, and was abrogated by the addition of 10^{-4}M glutathione. One possible explanation for the decrease in ESR signal is the chemical reduction of the nitroxyl free radical by biochemical reactions triggered by MLR. The changes in order parameter observed here, suggest that plasma membranes undergo dynamic fluidity changes during the process of antigenic recognition. It is possible that spin labeling can provide a rapid and effective tool for the analysis of histocompatibility matching.

T-Pos84 PHORBOL ESTERS STIMULATE AMILORIDE-SENSITIVE NA INFLUX INTO CULTURED RAT GLIOMA CELLS.

Dale J. Benos and Victor S. Saperstein, Departments of Physiology and Biophysics and Biological Chemistry, Harvard Medical School, Boston, Massachusetts, 02115.

Phorbol ester tumor promoters can induce certain cells to proliferate. The biochemical mechanism of action of these compounds is unknown, although it appears that phosphorylation of cellular proteins is somehow involved. Recently, it has been shown that phorbol esters increase the amount of a Ca^{2+} -activated, phospholipid-dependent protein kinase activity in the plasma membrane of parietal yolk sac cells (Kraft and Anderson, *Nature* 301:621;1983). In an effort to understand the relationship between the stimulation of quiescent rat C6 glioma cells in culture to proliferate and the initial appearance of an amiloride-sensitive component to Na-influx, we studied the effects of phorbol esters, Ca^{2+} , diacylglycerol and cyclic AMP on the activation of this Na transport system. We also examined the role that cytoskeletal elements play in the expression of this system. We found that epidermal growth factor (1 μM), dibutyryl cAMP (1 mM), bradykinin (1 μM), phorbol ester (1 μM) and diacylglycerol (10 μM) all induce a comparable increase in amiloride-sensitive Na-entry into serum-deprived glial cells. Long term exposure (24h) to dibutyryl cAMP (1 mM), on the other hand, did not. Colchicine (0.1 mM, 3h incubation), prevented the appearance of this transport system when quiescent cells were exposed to serum, but not when phorbol ester was used as inducer. Dihydrocytochalasin B had no effect. Our results indicate that phorbol esters may act to cause cellular proliferation by activating an amiloride-sensitive Na transport system. However, the mechanism of activation of this ion transport system by phorbol esters is different from that of serum or growth factors, in that phorbol ester activation apparently bypasses the stage of microtubular involvement. Supported by NIH Grants AM 25886, HD 05515, and NS 16186.

T-Pos85 FTIR EVIDENCE FOR CHARGE SEPARATION AT THE BACTERIORHODOPSIN SCHIFF BASE

Kenneth J. Rothschild and Johan Lugtenburg⁺ Department of Physics and Physiology, Boston University Boston, MA 02215 and ⁺Chemistry Department, Gorlaeus Laboratories, Leiden, The Netherlands

The mechanism by which bacteriorhodopsin (BR), a protein in the purple membrane of *Halobacteria halobium*, acts as a light driven proton pump is being investigated by using FTIR difference spectroscopy. In this study, we have focussed on the primary photoreaction, BR570 to K. While the K photoproduct has been studied previously with FTIR and resonance Raman spectroscopy, the vibrational frequency of the C=N Schiff base bond stretching mode has not been clearly assigned. We previously suggested that the K $\nu_{\text{C=N}}$ may be as low as 1609 cm^{-1} relative to a BR $\nu_{\text{C=N}}$ of 1640 cm^{-1} . Such a large perturbation could originate from a charge separation of the protonated Schiff base from a counterion. This assignment is now further supported by additional measurements of bacteriorhodopsin regenerated with isotopically substituted retinals. A comparison of BR regenerated with $^{13}\text{C}(10)$ -retinal in H_2O and D_2O indicates that a peak shift occurs from 1610 cm^{-1} to 1580 cm^{-1} . A similar shift of the 1610 cm^{-1} peak is observed for other isotopic substitutions at the C=N bond. This evidence supports our original assignment of the 1609 cm^{-1} peak in the spectrum of the K intermediate as due to the C=N stretch mode. (This work was supported by NSF grant PCM 2-08559 and an American Heart Association Established Investigatorship to KJR).

T-Pos86 N-15 NMR STUDIES ON OCTYLGLUCOSIDE - SOLUBILIZED BACTERIORHODOPSIN BIOSYNTHETICALLY ENRICHED WITH [ϵ - ^{15}N]-LYSINE. D. D. Muccio. Department of Chemistry, University of Alabama in Birmingham, Birmingham, Alabama 35294.

The characterization of hydrogen bonded and ion paired charged residues in bacteriorhodopsin is essential in order to understand the proton pumping ability of this membrane protein. In this endeavor, *Halobacterium halobium* S9 was grown on a synthetic medium containing [ϵ - ^{15}N]-DL-lysine (99% enrichment). Gas chromatography and mass spectroscopy on the acid hydrolysis of bacteriorhodopsin isolated from these growths indicated that the lysine residues (seven total) in the protein were N-15 enriched. The N-15 NMR spectrum (30.4 MHz) of N-15 labeled bacteriorhodopsin solubilized in octylglucoside yielded four resonances in the amino region of the spectrum which can be attributed to the amino groups from six lysine residues in the protein. Three of the signals were overlapping and centered at a frequency characteristic of fully protonated amino groups. Based on the deconvoluted natural linewidths of 1 to 2 Hz, the N-15 resonances were typical of amino groups with rapid motion. In contrast to these signals, the fourth resonance was shifted upfield from the center of the fully protonated signals by about 1.5 ppm and displayed a significantly larger linewidth of about 10 Hz. It is suggested that this signal be assigned to an amino group(s) which is immobilized by hydrogen bonding interactions with another polar residue in the protein. No N-15 resonance was observed for the seventh lysine amino residue which is bound to retinal as a Schiff base, even though resonance Raman spectra of the labeled membranes displayed a Schiff base signal characteristic of isotopic labeling.

T-Pos87 VIBRATIONAL ANALYSIS OF THE RETINAL CHROMOPHORE IN BACTERIORHODOPSIN: BR₅₆₈ AND BR₅₄₈.

S.O. Smith, A.B. Myers, M. Braiman, J.A. Pardo, C. Winkel, P.P.J. Mulder, J. Lugtenburg and R. Mathies. Department of Chemistry, University of California, Berkeley, CA 94720.

We have obtained resonance Raman spectra of light-adapted bacteriorhodopsin (BR₅₆₈) and the 13-*cis* component of dark-adapted bacteriorhodopsin (BR₅₄₈) using purple membrane regenerated with ^{13}C - and deuterium-labeled retinals. ^{13}C substitutions were at carbons 9, 10, 11, 12, 13, 14, 15, 19 and 20, while deuterium substitutions were at positions 5, 7, 8, 10, 11, 12, 14, 15, N, 18, 19 and 20. Based on the observed isotopic shifts, empirical assignments have been made for the vibrations between 700 and 1700 cm^{-1} . Except for vibrations localized in the Schiff base region, the pattern of fingerprint vibrations (1100-1400 cm^{-1}) observed in BR₅₆₈ and BR₅₄₈ is very similar to that previously identified in all-*trans* and 13-*cis* retinal (Curry *et al.*, J.A.C.S. 104, 5274 [1982]; J. Phys. Chem., in press). Normal modes predominantly made up of the C₆-C₇ and C₁₀-C₁₁ stretches are found between 1160 and 1180 cm^{-1} . The C₈-C₉ and C₁₂-C₁₃ stretches are higher in frequency (1200-1240 cm^{-1}) because of coupling with the stretches of the adjacent methyl groups. This ordering is kinetic in origin and is thus the same in the retinals and in the pigments. The C₁₄-C₁₅ stretch is sensitive to protonated Schiff base formation, shifting from 1111 cm^{-1} in all-*trans* retinal to 1201 cm^{-1} in BR₅₆₈, and from 1114 cm^{-1} in 13-*cis* retinal to 1167 cm^{-1} in BR₅₄₈. In addition to causing the higher C₁₄-C₁₅ stretch frequency, increased delocalization of the conjugated π -system in the pigments results in increased interaction of both the C-C and C=C stretches which leads to more "delocalized" skeletal normal modes. Modified Urey-Bradley force fields have been refined to reproduce the observed frequencies and isotopic shifts in BR₅₆₈ and BR₅₄₈. Features of the spectra which are diagnostic of C₁₃=C₁₄ and C=N configuration will be discussed.

T-Pos88 LOCATION OF RETINAL IN PURPLE MEMBRANE. Glen King (Intr. by Russell Jacobs) Dept. of Physiology and Biophysics, Univ. of Calif., Irvine, CA. 92717

Neutron diffraction studies have been performed on purple membrane samples regenerated with perdeuterated, partially deuterated and protonated retinals, respectively. The purpose of these studies was the localization of the retinal molecule in the plane of the membrane, relative to the protein. The experiments and results with the perdeuterated and protonated retinals have been previously described in King, Mowery, Stoeckenius, Crespi and Schoenborn (1980) PNAS 77, 4726. Here we describe the additional information which has been obtained from experiments done with retinal (synthesized by H. Akita and K. Nakanishi) which is deuterated only in the hydrocarbon chain part of the molecule. The difference map between perdeuterated retinal and protonated retinal should reveal the position(s) of the retinylidene moieties projected onto the membrane plane. The major peak labeled 1 in King, et al (ibid.) represents the ionone ring portion of the retinal but it is not clear where the hydrocarbon chain of the retinal is in this map. Previously, we tentatively identified peak 2 as the Schiff base position of the molecule, although other possibilities could not be ruled out. The difference map which results between data from samples regenerated with perdeuterated retinal and partially deuterated retinal should have as its only real feature the ionone ring. This map is virtually identical to the former one except for the missing weaker density bands connecting peaks 1 and 2 and another one extending down the protein "cleft".

T-Pos89 LIGHT-INDUCED $\text{Ca}^{++}/\text{Mg}^{++}$ RELEASE FROM PURPLE MEMBRANE AND PHOTOCHEMISTRY OF BLUE MEMBRANE
C.-H. Chang, C.-K. Suh, R. Govindjee, and T. Ebrey, Department of Physiology and Biophysics, University of Illinois, Urbana, IL 61801

Calcium-sensitive microelectrode and the magnesium-sensitive dye, Eriochrome Blue S, have been used to measure the concentration of free Ca^{++} and Mg^{++} , in purple membrane suspensions and in blue membrane suspensions, obtained by either NaCl^{++} -treatment, EDTA-treatment, or acid treatment. A significant amount of light-induced Ca^{++} and Mg^{++} release was detected from purple membrane, but almost no Ca^{++} release was seen from any type of blue membrane.

The photochemistry of blue membrane is quite different from that of purple membrane. After light-adaptation, the λ_{max} of EDTA-treated blue membrane blue-shifts with a decrease in the extinction coefficient. Flash-induced absorbance changes in submillisecond to millisecond time scale show that there is a small absorbance increase at 400 nm in both NaCl -treated and EDTA-treated blue membranes. The amplitude of the absorbance change is significantly smaller than that seen for native purple membrane (12% for EDTA-treated blue membrane) and may be due to unconverted purple membrane. Flash-induced difference spectrum has a peak around 500-510 nm in the EDTA-treated blue membrane. This absorbance increase closely resembles that reported for acid purple membrane (pH 2.0) (Mowrey et al., *Biochemistry*, 1979, 18, 4100).

T-Pos90 PRESSURE EFFECTS ON PURPLE MEMBRANE PHOTOCYCLE. Jeffrey Marque and Laura Eisenstein, Department of Physics, University of Illinois, Urbana, IL 61801.

We present data on the effects of hydrostatic pressure on the kinetics of the photocycle of purple membrane from *Halobacterium halobium*. The data were collected between 1°C and 50°C and between atmospheric pressure and 1.7 Kbar. These data show that pressure retards all of the transitions $\text{K} \rightarrow \text{L}$, $\text{L} \rightarrow \text{M}$, $\text{M} \rightarrow \text{O}$, and $\text{O} \rightarrow \text{bR}$ and that the earlier stages of the photocycle are less strongly affected by pressure than are the later stages. The retardation of the slowest steps by pressure shows a saturation effect, particularly at the lower temperatures. There is strong suppression of O formation as pressure is raised and/or temperature is decreased. This, together with the observation that O production is suppressed at high pH, suggests that O contains an undissociated acid group, and that this group is dissociated by pressure or low temperatures. In addition, the qualitative behavior of the rates' pressure dependence is similar to their solvent viscosity dependence. We conclude that a major effect of pressure is to decrease the fluidity of the membrane by decreasing its volume.
Supported in part by grants NSF PCM82-09616 and HEW PHS GM18051.

T-Pos91 FOURIER TRANSFORM INFRARED DIFFERENCE SPECTROSCOPY OF BACTERIORHODOPSIN.

Kimberly Bagley, Gavin Dollinger, Laura Eisenstein, Mi Kyung Hong, Agnes Jánosházi, Joseph Vittitow, Physics Dept., University of Illinois, Urbana, IL 61801.

We have used Fourier transform infrared (FTIR) difference spectroscopy to study changes of the retinal chromophore and opsin moieties of bacteriorhodopsin (bR) during its proton pumping photocycle. As a continuation of earlier work on the chromophore changes (K. Bagley, G. Dollinger, L. Eisenstein, A. K. Singh and L. Zimányi, Proc. Natl. Acad. Sci. USA **79**, 4972 (1982)) we have studied bR regenerated with two additional retinal analogues, a retinal with a photoaffinity label at C-3 on the β -ionone ring and a retinal labelled with ^{13}C at the aldehyde. The results of these measurements will be briefly discussed. However the strength of FTIR difference spectroscopy is its ability to observe opsin changes that are difficult to study with resonance Raman and visible techniques. We have focussed our attention on those amino acids that are thought to be directly involved in the photocycle and proton pumping such as tryptophane, tyrosine, aspartic and glutamic acids. Specifically we have studied bR from bacteria grown on isotopically labelled amino acids and, in the case of the carboxylic amino acids, bR which has been subjected to papain digestion, cation exchange, or has been reacted with carbodiimides. We will report on the differences which we observed in the difference spectra between these samples and normal bR for dark-adapted, light-adapted, K and M intermediates. (We would like to thank C. H. Chang, A. A. Croteau, V. Balogh-Nair, T. Ebrey, R. Govindjee, K. Nakanishi, E. Oldfield and L. Packer for providing bR samples. This work was supported in part by grant HEW PHS GM32455.)

T-Pos92 TESTING KINETIC MODELS FOR THE BACTERIORHODOPSIN PHOTOCYCLE: INCLUSION OF AN O TO M

BACKREACTION. Luis A. Parodi, Clinical Research Laboratory, Upjohn Co., Mail Stop 7262-209-5, Kalamazoo, MI 49001 and Richard H. Lozier, Cardiovascular Research Institute, University of California, San Francisco, CA 94143 and Somendra M. Bhattacharjee and John F. Nagle, Departments of Physics and Biological Sciences, Carnegie-Mellon University, Pittsburgh, PA 15213.

Using our previously established procedures (Biophysical Journal **38**, 161 (1982)) we have tested a kinetic model of bacteriorhodopsin involving a backreaction from O to M. This model is superior to the previously tested models involving only unidirectional reaction paths. However, the spectrum of O is still too strongly temperature dependent in the red. Therefore, at least one additional feature is necessary to obtain a completely consistent kinetic model of the bacteriorhodopsin photocycle.

T-Pos93 A DEFORMATION WAVE MODEL FOR THE PHOTOINDUCED TRANSMEMBRANE VECTORIAL PROTON TRANSPORT IN THE PURPLE MEMBRANE. J.E. Draheim, N.J. Gibson, S.C. Hartsel and J.Y. Cassim, Department of Microbiology, The Ohio State University, Columbus, Ohio 43210.

Currently, a solid state protonic semiconductor model has been proposed to explain the photo-induced vectorial translocation of protons through the purple membrane bilayer which appears to be void of permanent transmembrane channels. The key feature of this model is continuous ordered chains of hydrogen bonds formed from the protein side groups through which protons could be conducted in a relay fashion similar to protonic conduction in ice. Recently this laboratory showed that the membrane may undergo large scale global structure changes during the photocycle (Draheim *et al.*, Photochem. Photobiol. **37**, 1983, TPM-B20, S54 (abstr.)). Two important consequences of these changes are the loss of integrity of the membrane crystallinity and a net tilting of the polypeptide segments of the bacteriorhodopsins away from the membrane normal. Clearly, these structural changes are not consistent with the proposed solid state model of the membrane. Theoretically, such changes should encourage the formation of pulsating transmembrane channels normal to the membrane plane. A more realistic view of pulsating channels, considering the time scale involved, would be deformation waves traversing the membrane rather than physical channels. Therefore, during the photocycle there would be outward and inward moving deformation wave fronts which could be the driving force for the protonic translocation process of the membrane. Net vectorial translocation could be realized by assuming two possible pathways in the membrane, differentially resistant to protonic movement, to which this driving force may be coupled.

T-Pos94 IDENTIFICATION AND FUNCTION OF CYTOCHROME O IN THE BROWN MEMBRANE OF HALOBACTERIUM HALOBIVM. S.C. Hartsel, B.J. Kolodziej and J.Y. Cassim. Department of Microbiology, The Ohio State University, Columbus, Ohio 43210.

The brown membrane is the precursor of the purple membrane Halobacterium halobium. It consists of b-type cytochrome in addition to bacterioopsin, the apoprotein of bacteriorhodopsin of the purple membrane (G.K. Papadopoulos *et al.*, Photochem. Photobiol. 33,1981,455). Previously this cytochrome had been identified tentatively as cytochrome b-561. New evidence will be presented to show that this cytochrome is most likely cytochrome o, a CO-binding terminal oxidase, and can account for nearly all of the assayed heme content of this membrane domain. The reduced, oxidized and carbonyl states of this cytochrome were studied by linear and circular dichroic spectroscopy. Although the orientation of the heme plane relative to the membrane plane remained invariant to these state changes, the protein tertiary structure did not. Cytochrome o has been proposed to be a mixed function oxidase in Pseudomonas putida (J.A. Peterson, J. Bacteriol. 103,1970,714) and has also been shown to increase quantitatively relative to other cytochromes in stationary phase cultures of H. halobium (K.S. Cheah, Biochim. Biophys. Acta 205,1970,148). We propose that the function of this cytochrome in the brown membrane may involve catalysis of the oxidative cleavage of β -carotene to retinal which is essential for purple membrane formation.

T-Pos95 QUASI-ELASTIC LASER LIGHT SCATTERING AND DOPPLER ELECTROPHORESIS. Bernard Arrio*, Georges Johannin*, Pierre Volfin* and Lester Packer†. *Institut de Biochimie, Bat. 43 Université de Paris XI, 91405 Orsay, France and †Membrane Bioenergetics Group, Applied Sciences Division, Lawrence Berkeley Laboratory. University of California, Berkeley, California 94720 USA.

Quasi-elastic light scattering (QELS) and electrophoretic light scattering, e.g. laser-doppler velocimetry (LDV), were used to measure apparent size and surface charge of purple membrane (PM) suspensions and PM reconstituted into lipid vesicles. QELS showed that reconstitution of hydroxylamine-bleached membranes with all-trans retinal caused a 7 percent increase in PM size. This suggests that under these conditions 2° structural changes of retinal with the apo-protein cause long range effects on PM structure. PM suspensions show light-induced changes in negative surface charge density which are reversible in the dark. Light-induced changes in populations of PM-reconstituted lipid vesicles which can be observed by electrophoretic mobility (LDV) are reversible in the dark. QELS and LDV afford a convenient measure of surface charge (zeta-potential) and size (hydrodynamic radius) of PM suspensions and PM reconstituted vesicles.

[Research supported by the Centre National de les Recherche Scientifique (A.T.P."Bioenergetique" n°3093/79), France] and the Office of Biological Energy Research, Division of Basic Energy Sciences, Department of Energy, USA.

T-Pos96 COMPARISON OF PROTON TRANSFERS BETWEEN CARBONYL AND HYDROXYL GROUPS. Steve Scheiner, Dept. of Chemistry & Biochemistry, Southern Illinois University, Carbondale, IL 62901

The differences in proton-transfer properties between oxygen atoms in two distinct bonding situations are investigated using ab initio molecular orbital methods. In the hydroxyl group, the O is involved in single bonds only whereas a double bond is present between O and C in the carbonyl moiety. Within the context of the calculations, the -OH group is placed in the HOH (or CH₃OH) molecule; formaldehyde H₂C=O is used as the prototype carbonyl-containing molecule. An energy barrier is found along the proton transfer path separating H₂COH--OH₂ and H₂CO--HOH₂. The height of this barrier is quite sensitive to the H-bond length R(OO), increasing rapidly as this bond is elongated. Of particular interest is the observation that the relative stabilities of the two configurations may be reversed by alterations in their relative orientations. That is, the situation in which the proton is located on the carbonyl (H₂COH--OH₂) is more stable than (H₂CO--HOH₂) when the water lies along a "lone pair" direction of the carbonyl oxygen; i.e. $\theta(\text{COO})=120^\circ$. On the other hand, when the water is placed along the C=O axis ($\theta(\text{COO})=180^\circ$) the proton prefers the hydroxyl group of the water. This fact points to a possible mechanism for a conformation-induced local pK shift in a protein. By altering the angular features of a H-bond between a hydroxyl and carbonyl group, a protein may control on which group the proton prefers to be located despite the "normal" ordering of pK. Implications for proposed mechanisms of proton translocation along H-bond chains within proteins such as bacteriorhodopsin and H⁺-ATPase will be discussed.

T-Pos97 DEUTERIUM NMR STUDIES OF MOLECULAR DYNAMICS IN BACTERIORHODOPSIN: ANALYSIS OF LINESHAPES AND INTENSITIES FOR PHENYLALANINE, TYROSINE, AND LEUCINE SIDECHAINS. B.A.Lewis*, D.M. Rice**, E.T. Olejniczak*, S.K. Das Gupta*, J. Herzfeld***, and R.G. Griffin*. *Francis Bitter Natl Magnet Laboratory, M.I.T., Cambridge MA 02139, **Dept. of Chemistry, Univ. of Mass., Amherst, Amherst, MA 01002, ***Biophysical Lab., Harvard Medical School, Boston, MA 02115

^2H quadrupole lineshapes, intensities, and spin lattice relaxation times have been observed from native bacteriorhodopsin (BR) labeled at the δ and ϵ positions of the phenylalanine rings. Between -50° and $+40^\circ\text{C}$ the lineshapes are characteristic of a 180° rotational jump of the phenyl ring, and the jump rates inferred from the lineshapes vary between 5×10^2 and $2 \times 10^6 \text{ sec}^{-1}$, with activation energy of 12 kcal/mole. The temperature dependence of the echo intensity indicates that at least 10 of the 13 phenylalanine rings have very similar jump rates. T_1 relaxation times are approximately 100 times faster than predicted by the observed jump rate, suggesting that spin lattice relaxation is dominated by a faster motion with a small amplitude. T_1 decreases with increasing temperature, reaching a minimum of about 15 msec near 25°C . Such relaxation can be caused by motion with a correlation time in the range of 10^{-8} sec. Short T_1 's and a low ring flip activation energy suggest that the interior of the protein is relatively disordered.

The $(\delta, \epsilon\text{-d}_4)$ -tyrosine-BR results are similar to those for phenylalanine, while the $(\delta\text{-d}_3)$ leucine BR spectra show fast methyl rotation plus a small amount of tetrahedral jump, probably about the $\text{C}_\beta\text{-C}_\gamma$ bond.

T-Pos98 EVIDENCE FOR A SULFHYDRYL GROUP NEAR THE RETINAL BINDING SITE OF HALORHODOPSIN. M. Ariki and J.K. Lanyi. Dept. of Physiology and Biophysics, University of California, Irvine, CA 92717

Amino acid analysis of halorhodopsin chromoprotein shows a cysteine residue which is absent in bacteriorhodopsin. Since preliminary results had shown that mercurials inhibit ion transport by cell envelope vesicles, HgCl_2 effects on the properties of halorhodopsin were studied. We find that low concentrations (μM) of HgCl_2 inhibit the light-induced chloride transport of halorhodopsin in L-33 vesicles and increase the K_m of chloride for halorhodopsin. Photocycle measurements show that the decay rate of the absorption change at 570 nm for halorhodopsin is considerably slowed by HgCl_2 , while that of slow rhodopsin is virtually unaffected. The magnitude of the flash-induced absorption change is likewise reduced to zero by HgCl_2 . The HgCl_2 effect is counteracted by higher concentrations of chloride. The inhibitory effects of HgCl_2 are also observed with the purified halorhodopsin chromoprotein. The photocycle of bacteriorhodopsin is not affected even by 1 mM HgCl_2 . Upon addition of HgCl_2 to chromoprotein at low chloride concentration in the dark, a decrease at 570 nm in chromophore spectrum occurs, accompanied by blue shift (20 nm), which is eliminated at high chloride concentration. Sustained illumination of halorhodopsin produces a 410 nm photoproduct, which slowly reconverts to the 580 nm chromophore. HgCl_2 inhibits this step, indicating that SH group is located near the chromophore.

T-Pos99 NEW EVIDENCE FOR BRANCHING IN THE BACTERIORHODOPSIN PHOTOCYCLE. James M. Beach and Roger S. Fager, Department of Physiology, University of Virginia, Charlottesville, VA 22908.

Kinetics of transitions in the photocycle of bacteriorhodopsin and their relation to proton pumping in purple membranes have been extensively studied (1,2,3). The organization and temperature dependence ($10^\circ\text{--}40^\circ\text{C}$) of transition pathways is tested in this flash photolysis study of bacteriorhodopsin in aqueous suspensions of purple membranes from *Halobacterium halobium*. In order to conform with theoretical kinetic models, flash absorption records were transformed into relative concentration time courses using simultaneous solutions to the Lambert-Beer equation with published molar extinction coefficients (1). Comparison of the data with various kinetic models was performed by simulation methods which reconstruct estimates of intermediate concentration changes from the solutions to model dependent flux equations. Parallel decay from the "M" form, directly into bR_{570} and indirectly to bR_{570} through an intermediate O_{640} , most accurately described our data. This result is in agreement with a study based on analysis of absorption transients (3), and in disagreement with another kinetic model testing procedure (2). Our analysis suggests that (i) the transition from "M" is the sole rate-limiting step in the photocycle, and (ii) temperature dependent formation of "O" is explained by changes in the relative utilization of the branched pathways as a function of temperature. Data were collected on a home-built photodiode array spectrographic photometer, giving 22 wavelengths between 400–700 nm at 0.5 millisecond temporal resolution. Supported by NIH Grants EY 01505 and EY 00142.

1) R.H. Lozier, et al. (1975), *Biophys. J.* 15:955–962. 2) J.F. Nagle et al. (1982), *Biophys. J.*, 38:161–174. 3) W. Sherman et al. (1979), *Photochem. Photobiol.*, 30:727–729.

T-Pos100 BACTERIORHODOPSIN'S PURPLE COLOR IS PARTIALLY DUE TO DIVALENT CATIONS

J.G. Chen, C.-H. Chang, R. Govindjee, and T. Ebrey (Intr. by D. DeVault), Department of Physiology and Biophysics, University of Illinois, Urbana, IL 61801

Atomic absorption spectrometry shows that purple membrane (PM) from *Halobacterium halobium* binds approximately 1 Ca^{++} and 3 Mg^{++} ions per bacteriorhodopsin (BR). Incubation of purple membrane with EDTA or 4 M NaCl followed by washing in distilled water results in a shift of the λ_{max} of BR from 569 to longer wavelengths, 595-600 nm with the purple membrane turning blue. Elemental analysis shows there is almost no Ca^{++} and Mg^{++} present in these blue membrane preparations. The purple color recovers when a mole of Ca^{++} and/or Mg^{++} per mole of BR is added back to blue membrane. The titration curves of blue membrane with various salts have a single isosbestic point at 575 nm indicating that only two species, PM and the blue membrane, are involved in the blue-purple transition. Incubation of PM in mM concentration of either ionic species replaces the other, thus the binding site is nonspecific for Ca^{++} and Mg^{++} , like other Ca-binding proteins, Ca^{++} and Mg^{++} can be replaced by La^{3+} .

It is known that the λ_{max} of BR shifts to about 595 nm at pH 2.0 (acid blue membrane). Elemental analysis shows there is almost no Ca^{++} and Mg^{++} in the acid blue membrane suspension. Therefore, removal of the divalent cations from their binding sites in the purple membrane probably is responsible for the spectral change of BR upon lowering the pH to 2.0. Chemical modification of the COOH-groups with 1-amino-naphthalene-3,6,8-tri sulfonic acid also results in a shift of the λ_{max} to 580 nm-590 nm, and a loss of Ca^{++} and Mg^{++} . Evidence will be presented to show that the COOH groups on the C-terminal tail are involved in the binding of these metal ions.

T-Pos101 CONFORMATIONAL CHANGES OF BACTERIORHODOPSIN AS PROBED BY A FLOURESCENT DYE

R. Govindjee, K. Kinoshita, A. Ikegami, and T. Ebrey, Department of Physiology and Biophysics, University of Illinois, Urbana, IL 61801, and Laboratory of Biophysics, RIKEN, Wako-Shi, Saitama 351 Japan.

By measuring the fluorescence properties of a fluorophore, 1-amino naphthalene -3,6,8-tri sulfonic acid (ANTSA), covalently attached to the COOH-groups of bacteriorhodopsin (BR), we studied conformational changes of BR, specifically those of the COOH-terminal region. Approximately 2 dye molecules were bound per BR. After papain digestion of the PM which removes the C-terminal region, however, 1 dye molecule/BR was released into the supernatant. Thus, one dye molecule must be bound to some site on the membrane surface and another on the COOH-terminal region. Time-resolved fluorescence decay of ANTSA-BR could be resolved into 3 components, ~50% with life-time of 1 to 2 nsec, ~40% with $\tau = 4$ nsec and a very small component ~10% of $\tau \sim 8$ nsec. After digestion with papain the shortest τ component comprised almost 85% of the total fluorescence, and the 4 nsec component approximately 10%. This suggests that the 1 nsec component is from the dye bound to the membrane surface, and the 4 nsec component must be from the dye attached to the COOH-terminal region. The fluorescence intensity of ANTSA-BR increases, and the fluorescence anisotropy decreases as the concentration of NaCl is increased. This result suggests that there is salt-induced conformational change in BR. In contrast the papain treated ANTSA-BR shows very little salt effect. Relationship with H^+ changes will be discussed.

T-Pos102 ISOLATION, PURIFICATION AND PARTIAL CHARACTERIZATION OF BACTERIORHODOPSIN IN SUCROSE ESTER. Johanne Baribeau and François Boucher, Centre de Recherche en Photobiophysique, Université du Québec à Trois-Rivières, Trois-Rivières, Québec, Canada. G9A 5H7

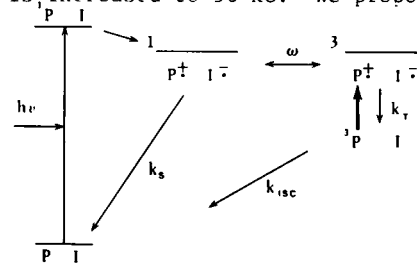
Bacteriorhodopsin has been isolated from purple membranes of *Halobacterium halobium*. The protein was solubilized and delipidated according to standard procedures and further purified by chromatography on Phenyl-Sepharose using lauryl sucrose (L-1690) as the detergent. The purified bacteriorhodopsin in L-1690 has maximum absorption at 540 nm; it is light adaptable and it reversibly forms, under illumination, a meta intermediate which absorbs maximally at 385 nm. Upon alcalinization of the medium, BR-540 is reversibly converted, in the dark, to another species absorbing at 480 nm. The pK_a of the reaction is 8.5 and the equilibrium between BR-540 and BR-480 is temperature dependant. The comparison between the photochemical properties of both bacteriorhodopsin species will be presented.

T-Pos103 $P^+Q_B^-$ RECOMBINATION LUMINESCENCE FROM RHODOPSEUDOMONAS VIRIDIS. Darrell Fleischman, Charles F. Kettering Research Laboratory, Yellow Springs, Ohio 45387

Chromatophores of *R. viridis* display a delayed fluorescence component whose first order decay constant is about 1.5 sec^{-1} at 20°C and pH 7. The delayed fluorescence decay parallels P^+ reduction and the reversal of a light-induced ultraviolet absorbance change whose spectrum resembles that of a semiquinone anion. We attribute this delayed fluorescence to $P^+Q_B^-$ charge recombination. The Arrhenius activation energy for the light emission is 0.42eV , while that for the decay of delayed fluorescence and P^+ is 0.2eV . We suggest that $P^+Q_B^-$ lies energetically 0.42eV below P^+Q_B and 0.2eV below $P^+Q_A^-$, which is an obligatory intermediate in the $P^+Q_B^-$ charge recombination. A comparison of the initial intensities of $P^+Q_B^-$ and $P^+Q_A^-$ recombination luminescences indicates that $P^+Q_B^-$ lies 0.08eV below $P^+Q_A^-$ in free energy at pH 8. The rate constant for $P^+Q_A^-$ recombination is pH-dependent and appears to be determined by protonation of a base whose pK is 6.5 when Q_B is oxidized. Proton release parallels $P^+Q_B^-$ charge recombination. It appears that formation of the Q_B semiquinone shifts the pK of the Q_B^- associated base to a value greater than 8. The $P^+Q_B^-$ charge recombination rate is sensitive to the presence of salt. A comparison of the effect of MgSO_4 and KCl and application of the Guoy-Chapman treatment, with the assumption of uniform planar surface charge distribution, yields a chromatophore surface charge density of 0.14C/m^2 .

T-Pos104 MAGNETIC FIELD EFFECTS ON THE LIFETIME OF THE TRIPLET STATE IN PHOTOSYNTHETIC REACTION CENTERS: EVIDENCE FOR THERMAL RE-POPULATION OF THE PRIMARY RADICAL PAIR S.G. Boxer, C.E. D. Chidsey, L. Takiff, and R. Goldstein, Department of Chemistry, Stanford University, Stanford, CA 94305

The reaction scheme for the initial events in quinone depleted photosynthetic reaction centers from the R-26 mutant of *R. sphaeroides* is shown below. It is generally accepted that the molecular triplet state of the primary electron donor (3P) is formed by charge recombination of the triplet radical pair, $^3(P^+I^-)$, and that 3P decays to the ground state by ordinary intersystem crossing. We have discovered that the lifetime of 3P shows a strong dependence on magnetic field: in non-viscous buffer the lifetime at room temperature increases from about 30 to $60 \mu\text{s}$ when the applied field is increased from 0 to 1 kG, and decreases to about $30 \mu\text{s}$ as the field is increased to 50 kG. We propose that these effects are a result of thermal re-population of the triplet radical pair from 3P (bold vertical arrow), i.e., the triplet state decays predominantly by a thermal reversal of the reaction which formed it, rather than intersystem crossing. As expected, the magnetic field effects on the lifetime disappear at low temperature. Assuming that the $150 \mu\text{s}$ 3P lifetime at low temperature represents the intrinsic lifetime in the absence of back-reaction, the temperature dependent lifetime gives an estimate for the energy gap between the triplet and the ion-pair of about 1000 cm^{-1} . A detailed theoretical treatment of the problem will be presented to quantitatively analyze the field dependence.



T-Pos105 MODELS OF PHOTOSYNTHETIC REACTION CENTERS. STRUCTURE, AGGREGATION AND RADICALS OF A BACTERIOPHEOPHYTIN b ANALOG. K.M. Barkigia, C.K. Chang, I. Fujita, T. Horning and J. Fajer, Department of Applied Science, Brookhaven National Laboratory, Upton, NY 11973.

The structure of **1**, a metal-free model of BChl and BPheo b, has been determined by X-ray diffraction. The molecule is planar and aggregates via π - π interactions to form head-to-tail polymers $\sim 3.6\text{\AA}$ apart. In solution, radicals of the model exhibit optical, ESR and ENDOR properties similar to those of BPheo b radicals. The molecule thus provides a reasonable chemical analog of the biological pigment. In addition, dimeric subunits of the crystalline polymer display a structural arrangement (Fig. 1) similar to that recently proposed by Mobius and coworkers (PNAS, in press) for the primary donors or special pairs of bacterial reaction centers. Although structural data for bacteriochlorins are sparse, the present results and those previously obtained for methylbacteriopheophorbide a (JACS 1981, **103**, 5890) and a metal-free isobacteriochlorin (JACS 1982, **104**, 315) suggest that π - π interactions may provide a common mode of aggregation for these derivatives in vitro and in vivo. (Work supported by the Chemical Sciences Division, U.S. Dept. of Energy.)

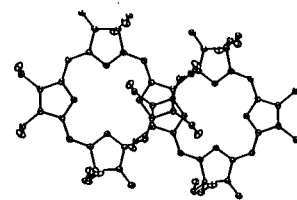
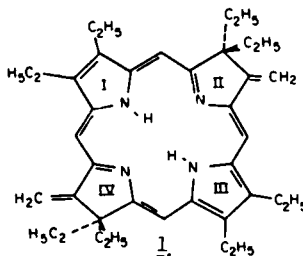


Fig. 1

T-Pos106 SPECTRAL PROPERTIES OF PROTONATED SCHIFF'S BASE PORPHYRINS AND CHLOROPHYLLS. INDO-CI CALCULATIONS AND RESONANCE RAMAN STUDIES. L.K. Hanson and J.D. Head, Dept. of Applied Science, Brookhaven National Laboratory, Upton, NY 11973; C.K. Chang, B. Ward, P.M. Callahan and G.T. Babcock, Dept. of Chemistry, Michigan State University, East Lansing, MI 48824.

The chlorophylls which function as the primary electron donors within photosynthetic reaction centers have red-shifted absorption spectra relative to monomer species in solution. In green plants, the donors may be monomers whose electronic properties have been altered by the protein environment. Recent suggestions include the derivatization of the Ring V carbonyl to a Schiff's base (SB) by an amine side chain of the protein.¹ Protonation of the SB substituents of model porphyrins (P), chlorins (C), and bacteriochlorins (BC) can lead to dramatic red-shifts of the long wavelength absorption band accompanied by splitting or broadening of the Soret band. Calculations by a spectroscopic INDO method on these P, C and BC complexes as well as on ketimine and enamine isomers of pyrochlorophyll (Pchl) will be presented, along with RR results on chlorin adducts. The calculations successfully reproduce the changes in optical spectra which occur upon protonation. They ascribe the changes to SB C=N π^* orbitals which drop in energy and mix with and perturb the π^* orbitals of the macrocycle, a result consistent with RR data. The red band of chlorins is predicted to red-shift or blue-shift, depending on the substitution site of the SB. Blue-shifts are calculated for protonation of ketimine and enamine isomers of pyrochlorophyll a (Pchl). Comparison with reported optical spectra¹ suggests that Pchl a SB may undergo isomerization upon protonation. (Supported by the Department of Energy, the NSF and the NIH.) 1) R.M. Pearlstein, et al., *Biophys. J.* **37**, 112a (1982). L.L. Maggiora and G.M. Maggiora, *JACS* (1983) submitted.

T-Pos107 CHLOROPHYLL FLUORESCENCE KINETIC STUDIES OF PHOTOSYNTHETIC MEMBRANE ORGANIZATION, Kerry K. Karukstis and Kenneth Sauer, Dept. of Chemistry and Lab. of Chemical Biodynamics, University of California, Berkeley, CA 94720

The chlorophyll (Chl) fluorescence decay kinetics of higher plant chloroplasts monitors the primary processes of photosynthesis and reflects photosynthetic membrane organization [Haehnel, W., Nairn, J.A., Reisberg, P. and Sauer, K. (1982) *Biochim. Biophys. Acta* **680**, 161-173]. We have extended these studies by measuring the Chl fluorescence decay kinetics of peas at various stages of chloroplast development as controlled by the mode of illumination during plant growth. Changes in the kinetics of a slow decay component (1-4 ns) during etioplast-to-chloroplast differentiation are associated with incorporation of Chl a into PS1 and PS2 reaction centers, formation of grana, and development of communicating PS2 reaction centers (α -centers). The kinetics of a middle phase (300-600 ps) also reflects the formation of a heterogeneous population of PS2 units (α - and β -centers), while the kinetics of a fast phase (100 ps) is independent of plant development. We have also monitored the Chl fluorescence decay as a function of thylakoid membrane composition by examining Chl b-deficient *chlorina f-2* barley mutant chloroplasts. These decays are characterized by a 400-ps component and a fast (100 ps) component; we do not find a variable ns decay component in this mutant. We use these data to formulate a model for the origin of the Chl fluorescence decay components in higher plant chloroplasts.

This work was supported by the Department of Energy (Contract No. DE-AC03-76SF00098), the National Science Foundation (PCM 82-10524), and the National Institutes of Health (National Research Service Award 1 F32 GM08617-03).

T-Pos108 A MODEL FOR THE POSITION OF THE HEMES OF CYTOCHROME b_6 IN THE CHLOROPLAST MEMBRANE-IMPLICATIONS FOR THE ORIGIN OF THE SLOW ELECTROCHROMIC BAND SHIFT. W. R. Widger¹, W. A. Cramer¹, R. G. Herrmann², and A. Trebst³, Dept. of Biol. Sci.,¹ Purdue Univ., W. Lafayette, IN 47907, U.S.A., Bot. Inst. der Univ. Düsseldorf², FRG, and Lehrstuhl für Biochemie der Pflanzen³, Ruhr-Univ. Bochum, FRG.

The amino acid sequences of the b_6 cytochrome of complex III from five different mitochondrial sources (human, bovine, mouse, yeast, and *A. nidulans*) and the chloroplast cytochrome b_6 from spinach show a high degree of homology. Calculation of the distribution of hydrophobic residues, using a 'hydropathy' function that is conserved in this family of proteins, implies that the membrane folding pattern of the 42 kDa mitochondrial cytochromes involves 8-9 membrane spanning domains. The smaller 23 kDa chloroplast cytochrome appears to fold in 5 spanning domains that are very similar to the first 5 of the mitochondria. 4 highly conserved histidines are considered to be the likely ligands for the 2 hemes. The position of the histidines along the spanning segments and in a cross section of the membrane spanning α -helices implies that two ligand pairs, HIS 82 - HIS 197 (198) and HIS 96 - HIS 183, bridge the spanning peptides II and V, and the two hemes reside on opposite sides of the hydrophobic membrane core. In addition, the 17 kDa protein of the $b_6 - f$ complex (subunit 4), whose sequence is also known, appears to contain one or more of the functions of the C-terminal end of the mitochondrial cytochrome b_6 polypeptide.

This heme arrangement has implications for 'Q cycle' models developed to explain the origin of the slow electrochromic band shift. The hydrophobic membrane span between the hemes, $\sim 12\text{\AA}$ edge to edge, is larger than that between either heme and the polar interface. Thus, if oxidation of cyt b_6 is electrogenic, the main step in field generation would be the heme \rightarrow heme transfer.

T-Pos109 CRYOGENIC PHOTOGENERATION OF AN INTERMEDIATE SPECIES IN PHOTOSYNTHETIC OXYGEN EVOLUTION OBSERVED BY EPR. J.L. Casey, and K. Sauer, Department of Chemistry and Laboratory of Chemical Biodynamics, Lawrence Berkeley Laboratory, University of California, Berkeley, California 94720.

The ability at low temperature to generate and trap an intermediate state between the S_1 and S_2 states of the Kok scheme¹ for photosynthetic oxygen evolution has been demonstrated. Illumination of oxygen-evolving photosystem 2 preparations² at 140 K produced a 350 Gauss wide EPR signal centered at $g=4.3$ when observed at 10 K. This signal appeared on top of a five-fold larger, narrower background signal; hence, it was best observed in difference spectra. The light-induced signal appeared to be structureless when observed with 8 Gauss field modulation. Warming of illuminated samples to 190 K in the dark resulted in the disappearance of the light-induced $g=4.3$ feature and the appearance of the multiline EPR signal associated with the S_2 state³. Inhibition of oxygen evolution by incubation of photosystem 2 preparations in 0.8M NaCl or by the addition of 0.4mM NH_2OH prevented the light-induced formation of the $g=4.3$ signal and the multiline signal. Samples in which oxygen evolution was inhibited by replacement of Cl^- with F^- exhibited the $g=4.3$ signal when illuminated at 140 K, but subsequent warming to 190 K neither diminished the amplitude of this signal nor produced the multiline signal. The broad signal at $g=4.3$ is typical for a $S=5/2$ system in a rhombic environment, suggesting the involvement of non-heme iron in oxygen evolution.

1. B. Kok, B. Forbush and M. McGloin, *Photochem. Photobiol.*, **11**, 457-475 (1970)

2. T. Kuwabara and N. Murata, *Plant Cell Physiol.*, **23**, 533-539 (1982)

3. G.C. Dismukes and Y. Siderer, *FEBS Lett.*, **121**, 78-80 (1980)

T-Pos110 TRANSIENT CONDUCTIVITY CHANGES IN SOLUTIONS OF PHOTOEXCITED BACTERIAL REACTION CENTERS*

T. Marinetti, Rockefeller University, 1230 York Avenue, New York NY 10021.

Using a sensitive 100kHz conductivity bridge, proton uptake has been detected in solutions of reaction centers[†] (RCs) from *Rhodospseudomonas sphaeroides* R-26 following flash excitation (590 nm, ~ 1 μ s, ~ 1 mJoul). The observed risetime of the transient conductivity change is limited by the time constant of the instrument (1 ms); the transient decays with a half-time which decreases from 1 s to 0.6 s as the pH of the solution is raised from 8 to 10. At pH 8, addition of o-phenanthroline (4 mM) to block electron transfer from Q_A to Q_B does not affect the signal amplitude. The decay half-time, however, shortens to about 50 ms. At pH 10.7, addition of o-phenanthroline (2 mM) causes a decrease in the amplitude of the transient and reduction of the decay half-time from 0.2 to 0.1 s. These time constants are similar to those observed for the back reaction of the charge separation. (cf, Blankenship & Parson, *BBA* **545**, 429 (1979); Kleinfeld, Okamura & Feher, *Biophys. J.*, **37**, 110a (1982)). Variation of the composition of the buffer, and the ensuing changes in the conductivity signal, proves that the observed transients are due to proton uptake. For example, at pH 8 when glycylglycine is titrated into Tris-buffered RCs--buffers which have similar pK 's but opposite changes in charge upon deprotonation--the transient conductivity is expected to change sign and does so. These data show that photoexcited RCs take up protons even when electron transfer to the secondary ubiquinone is blocked.

[†] Samples of RCs were generously provided by D. Kleinfeld and E. Abresch, UCSD, La Jolla CA.

* This work was supported by NIH grant GM 25693-05

T-Pos111 AGGREGATION OF CHLOROPHYLL *a* IN MONO- AND MULTILAYER. C. Chapados, L. Parent*,

S. Hotchandani*, and R.M. Leblanc, Centre de recherche en photobiophysique, Université du Québec à Trois-Rivières, C.P. 500, Trois-Rivières, Québec, Canada, G9A 5H7.

The nature of the interactions between chlorophyll *a* (Chl *a*) in mono- and multilayer arrays obtained by the Langmuir-Blodgett technique, is examined by electronic, fluorescence, and infrared spectroscopies. In the electronic spectra, the λ max of the red band (679 ± 1 nm) of the monolayer at the air/solid interface is approximately the same as that of the multilayer but the half-band width ($\Delta\lambda_{1/2}$) increases in passing from monolayer (32.5 ± 1 nm) deposited on a hydrophilic surface to bi-layer (43 ± 2 nm) and multilayer (48 ± 2 nm) deposited on an hydrophobic surface. The increase in $\Delta\lambda_{1/2}$ is an indication of the presence of Chl *a* in different states of aggregation. The fluorescence spectra of the monolayer on an hydrophilic surface shows a strong band at ~ 690 nm and a weak one at ~ 735 nm. For multilayers deposited on an hydrophobic surface, this intensity pattern is progressively reversed as more and more layers are added to the sample. Similar arrays are examined by infrared spectroscopy in the carbonyl region. This technique shows that for the monolayer there is little absorption in the coordinated ketone carbonyl and C=C, C=N regions (1680 to 1500 cm^{-1}) while there are some well defined bands in the multilayer organisation. These many bands are an indication of the presence of different species in the multilayers which will broaden the band width of the electronic spectra when passing from a monolayer to a multilayer organisation. This interpretation is not inconsistent with the fluorescence data which suggest one species because only monomeric form of Chl *a* is known to fluoresce in the 672-690 nm region. The electronic, fluorescence and infrared spectra are discussed along with the recently proposed model of Chl *a* at the air/solid interface (C. Chapados and R.M. Leblanc, *Biophysical Chemistry* **17** (1983) 211).

T-Pos112 CONFORMATION CHANGES IN CHLOROPLAST PLASTOCYANIN J. Draheim, G. Anderson and E. L. Gross. Dept. of Biochemistry, The Ohio State University, Columbus, Ohio 43210.

Plastocyanin (PC) is a 10.7 kD copper protein which functions as a mobile electron carrier in photosynthetic electron transport between cytochrome f and P700. We have found conformation changes in spinach PC both upon reduction and chemical modification of carboxyl groups. Reduction causes an increase in extinction at 278 nm and 261 nm of ca. 25% and 36%, respectively. Reduction causes an increase in ellipticity at 260 nm of ca. 124% with minimal change at 278 nm. Tyrosine fluorescence emission at 314 nm increase ca. 90% upon reduction when excited at 275 nm. Chemical modification causes a decrease in extinction at both 278 and 261 nm of ca. 17% for both the oxidized and reduced forms of PC. Chemical modification causes decrease in ellipticity at 260 nm at ca. 35% with minimal change at 278 nm. Chemical modification also appears to inhibit the fluorescence increase upon reduction. Similar spectral changes were observed for poplar PC upon reduction which contains one fewer tyrosine residues. These PC conformation changes could be related to possible differential binding affinities for PC with cytochrome f and P700 upon a change in its oxidation state.

T-Pos113 TIME-RESOLVED OPTICAL AND ELECTRON SPIN RESONANCE STUDIES IN PHOTOSYSTEM 2: THE MECHANISM OF LINOLENIC ACID-INDUCED INHIBITION. Joseph T. Warden and John H. Golbeck, Department of Chemistry, Rensselaer Polytechnic Institute, Troy, NY 12181.

Time-resolved spectroscopic techniques (optical flash photolysis and flash-photolysis electron spin resonance spectroscopy) have been utilized to monitor electron transport in Photosystem 2 (PS2) of chloroplasts and subchloroplast preparations from spinach. In particular an emphasis has been applied toward the elucidation of the mechanism for the reversible inhibition of PS2 by the fatty acid, linolenic acid (Golbeck et al., *Plant Physiol.* (1980) 65, 707-713).

Our studies have demonstrated that in the presence of linolenic acid: (1) Absorption transients ($\tau \geq 10 \mu s$) in the region of 820 nm, attributed to $P680^+$, are abolished. (2) Transient electron spin resonance signals at $g = 2.0025$ arising from $P680^+$ are also abolished. (3) Electron spin resonance Signal 2s and Signal 2f ($Z^{+?}$) are not detectable. (4) A high initial fluorescence yield (F_i) is observed upon illumination of the inhibited sample.

Upon reversal of linolenic acid inhibition by washing or addition of bovine serum albumin, optical and electron spin resonance transients, originating from the photooxidation of $P680$, are restored. Similarly the variable component of fluorescence is recovered with an accompanying restoration of a low F_i . The reversal of linolenic acid inhibition is characterized also by a light-mediated restoration of Signal 2s and Signal 2f.

These observations combined with esr studies at cryogenic temperatures will be interpreted within a proposed topological model for PS2. This work was supported by the National Institute of Health (2R01 GM26133-04). JHG was on leave from Martin Marietta Laboratories.

T-Pos114 EFFECT OF FUSION OF LIPOSOMES TO *RHODOPSEUDOMONAS SPHAEROIDES* PHOTOSYNTHETIC MEMBRANES ON THE STRUCTURAL ORGANIZATION OF THE LIGHT-HARVESTING SYSTEM. J. D. Pennoyer^a, H. J. M. Kramer^b, W. Westerhuis^b, R. van Grondelle^c and R. A. Niederman^a. ^aRutgers Univ., Piscataway, NJ, ^bState Univ., Leiden and ^cFree Univ., Amsterdam, The Netherlands.

Membranes of *R. sphaeroides* contain both core (B875) and peripheral (B800-850) light-harvesting complexes. The affinity of B800-850 for phospholipids was examined further by fusion of membranes to liposomes. Low-pH and polyethylene glycol (PEG)-induced fusion gave preparations with >20-fold phospholipid enrichment. Although B800 losses occurred, the polypeptide composition, reaction center activity and carotenoid absorbance changes were preserved. Fluorescence yields from B800-850 and B875 were examined as probes of interactive associations of the complexes within the lipid-enriched membranes. Fluorescence emission at $\sim 300^\circ K$ from B850 was increased up to 3.3-fold while increases of <1.5-fold were observed from B875. Liposomes formed from native phospholipids or phosphatidylcholine gave similar results, but the latter caused fluorescence quenching. Fluorescence excitation spectra at 77°K indicated that energy transfer efficiency from B850 to B875 was decreased by 39 and 28%, respectively, in preparations from the PEG and low-pH procedures. In contrast, energy transfer from carotenoids was unaffected. Overall, these results suggest that some peripheral B800-850 antenna (possibly the outer B800-850 array) has become dissociated. In contrast, protein-protein interactions between B875 and reaction centers within the core may be sufficiently strong to maintain these associations even in the presence of a large phospholipid excess. (Supported by PHS grant GM26248 and NSF grants PCM79-03665 and PCM82-09761 and a Busch fellowship award to J.D.P.)

- T-Pos115** HYPERFINE SPLITTING FROM A SINGLE METHYL GROUP DETERMINES THE EPR SPECTRAL SHAPE OF SIGNAL II. P.J. O'Malley* and G.T. Babcock, Michigan State University, East Lansing, MI 48824-1322 and R.C. Prince, Johnson Research Foundation and Department of Biochemistry and Biophysics, University of Pennsylvania, Philadelphia, PA 19104.

The proposal that EPR Signal II in spinach chloroplasts is due to a plastoquinone radical (O'Malley, P.J. and Babcock, G.T., *Biophys. J.* 41, 315a) is investigated. The similarity in spectral shape between Signal II and the 2-methyl-5-isopropylhydroquinone cation radical is shown to arise from hyperfine coupling to one methyl group for both radicals. A well resolved four line EPR spectrum of approximate relative intensity 1:3:3:1 for membrane orientation parallel and perpendicular to the applied magnetic field direction indicates that the partially resolved structure of Signal II is due to hyperfine interaction with one methyl group i.e. the 2-CH₃ group of the plastoquinone cation radical. The ENDOR band observed for this coupling is similar to previously observed methyl group bands for model quinone radicals and allows us to obtain the principal hyperfine tensor values for the methyl group interaction. The large isotropic coupling value of the plastoquinone cation radical's 2-methyl group *in vivo* indicates that the antisymmetric orbital is the sole contributor to the spin density distribution of Signal II. The orientation data also suggest that the plastoquinone cation radical is oriented on the membrane such that the C-CH₃ bond direction and the aromatic ring plane lie perpendicular to the membrane plane.

- T-Pos116** THE EFFECT OF OXYGEN ON THE AMPLITUDE OF PHOTO DRIVEN ELECTRON TRANSFER ACROSS THE LIPID BILAYER-WATER INTERFACE. Asher Ilani, Tong-Ming Liu and David Mauzerall, The Rockefeller University, 1230 York Avenue, New York, New York 10021.

The surprisingly small effect of oxygen on photoelectron transfer in pigmented lipid bilayers is traced to a short lifetime of the excited states. Changing the oxygen concentration from $<10^{-6}$ M to air level increases the half-saturating concentration of acceptor by about threefold but has no effect on the maximum photovoltage observed at acceptor saturation. Analysis of this competition as a function of pigment concentration indicates that pigment ions are formed by excited state self or concentration quenching. The acceptor, or O₂, reacts with the pigment anion forming the stabilized, interfacial photovoltage. The lipid-water interfacial region appears to favor longer lived ion formation in contrast to the usual concentration quenching in homogeneous solvents. Direct evidence for concentration quenching was obtained by measuring decreased yields and shortened lifetimes of the triplets in liposome preparations. Since the fluorescence is quenched at 100 times higher concentration of acceptors than required for the photoeffect, it is the triplets that react at the usual acceptor concentrations. This research was supported by NIH-Grant #GM 25693-05.

- T-Pos117** BIOLOGICAL SIGNIFICANCE OF MOLECULAR CHIRALITY IN ENERGY BALANCE. A. S. Garay. Department of Biochemistry and Biophysics, Texas A&M University, College Station, Texas 77843.

In Biological electron transport the spin, and thus the magnetic property of electrons, is neglected. Furthermore, no attention is paid to the fact that the great majority of biologically important molecules are chiral, and during excitation a magnetic moment is induced in them. It is shown, both theoretically and experimentally, that the magnetic moment of the electron and the magnetic transition moment of the optically active molecules may interact. The main consequences of such an interaction are a higher probability of the occurrence of optically active molecules in triplet states, and the polarization of transported electrons. With respect for theoretical approach I rely on the fact that the symmetry properties of optical isomers are compatible with the existence of second order pseudotensors characterizing the enantiomers. The correlation tensor between the velocity and the spin of electrons is of this type. With respect to experiments the magnetic transition dipole has been determined in a series of experiments. Results show a marked correlation between magnetic transition dipole and quantum yield of luminescence. Furthermore, if we consider the transported electrons as electron gas and apply the Fermi-Dirac statistics then the energy of the transported electrons are higher as compared to that of the random ones.

T-Pos118 REDUCTION KINETICS OF CLOSTRIDIUM PASTEURIANUM RUBREDOXIN (Rb) BY PHOTOREDUCED SPINACH FERREDOXIN: NADP+ REDUCTASE (FNR) AND FREE FLAVINS. C.T. Przysiecki, A.K. Bhattacharyya, G. Tollin, and M.A. Cusanovich, Dept. of Biochemistry, University of Arizona, Tucson, AZ 85721.

Laser flash photolysis of anaerobic solutions containing C. pasteurianum Rb, spinach FNR and/or free flavins have been used to measure direct free flavin and FNR semiquinone reduction of Rb. Rapid reduction of FNR by 5-deazariboflavin semiquinone (dRF \cdot) at pH 7, μ =10 mM produces a stable FADH semiquinone (FADH \cdot) monitored at 580 nm, addition of a substoichiometric amount of Rb results in monophasic decay of FADH \cdot . At 480 nm, a wavelength of Rb bleach and FNR isosbestic, Rb reduction is biphasic with the fast phase apparently due to direct Rb reduction by dRF \cdot . The slow phase rate constant is identical with that obtained at 580 nm. Second-order plots of the slow phase display saturation kinetics, which upon analysis yield a second-order rate constant of $\sim 3 \times 10^8$ M $^{-1}$ s $^{-1}$ and a limiting first-order rate constant of $\sim 8 \times 10^3$ s $^{-1}$. Spectroscopic studies at this ionic strength provide evidence for a strong 1:1 complex between Rb and FNR. Thus Rb reduction occurs via uncomplexed FNR and as the FNR/Rb ratio approaches unity intracomplex electron transfer becomes rate limiting. Both second-order and first-order rate constants decrease with increasing μ suggesting an electrostatic bimolecular reaction and an electrostatic rearrangement within the Rb:FNR complex, respectively. FNR is not reduced by lumiflavin semiquinone (LF \cdot). Reduction of Rb by LF \cdot is unaltered in the FNR:Rb complex. These results are interpreted in terms of suggested reductase recognition sites on Rb. (Supported by NIH Grants GM21277 to MAC and AM17072 to GT).

T-Pos119 COLOCALIZATION OF BIOLUMINESCENCE AND ENDOGENOUS FLUORESCENCE IN SUBCELLULAR SITES OF THE DINOFLAGELLATE GONYAULAX POLYEDRA Carl Johnson*, J. W. Hastings, and Shinya Inoue*, Biological Labs, Harvard Univ., Cambridge, MA 02138 and Marine Biological Lab, Woods Hole, MA 02543

The bioluminescent flashes of the photosynthetic dinoflagellate Gonyaulax polyedra have been reported (Biol. Bull, 137:411, 1969) to originate from many discrete subcellular loci which, however, have not yet been definitively identified. Using an inverted microscope coupled with a Zeiss/Venus 3-stage intensified camera, we have found that flashes emanate from subcellular sites which colocalize with newly discovered fluorescent granules (0.3-1.0 μ m in diameter). Several lines of evidence indicate that the fluorescence is that of the substrate molecule (luciferin) for dinoflagellate luminescence: its color, its circadian change in intensity, and the fact that the fluorescence is lost subsequent to stimuli which evoke bioluminescence. Studies of the flashing were carried out with cells taken from the dark phase of a light-dark cycle when the fluorescence and bioluminescent capacity are greatest. Cells were immobilized in 2% agarose and maintained at 19°C. First, the distribution of the fluorescent sites in an individual cell was recorded on video-tape. Then, bioluminescence was stimulated with either acetic acid, ammonia, or calcium, and the cellular location and kinetics of flashes recorded. The bioluminescent and fluorescent granules were found to be co-localized cortically and to number in the dozens per cell. Following stimulation, a given site may emit several sequential flashes; the disappearance of granular fluorescence lags behind the decay of bioluminescence. Based on these observations and *in vitro* studies, we believe these fluorescent granules are the subcellular source of Gonyaulax bioluminescence, and that they may be identical with the previously described "scintillons" (J. Cell Sci. 11:305-317, 1972). (Supported in part by NIH 5-R01-GM31617 and NSF PCM83-09414.)

T-Pos120 THE EFFECT OF TROPONIN-TROPOMYOSIN ON THE BINDING OF SKELETAL MUSCLE HMM TO ACTIN IN THE PRESENCE OF ATP. Joseph M. Chalovich and Evan Eisenberg, NHLBI, NIH, Bethesda, MD.

We have reported that the binding of myosin subfragment-1 to regulated actin, was not greatly inhibited in the absence of Ca^{2+} although the ATPase rate was 95% inhibited (Chalovich et al. (1981) JBC 256, 575 and (1982) JBC 257, 2432). In contrast, a recent report suggests that the binding of heavy meromyosin (HMM) is substantially weakened at low Ca^{2+} (Wagner and Stone (1982) Biochemistry 22, 1334). This conclusion was largely based on an observed biphasic binding in the absence of Ca^{2+} , with the HMM fraction containing intact light chain 2 binding very weakly. Using our Airfuge method we have now studied the binding of HMM with 90% intact light chain 2, and showing 94% Ca^{2+} sensitivity. At $\mu=19$ mM, the binding constant in the presence of Ca^{2+} is only about 3 times larger than in the absence of Ca^{2+} ($2.4 \times 10^4 \text{ M}^{-1}$ compared to $8.8 \times 10^3 \text{ M}^{-1}$). We have consistently measured more than 50% binding with no evidence of multiple populations. As a further test for heterogeneity we did a double binding experiment; after binding 50% of the HMM, in the absence of Ca^{2+} , the unbound HMM was again mixed with regulated actin. Here again 50% of the HMM bound to actin. Therefore, HMM binds as a single population. Our results are consistent with the demonstration of Brenner et al. (Proc. Natl. Acad. Sci. USA 1983, 79, p. 7288) that at low ionic strength a substantial number of cross-bridges are attached in relaxed skinned rabbit psoas fibers. We conclude that regulation of acto-HMM ATPase activity by troponin-tropomyosin is similar to regulation of the acto-S-1 ATPase activity; the troponin-tropomyosin inhibits a kinetic step in the ATPase cycle rather than the binding of HMM to actin.

T-Pos121 IONIC STRENGTH EFFECTS ON THE INTERACTION BETWEEN ACTIN AND THE MYOSIN SUBFRAGMENT-1 ISOZYMES A1 AND A2. Chalovich, J.M., Stein, L.A., Greene, L.E., and Eisenberg, E. NHLBI, NIH, Bethesda, MD and Dept. Cardiology, State Univ. of New York at Stonybrook.

Myosin subfragment-1 can be fractionated into two isozyms, (A1)S-1 containing alkali light chain 1 and (A2)S-1 containing alkali light chain 2. The predominant difference in the behavior of the two isozyms of S-1 is that, at low ionic strength, the actin concentration required for half maximal activity is considerably less for (A1)S-1 than for (A2)S-1, that is, K_{ATPase} for (A1)S-1 is greater than K_{ATPase} for (A2)S-1 (Weeds and Taylor (1975) Nature 257, 54). This difference disappears at high ionic strength (Wagner et al. (1979) Eur. J. Biochem. 99, 385). In the present study we investigated whether the difference in the K_{ATPase} values of (A1)S-1 and (A2)S-1 is due to a difference in the actual binding of these S-1 isozyms to actin. Binding was measured in the presence of ATP, AMP-P[NH]P and in the absence of nucleotide at varied ionic strength. We found that at low ionic strength where K_{ATPase} is several times stronger for (A1)S-1 than for (A2)S-1, the binding of (A1)S-1 to actin is correspondingly stronger than that of (A2)S-1 irrespective of the nucleotide present. Furthermore, as the ionic strength is increased, just as the ratio of K_{ATPase} (A1)/ K_{ATPase} (A2) decreases toward 1 so too does the ratio of K_{BINDING} (A1)/ K_{BINDING} (A2). We conclude first, that the difference in K_{ATPase} between (A1)S-1 and (A2)S-1 is due to a difference in the binding affinity of these isozyms to actin, a difference which is maintained even in the absence of nucleotide. Second, we conclude that, although it is weak, the binding of S-1 to actin observed in the presence of ATP is a specific reaction because it reflects the difference in the affinity of (A1)S-1 and (A2)S-1 to actin.

T-Pos122 THE BINDING OF DIFFERENT pPDM-S-1-NUCLEOTIDE COMPLEXES TO ACTIN. Lois E. Greene, Joseph M. Chalovich, and Evan Eisenberg, NHLBI, NIH, Bethesda, MD.

The interaction of actin with myosin subfragment-one (S-1), modified by having its two reactive cysteines cross-linked by N-N'-p-phenylenedimaleimide (pPDM), was examined in the presence of different nucleotides. pPDM-S-1 initially has ~70% of its active sites occupied by ADP which was trapped at the active site during the cross-linking procedure (Wells and Yount, PNAS 76, 4966). We now find that in the presence of actin, nucleotide is rapidly exchanged at the active site of pPDM-S-1. Therefore, we were able to study the binding of different pPDM-S-1-nucleotide complexes to actin. In the presence of ATP, the binding of pPDM-S-1 to actin is virtually identical to that of unmodified S-1 in the presence of ATP. Specifically, at $\mu = 18$ mM, 25°, pPDM-S-1 + ATP binds to unregulated actin with the same affinity as does S-1+ATP and this binding is unaffected by troponin-tropomyosin. Similar results were obtained for the binding of pPDM-S-1 to actin in the presence of PPI. On the other hand, in the presence of ADP or absence of nucleotide (nucleotide removed from acto-pPDM-S-1 by Dowex treatment), there is a small, but significant difference between the binding of pPDM-S-1 to actin and the binding of S-1+ATP (see Chalovich et al. PNAS 80, 4909), pPDM-S-1 alone and pPDM-S-1-ADP both bind about 2-3 fold stronger to unregulated actin than does S-1+ATP. In addition, troponin-tropomyosin confers slight cooperative strengthening (2-3 fold) on the binding of pPDM-S-1 and pPDM-S-1-ADP to actin. This binding to regulated actin is only slightly affected by Ca^{2+} . Therefore, these results suggest that the nucleotide bound to pPDM-S-1 causes conformational changes in the protein which in turn subtly alters its interaction with actin.

T-Pos123 STOICHIOMETRY OF RECYCLED ACTO-S-1 CROSS-LINKED COMPLEX. Lois E. Greene, NHLBI, NIH, MD
 Mornet et al. (Nature 292, 301) have shown that myosin subfragment-one (S-1) which has been cross-linked to actin with the zero-length crosslinker, EDC, hydrolyzes ATP with a rate similar to the V_{max} of the actin-activated S-1 ATPase activity. The stoichiometry of the cross-linking appeared to show that one S-1 is cross-linked to two actin-monomers. However, Sutoh (Biochemistry 22, 1579) reported that S-1 is cross-linked to only one actin monomer. In both of these measurements, the stoichiometry was determined by separating the cross-linked complex from free actin on SDS-PAGE and then determining the concentration of actin and S-1 in the complex. In this study, a new approach was used to determine the stoichiometry of actin to S-1 in the cross-linked complex. The cross-linked acto-S-1 preparation, which was composed of [^{14}C]-iodoacetamide modified S-1 and [3H]NEM-actin, was passed through several cycles of actin depolymerization and polymerization. This had no effect on the ATPase activity of the cross-linked S-1, but it did preferentially remove actin which was not cross-linked to S-1. This increased the ratio of S-1 to actin from 1:5 to 1:2 in the recycled cross-linked preparation. The stoichiometry was now determined by measuring the concentration of free actin in the 42K band on SDS PAGE. This method predicts very different concentrations of free actin in the recycled preparation depending on whether 1 S-1 is cross-linked to 1 or 2 actins. If the stoichiometry of cross-linking were one S-1 per two F-actin monomers, the recycled acto-S-1 cross-linked preparation should show virtually no actin in the 42K band. However, SDS-PAGE of this recycled complex showed that the free actin concentration was equal to the concentration of cross-linked acto-S-1 complex. This establishes that the stoichiometry of the cross-linking is one S-1 per one F-actin monomer, in agreement with the results of Sutoh.

T-Pos124 REINVESTIGATION OF ACTIN CROSSLINKING TO S-1. T. Chen*, D. Applegate, and E. Reisler, Department of Chemistry and Biochemistry and the Molecular Biology Institute, UCLA, Los Angeles, CA 90024.

Recent crosslinking studies on acto-S-1 have shown that actin binds to the 50K and 20K fragments of tryptic S-1 [Mornet et al., Nature 292, 301 (1981); Sutoh, K., Biochem. 22, 1579 (1983)]. Yet it remains unclear whether this binding occurs at either site (Sutoh) or simultaneously at both of them (Mornet). We have reexamined the crosslinking of actin to S-1 by using two methods to quantitate the amount of 50K and 20K fragments crosslinked to actin. In the first method, we employed elastase to cleave the 50K/20K junction in crosslinked acto-S-1 thus allowing direct measurement of the crosslinked 20K (20K-actin) and 50K (50K-actin) and the free, uncross-linked 50K and 20K fragments. In the second method, we employed tryptic S-1 in the crosslinking experiments and measured the crosslinked versus uncrosslinked fragments on SDS gels. We found that both 50K and 20K were crosslinked to actin at pH 6; whereas at pH 7, the reaction proceeded preferentially at the 20K fragment. Although the particular reaction conditions affected the efficiency of 50K-actin crosslinking, in all cases tested the major product of the reaction was the 20K-actin species. These results may reflect the greater affinity of actin for the 20K than the 50K fragment of S-1. This research was supported by grants from MDA and USPHS (AM 22031) and a postdoctoral AHA fellowship.

T-Pos125 DETECTION OF SINGLE-HEADED BINDING OF HMM TO ACTIN. B.A. Manuck, J.C. Seidel, J. Gergely. Boston Biomedical Research Institute, Boston MA.

The mechanism of binding of HMM to actin in the presence of nucleotides (N) has been studied through titrations of acto-HMM (containing spin labelled HMM) with ADP or AMPPNP. The fraction of HMM heads bound to actin at each concentration of nucleotide was estimated by saturation-transfer EPR (ST-EPR) while the fraction of bound molecules was determined by sedimentation. The manner in which N_2 -HMM binds to actin varies with the nucleotide present. In the presence of ADP (at 0.2M KCl) the fraction (BDM) of bound molecules was larger than the fraction (BDHD) of bound heads, while with AMPPNP they were equal. Because ST-EPR is sensitive to the rate of motion of the HMM heads, there was a possibility that a head, although bound, might move rapidly enough to appear to be unattached to actin, resulting in BDHD < BDM. However, this is not very likely: use of the binding constants for the first and second heads of ADP_2 -HMM to actin (determined by the titration of actin with HMM in the presence of saturating ADP) in a computer fit of a one dimensional Ising model to the ADP titration of acto-HMM produces good agreement between the calculated curves and the data and accounts for the difference between BDM and BDHD by the binding of ADP_2 -HMM by only one of its heads. In the case of $AMPPNP_2$ -HMM, the binding of the first head of $AMPPNP_2$ -HMM is much weaker than that of ADP_2 -HMM; explaining why practically all of the bound $AMPPNP_2$ -HMM attach by two heads. Single headed binding is also not observed in the absence of nucleotide suggesting that ADP affects the HMM structure thereby favoring its binding by one rather than two heads. The experiments suggest that the unbound head in a single-headedly bound HMM is capable of independent motion.

T-Pos126 KINETIC MECHANISM OF ϵ -aza-ATP HYDROLYSIS BY MYOSIN-S1 AND MYOFIBRILS. Susan J. Smith and Howard D. White, Department of Biochemistry, University of Arizona, Tucson, AZ 85721

The fluorescence emission maximum of 1,N⁶-etheno-2-aza-ATP (ϵ -aza-ATP) has been shown by Miyata and Asai B.B.R.C. 105, 296-302 (1982) to be enhanced approximately three-fold and shifted from 485 nm to 453 nm during steady state hydrolysis by HMM. We have used the large change in fluorescence, which can be up to a twenty fold enhanced at 420 nm, to study the kinetic mechanism of ϵ -aza-ATP hydrolysis by myosin-S1 and relaxed myofibrils ($Ca < 10^{-7}M$). The k_{cat} of ATP hydrolysis by rabbit skeletal myosin-S1 determined by either the duration of the fluorescence enhancement or in single turnover experiments is $0.3 \pm .05 s^{-1}$. ϵ -aza-ATP binding to myosin-S1 measured by stopped flow fluorescence is accurately described by a single exponential if either $[myosin-S1] \gg [\epsilon\text{-aza-ATP}]$ or $[\epsilon\text{-aza-ATP}] \gg [myosin-S1]$ and has an apparent second order rate constant of $4\text{-}5 \times 10^5 M^{-1}s^{-1}$. The apparent second order rate constant and k_{cat} of ATP binding and hydrolysis are $2 \times 10^6 M^{-1}s^{-1}$ and $0.05 s^{-1}$, respectively. Thus the rate constant of ϵ -aza-ATP is reduced 4-5 fold with respect to ATP and the k_{cat} is increased six fold.

The time course of nucleotide fluorescence observed upon the addition of ϵ -aza-ATP to stirred suspensions of myofibrils is essentially the same as that with myosin-S1; a rapid increase to a steady state enhancement is followed by a decrease when the ϵ -aza-ATP is completely hydrolysed. Experimental conditions: 100 mM KCl, 20 mM bis-tris propane, 0.1 mM EGTA, 5 mM MgCl₂, pH 7, 20°C. This work has been supported by grants from the Muscular Dystrophy Association, HL 20984 and a British-American Heart Association Fellowship to SJS.

T-Pos127 ESTIMATION OF THE FRACTION OF ATTACHED CROSSBRIDGES FROM THE STEADY STATE V_{MAX} AND THE VELOCITY OF UNLOADED SHORTENING. R.F. Siemankowski. University Department of Biochemistry, Biosciences West Building, University of Arizona, Tucson, AZ 85721

The V_{max} observed for actomyosin-S1 ATPase should be a good estimate for the rate constant of the step(s), which limits the steady state rate of hydrolysis in muscle. k_{min} , the minimum value for the rate constant of the step, which limits the velocity of unloaded shortening, can be calculated from: $V_o S_L d^{-1}$, where V_o = velocity of unloaded shortening, S_L = length of the half sarcomere and d = maximum axial crossbridge translation. Since during the steady state, the flux of intermediates through each step in the reaction mechanism is the same, the ratio V_{max}/k_{min} should give a good estimate for the maximum fraction of crossbridges attached during an unloaded shortening. For chicken PLD, ALD, heart and gizzard, bovine ventricle, and rabbit psoas and soleus muscles, V_o varies from 0.8 to 16 ML/s (mean = 7.9, S.D. = 8.4) at 38°. However, V_{max}/k_{min} varies only slightly (mean = 0.09, S.D. = 0.03). Therefore, for muscles from homeothermic vertebrates, only ~ 10% of the total crossbridges can be attached during unloaded shortening. The fraction varies strongly with temperature for frog (poikilotherm) sartorius muscle, 0.1 at 20° and 0.02 at 0° [Homsher & Irving (1982) estimated < 3% at 0°, from the stoichiometry of ATP hydrolysis during shortening]. Furthermore, throughout the phylogenetic proliferation of muscle types, myosin isozymes have evolved such that the rate constant for the step, which limits the steady state rate of hydrolysis, is tightly kinetically coupled to the rate constant for the step, which limits V_o . (Supported by the Arizona Heart Association).

T-Pos128 PROXIMITY OF LC₃ THIOL TO THE REACTIVE LYSINE OF MYOSIN HEAVY CHAIN. Reiji Takashi, Peter Torgerson, Joseph Duke. UCSF, San Francisco, CA 94143.

Förster energy transfer techniques are being used to study the spatial relationship between two sites in myosin subfragment 1 (S-1), viz., the reactive lysyl residue (RLR) of S-1 heavy chain, and a single thiol residue of light chain 3 (LC₃). LC₃ labeled at its thiol with a donor, thiol-specific reagent, was incorporated into the chymotryptic S-1 by the exchange procedure of Wagner & Weeds [J. Mol. Biol. (1977) 109, 455]. The resulting S-1 was then selectively labeled at RLR with an acceptor, 2,4,6-trinitrobenzene sulfonate (TNP). Prior insertion of a donor on the LC₃ of S-1 slightly slowed the rate of trinitrophenylation on RLR. The emission of the donor on LC₃ was quenched, and its excited-state lifetime was reduced by TNP-RLR. In calculating distance (R) by Förster's equation ignorance of the orientation factor (κ^2) is usually countered by assuming sufficient dynamic randomization of dipoles to justify setting $\kappa^2 = 2/3$, but rarely is the assumption examined. Here we examined it by, (1) using 3 different fluorescent probes (1,5AEDANS, its 1,8isomer, and 5-IAS) and finding approximately the same R and by, (2) performing time-resolved fluorescence anisotropy decay experiments. The latter, in the Dale-Eisinger analysis, allowed us to limit how the calculated R could be from the R based on $\kappa^2 = 2/3$. Those R's were 2.7, 2.9, and 3.1 nm for 5-IAS-TNP, 1,8AEDANS-TNP, and 1,5AEDANS-TNP, respectively. Supported by HL-16683 and MDA.

T-Pos129 EFFECT OF DIFFERENT ANIONS AND PH ON THE THERMAL STABILITY OF SKELETAL MYOSIN ROD. Walter F. Stafford, Dept of Muscle Research, Boston Biomedical Research Inst., Boston, MA 02114.

The helix-coil transition of myosin rod was monitored under various ionic conditions by following the circular dichroic ellipticity at 222nm as a function of temperature. In 0.6M NaCl, 5mM phosphate, 0.1mM EDTA, pH 7.3, rod exhibited a biphasic melting curve with transitions at 45° and 54° as seen previously by Burke et al. [Biochemistry 12, 701, (1973)]. However, in 0.6M CH₃COONa, 5mM phosphate, 0.1mM EDTA, pH 7.3, the transitions occurred at 52° and 57°, respectively. The two transition temperatures, T_{m1} and T_{m2}, depended linearly on salt concentration such that increasing [NaCl] destabilized the helix while increasing [CH₃COONa] caused the helix to become more stable. The values of T_{m1} and T_{m2}, obtained by extrapolating the data to zero salt concentration, were T_{m1}=48° and T_{m2}=55°, respectively, giving an indication of the stability of the helix in the absence of specific salt effects. Substitution of ammonium or potassium for sodium ion had no significant effect on T_m showing that cation type is not important. At pH 9.3 in 2 mM PP_i, the melting profile became very broad exhibiting at least two transitions at T_{m1}=35° and T_{m2}=49° while at pH 9.5 in 0.6M KCl, 10mM PP_i, two transitions were observed at 39° and 54°, respectively, indicating that high pH destabilizes the helix. In 0.6M KCl, 10mM PP_i or 5mM MgATP, pH 7.3, the transitions occurred at 44° and 54° indicating that neither PP_i nor ATP at these concentrations had a significant effect on the helix stability. It is thought that the intracellular chloride ion concentration is about 2-3 mM [Bolton and Vaughan-Jones, J. Physiol. 270, 801(1977)] and that predominant anions are derived from organic carboxylic acids. These results suggest that myosin rod may be more stable *in vivo* and, therefore, not as flexible under physiological conditions as past solution studies have suggested. (Supported by NIH grant HL-26229)

T-Pos130 PROTEOLYTIC DIGESTION STUDIES ON THE S-1/S-2 SWIVEL IN MYOSIN. L. MILLER*, AND E. REISLER, Department of Chemistry and Biochemistry and the Molecular Biology Institute, UCLA, Los Angeles, CA 90024. Introduced by J. Horwitz, J. Stein Eye Institute, UCLA.

The S-1/S-2 swivel in myosin provides a flexible link between the head and tail portions of the molecule. We have investigated the properties of this swivel by employing limited proteolysis methods. Our results indicate that the binding of F-actin to HMM inhibits the chymotryptic cleavage of the S-1/S-2 swivel. However, this effect is dependent on the presence of intact LC-2 light chain. Actin did not slow digestions carried out using HMM previously treated with proteases to nick the LC-2 chain to 17K or 14K fragments. A small effect was observed using HMM with LC-2 nicked to an 18K fragment. Reactions carried out in the presence of divalent metals confirm that HMM with LC-2 degraded to 17K retains metal sensitivity of digestion. Thus, the effects of actin and divalent cations on the swivel can be clearly separated. Digestions of the S-1/S-2 swivel in HMM containing intact or proteolytically degraded LC-2 show significant temperature sensitivity between 5°C and 35°C. This sensitivity is much greater than the temperature dependence of chymotryptic activity. Our results suggest that the binding of actin to HMM as well as changes in temperature induce structural transitions in the S-1/S-2 swivel. In addition, actin-induced changes in this region seem to require the presence of intact LC-2. Supported by grants from USPHS (AM 22031) and MDA.

T-Pos131 EVIDENCE FROM OXYGEN EXCHANGE STUDIES THAT THE TWO HEADS OF MYOSIN ARE FUNCTIONALLY DIFFERENT. Kamal K. Shukla, Harvey M. Levy, Fausto Ramirez, and James F. Marecek. State University of New York at Stony Brook, Stony Brook, New York 11794.

Recent studies of intermediate oxygen exchange indicate two normal pathways for the hydrolysis of MgATP by myosin in the presence of actin, but only one in the absence of actin. The pathways are revealed by analyzing the distributions of (¹⁸O)_{P_i} species from the hydrolysis of (γ-¹⁸O)MgATP. It now appears that the single pathway in the absence of actin represents the operation of only one head of myosin (Head 1); and the two pathways in the presence of actin represent the operation of Head 1 and Head 2. Without actin, Head 1 reversibly cleaves bound MgATP and thereby supports oxygen exchange whereas Head 2 is enzymatically "silent". With actin, both heads support some oxygen exchange and release product P_i to the medium at the same high rate. We have examined the effects of certain changes in the substrate (Mn for Mg; dATP or ITP for ATP) on oxygen exchange. In general d-ATP was the same as ATP. However, Mn or ITP caused a ten-fold inhibition in the rate of oxygen exchange by Head 1 without actin, and by both heads with actin. Either Mn or ITP also caused a partial disinhibition of the overall hydrolysis by Head 1 without actin; but a double substitution (i.e. Mn ITP for MgATP) was required to disinhibit Head 2 without actin. Apparently, MgATP is positioned differently on the two heads when they are free of actin; this holds Head 2 in the M*ATP state (unable to exchange oxygen), but allows Head 1 to move reversibly to the M**ADP.P_i state (and support oxygen exchange). Actin, then, disinhibits both heads allowing overall rapid hydrolysis and release of product. The different state of the heads while free of actin could serve to make Head 1 react first with the actin filament, with Head 2 always following; thus they would exert their pull in a fixed sequence.

T-Pos132 BINDING OF ATP ANALOGS TO CROSS-BRIDGES IN STRIATED MUSCLE MYOFIBRILS PARTITIONS THEM INTO TWO POPULATIONS. Julian Borejdo and Olga Assulin, CVRI, University of California, San Francisco and Polymer Research Department, Weizmann Institute of Science, Rehovot, 76100, Israel. Tryptic digestion of myofibrils was used to assess the interaction of cross-bridges with thin filaments in the presence of ATP and its analogs. The relative amounts of 200 KD fragment produced by trypsin from myosin heavy chain when the cross-bridge was attached to actin, and of 160 KD fragment produced when the cross-bridge was detached from actin, served as a measure of cross-bridge-actin interaction. In the absence of added analogs only the 200 KD fragment was produced confirming the view that in rigor a great majority of cross-bridges were strongly attached to actin; in the presence of MgPP_i at 0°C only the 160 KD fragment was finally produced suggesting that eventually all cross-bridges detached from actin. In the presence of MgPP_i at 25°C, MgAMPPNP and MgADP at either 25°C or 0°C, both 200 and 160 KD fragments were present in unchanging amounts after several minutes of proteolysis suggesting that the two populations of cross-bridges (attached and detached) co-existed at the same time within the myofibril. In the presence of MgATP no attached cross-bridges at all were detected. During digestions of an isometrically held muscle, on the other hand, a significant fraction of cross-bridges interacted with actin. It is concluded that the cross-bridge population in muscle does not respond homogeneously to binding of ATP analogs, i.e. that the addition of ATP analogs to muscle does not affect simply the equilibrium of binding of myosin heads to actin but that it causes a rapid dissociation of one cross-bridge population without a significant effect on binding to actin on the remaining cross-bridge population.

T-Pos133 THE FREQUENCY DEPENDENCE OF SKELETAL MUSCLE MYOSIN P-LIGHT CHAIN PHOSPHORYLATION. R.L. Moore and J.T. Stull. Dept. Pharmacol., Univ. TX Hlth. Sci. Ctr., Dallas, Texas 75235. The kinetics of contraction-induced myosin P-light chain phosphorylation in rat hindlimb muscle were examined. Stimulation of the rat gastrocnemius muscle in situ produced a frequency-dependent increase in the 18.5 kDa myosin P-light chain phosphate content. Stimulation at 100 Hz resulted in P-light chain phosphorylation in the fast, white portion of the muscle at a rate of 57 μmol phosphate incorporated/l intracellular water $\cdot\text{sec}$. This rate was ~ 2 , 6 and 27 times greater than the initial rates of P-light chain phosphorylation observed when the muscle was stimulated at 10, 5 and 0.5 Hz, respectively. In all cases, isometric twitch tension potentiation increased and decreased concomitantly with the increase and decrease in P-light chain phosphate content. In response to constant muscle stimulation at 5, 10 and 100 Hz, myosin P-light chain phosphate content increased rapidly to maximal values of between 0.53 to 0.65 mol P/mol P-light chain. However, two 2-second tetanic contractions initiated 20 seconds apart resulted in a P-light chain phosphate content of 0.87 mol P/mol P-light chain. These results indicate that a major portion of the P-light chain is readily phosphorylatable. The plateau in P-light chain phosphate content observed during constant stimulation may have been associated with fatigue processes. The kinetic properties of myosin light chain kinase activation/inactivation and myosin P-light chain phosphorylation/dephosphorylation were used to construct a simple mathematical model to describe the contraction frequency dependence of myosin P-light chain phosphorylation in fast-twitch, white skeletal muscle. Consistent with previous reports, there was a positive correlation between the phosphate content of myosin P-light chain of fast skeletal muscle and isometric twitch potentiation. (Supported by GM09275 and HL06296)

T-Pos134 MYOSIN LIGHT CHAIN KINASE ACTIVITY IN SKELETAL MUSCLES FROM THE C57BL/6J dy^{2J}/dy^{2J} DYSTROPHIC MOUSE. L.G. JASCH, Dept. Anat., Un. British Columbia, Vancouver, Canada V6T 1W5 and J.T. Stull, Dept. Pharmacol., Un. Tx. Hlth. Sci. Ctr., Dallas, Tx. 75235. The extent of phosphorylation of myosin light chain LC2f isolated from fast-twitch extensor digitorum longus (EDL) and extensor carpi radialis longus (ECRL) muscles was less in 32-week-old dystrophic mice than in normal mice. Phosphorylation of myosin by Ca²⁺-calmodulin-dependent myosin light chain kinase (MLCK) and posttetanic potentiation of isometric twitch tension occurs in fast-twitch but not slow-twitch muscles. It has been reported that the magnitude of posttetanic potentiation of isometric twitch tension is attenuated in fast-twitch muscles from dystrophic mice which could be explained in part by decreased MLCK activity. Therefore, MLCK activity ($U = \text{nmol } 32\text{P incorporated into light chain/min/mg protein}$) was measured in extracts of normal and dystrophic skeletal muscles from 32-week-old mice. There were no significant differences in MLCK activities in slow-twitch soleus muscles from normal or dystrophic mice (5.2 ± 0.3 and 5.9 ± 0.8). The values for normal and dystrophic fast-twitch muscles, respectively, were 20.2 ± 2.2 and 6.9 ± 1.2 for gastrocnemius muscles, 19.9 ± 1.3 and 5.2 ± 0.6 for EDL, and 13.3 ± 1.4 and 5.6 ± 0.5 for ECRL. Thus, there was less MLCK activity in all fast-twitch dystrophic muscles, and these activities were similar to MLCK activity in soleus muscle. There were no differences in calmodulin content in the normal and dystrophic muscles. These results suggest that myosin light chain phosphorylation in dystrophic muscles could be attenuated due to decreased MLCK activity. Loss of MLCK activity may reflect loss of differentiable fast-twitch, glycolytic fibers from dystrophic fast-twitch muscles. (Supported by the Muscular Dystrophy Associations of Canada and USA)

T-Pos135 PROPERTIES OF CHICKEN SKELETAL MUSCLE MYOSIN LIGHT CHAIN KINASE. M.H. Nunnally, S.B. Rybicki and J.T. Stull. Dept. Pharmacol., Univ. TX Hlth. Sci. Ctr., Dallas, TX 75235

Myosin light chain kinase (MLCK) has been purified from chicken skeletal muscle with a procedure used for purification of rabbit skeletal muscle MLCK. The molecular weight of the purified chicken skeletal muscle MLCK was 150,000 as determined by SDS-polyacrylamide gel electrophoresis, whereas the values obtained for purified rabbit skeletal muscle and chicken gizzard MLCK were 87,000 and 130,000 respectively. Nondenaturing polyacrylamide gels demonstrated that chicken skeletal muscle MLCK activity was coincident with the protein band. The two MLCKs have similar K_m and V_{max} (Unit = $\mu\text{mol } ^{32}\text{P}$ incorporated/min/mg protein) values with either isolated rabbit or chicken skeletal muscle myosin P-light chains. For the rabbit skeletal muscle MLCK, K_m and V_{max} (\pm S.E.) values were $8.5 \pm 1.1 \mu\text{M}$, $56.0 \pm 6.0 \text{ U}$ and $8.3 \pm 1.5 \mu\text{M}$, $52.6 \pm 13.3 \text{ U}$ with rabbit and chicken P-light chains, respectively. Comparable data for the chicken skeletal muscle MLCK were $9.5 \pm 0.1 \mu\text{M}$, $29.0 \pm 4.7 \text{ U}$ and $7.7 \pm 1.3 \mu\text{M}$, $42.2 \pm 15.0 \text{ U}$ with rabbit and chicken skeletal muscle myosin P-light chains, respectively. Limited digestion by *S. aureus* V8 protease or chemical cleavage by cyanogen bromide of the chicken and rabbit skeletal muscle MLCKs followed by SDS-polyacrylamide gel electrophoresis, resulted in the generation of 8-10 distinct, nonoverlapping peptides. Affinity-purified antibodies to rabbit skeletal muscle MLCK inhibited chicken skeletal muscle MLCK activity, but the titer of crossreacting antibodies was at least 10-fold less than the total antibody concentration. These data suggest that the catalytic properties of chicken skeletal muscle MLCK are similar to rabbit skeletal muscle MLCK, but that there are significant differences in the primary structure of the two kinases. (Supported by HL23990, HL06335, and the Muscular Dystrophy Association)

T-Pos136 CALCIUM- AND CYCLIC AMP-DEPENDENT PHOSPHORYLATION OF SKELETAL MYOFIBRILLAR PROTEINS. Megan S. Lim and Michael P. Walsh, Department of Medical Biochemistry, University of Calgary, Alberta, Canada T2N 1N4.

Calcium, calmodulin-dependent phosphorylation of smooth muscle myosin plays an important role in regulating actin-myosin interactions in this tissue. Furthermore, cAMP-dependent phosphorylation of smooth muscle myosin light chain kinase (MLCK) has been implicated in relaxation of smooth muscle induced by β -adrenergic agents (Adelstein et al (1978) *J. Biol. Chem.* 253, 8347). This information, together with the earlier identification of Ca^{2+} -dependent MLCK in skeletal muscle (Pires et al (1974) *FEBS Letters* 41, 292), and a form of skeletal MLCK which is phosphorylated by cAMP-dependent protein kinase (Edelman and Krebs (1982) *FEBS Letters* 138, 293), raises the possibility that similar mechanisms exist to regulate the interaction between skeletal muscle actin and myosin. To gain more insight into the roles of Ca^{2+} and cAMP in regulating skeletal muscle function, we have studied protein phosphorylation in myofibrils prepared from fresh canine quadriceps femoris. These myofibrils bound ^{125}I -calmodulin in a Ca^{2+} -dependent manner; this binding was inhibited by unlabeled calmodulin. Incubation of myofibrils with $[\gamma\text{-}^{32}\text{P}]\text{ATP}$ and Mg^{2+} indicated the presence of endogenous kinase activity which phosphorylated the regulatory light chain (LC2) of myosin; this phosphorylation was enhanced by Ca^{2+} , calmodulin and phosphatase inhibitor. Treatment of the myofibrils with the pure catalytic subunit of cAMP-dependent protein kinase in the presence of $[\gamma\text{-}^{32}\text{P}]\text{ATP}$ and Mg^{2+} resulted in phosphorylation of 2 major proteins: a 143,000-dalton protein (which is either C protein or a protein that co-electrophoreses with C protein) and an unidentified protein of $M_r = 36,000$.

T-Pos137 DETERMINATION OF PHOSPHORYLATION AND THIOPHOSPHORYLATION LEVELS IN RABBIT SKINNED MUSCLE FIBERS USING HIGH VOLTAGE VERTICAL SLAB ISOELECTRIC FOCUSING (HVVS-IEF). Gary G. Giulian, Richard L. Moss, and Marion L. Greaser, Department of Physiology and the Muscle Biology Laboratory, University of Wisconsin, Madison, WI 53706.

The physiological role of phosphorylation of myosin LC2 in muscle contraction has been studied in skinned rabbit muscle fiber preparations. In order to determine the levels of phosphorylation in small numbers of fibers, high voltage vertical slab isoelectric focusing (HVVS-IEF) was performed in a one-dimensional system to resolve LC2 and LC2p. Fibers were dissolved in 8 M urea using sonic disruption. After solubilization, the muscle preparations were loaded into a vertical slab gel 0.35 mm thick. The gel contained 8 M urea, 2.0% (v/v) Triton X-100, 10% (v/v) glycerol, and 3.3% (w/v) total ampholytes. The gel was run in approximately 4 hours at 24°C with N_2 purge, for 10,000 volt-hours at a maximum of 3,000 volts. The gel was subsequently fixed and stained with Coomassie R-250, and the stained bands were quantified with a laser scanner and digital computer integrator. Multiple samples on the same gel (up to 15) allow for direct comparison of their isoelectric points. The gel system will resolve actin, LC1, LC2, TM, LC2p, LC3, and TnC on a single slab. When $\text{ATP}_{\gamma}\text{S}$ is used as a substrate along with myosin light chain kinase, and calmodulin at $\text{pCa}=4.5$, a distinct thiophosphorylated band is resolved from LC2, TM, and LC2p. The high resolution of the HVVS-IEF method eliminates the need for prior myosin purification or a second dimension gel. Thus, one-dimensional HVVS-IEF is a direct and rapid means of determining the degree of myosin light chain phosphorylation and thiophosphorylation in muscle fiber preparations. (Supported by grants from NIH and the American Heart Association)

T-Pos138 "TRAPPED" ADP INDUCES AN ATP-LIKE UV DIFFERENCE SPECTRUM IN MYOSIN SUBFRAGMENT-1, Kathy Cunningham and John W. Shriver, (Intr. by Paul Hargrave), Dept. of Medical Biochemistry, and Dept. of Chem. & Biochem., Southern Illinois University, Carbondale, IL 62901.

Myosin heads exist in two discrete states under a wide variety of conditions. The relative population of the two states is determined by such factors as the nucleotide in the active site and temperature. One state, the "R" state, is preferentially populated by ATP and AMPPNP (at 25°C). The other state, the "T" state, is populated by ADP (at 25°C) and AMPPNP (at 0°C). The ability of AMPPNP to populate either state has led us to expect that ADP may populate the "R" state under certain conditions.

We have obtained the UV difference spectrum induced by trapping $Mg \cdot ADP$ on myosin S-1 with the bifunctional sulfhydryl reagent p-phenylenedi-maleimide (pPDM). $Mg \cdot ADP$ (50 μM) and pPDM (18 μM) were placed in one half of a 1.0 cm tandem cell and subfragment-1 (19 μM) was placed in the other. The buffer throughout was 0.1 M KCl, 50 mM TRIS, pH 7.9, 1 mM $MgCl_2$. After equilibration a baseline was programmed on a Cary 210 interfaced to an Apple II+ microcomputer. The difference spectrum was recorded from 250 nm to 400 nm within ten minutes of mixing by inversion of the cell at 5°C. The spectrum was essentially identical to that obtained for ATP (at 25°C) or AMPPNP (at 25°C). Thus trapping $Mg \cdot ADP$ forces the myosin S-1 into an ATP-like structure, as indicated by the contribution of the tryptophans of S-1 to the UV spectrum. This may explain the dramatic increase in nucleotide affinity resulting from crosslinking. Preliminary results indicate that crosslinking in the total absence of nucleotide results in the ATP-like difference spectrum. (Supported by the Muscular Dystrophy Association).

T-Pos139 TRYPTOPHAN EMISSION FROM MYOSIN SUBFRAGMENT ONE: ACRYLAMIDE AND NUCLEOTIDE EFFECTS MONITORED BY DECAY-ASSOCIATED SPECTRA. Peter M. Torgerson. Cardiovascular Res. Inst., Univ. of Calif., San Francisco CA 94143

The intrinsic fluorescence due to the tryptophan residues of myosin chymotryptic subfragment one can be divided into three classes, with lifetimes of 8.8, 4.6, and 0.72 ns. The percentage contribution of each component to the total emission is 46%, 45%, and 9%, respectively. Low concentrations of acrylamide quench the long component with a Stern-Volmer constant of $14.9 \pm 2.9 M^{-1}$, while the intermediate and short components are unaffected. Addition of $MgATP$ results in an increase in the total intensity by 17%. The bulk of this increase is in the intermediate component, which goes up by 29%, while the long-lived component increases by 9% and the short component is unchanged. In contrast to the acrylamide quenching case, these intensity changes are not accompanied by corresponding lifetime changes. Quenching by acrylamide in the presence of $MgATP$ again quenches only the long lifetime component with a quenching constant not significantly different than previously. The above results indicate that the tryptophan residues perturbed by the binding of nucleotide are different from those accessible to acrylamide. (Supported by a Muscular Dystrophy Association Postdoctoral Fellowship and HL-16683.)

T-Pos140 STRUCTURAL COMPARISON OF PAPILLARY AND VENTRICULAR MYOSIN ISOZYMES. Pagani E.D., Faris R., and Julian F.J. Dept. Anes. Res. Labs., Brigham and Women's Hosp., Boston, MA

In many studies, data obtained in experiments that measure force development and shortening velocity of papillary muscles (paps) are used to make inferences about the contractile properties of the cardiac ventricle. This practice would appear to be acceptable if the molecular structure of the paps and the cardiac ventricle was the same. In the studies described here we tested if rabbit cardiac myosins (RV_1 , RV_2 , RV_3) of paps are structurally similar to myosins of the ventricular free wall (fw) and septum (s). Myosin isoforms of paps and the corresponding fw and s were examined under native and denatured conditions by polyacrylamide gel electrophoresis. In addition, myosin isoforms purified on pyrophosphate gels were evaluated by polypeptide mapping of the proteolytic fragments of the heavy chains. On pyrophosphate gels, under native conditions, the RV_1 , RV_2 , and RV_3 myosin isoforms of paps had the same mobility as the myosin isoforms of the fw and s. The RV_1 and RV_3 myosins of paps, fw and s were sliced from pyrophosphate gels, layered on 14% SDS gels, and electrophoresed to separate the myosin light chains (LC_1 and LC_2). After silver staining, SDS gels of all three preparations showed that the molecular weight of RV_1 and RV_3 myosin LC_1 was 27,000 daltons and that the molecular weight of LC_2 was 21,500 daltons. Moreover, examination of the polypeptide maps of the RV_1 and RV_3 heavy chains of paps, fw and s indicated that there were no differences among the RV_1 myosins or among the RV_3 myosins. However, as previously reported by Chizzonite et al. (J. Biol. Chem., 257, 1982) there were differences between the polypeptide maps of the RV_1 and RV_3 heavy chains. Our results indicate that the myosin isoforms of paps, fw and s are structurally similar. Supported by NIH grants HL30133 (FJJ) and HL06563 (EDP.)

T-Pos141 HIGH PERFORMANCE LIQUID CHROMATOGRAPHIC PURIFICATION OF BOVINE CARDIAC AND RABBIT SKELETAL TROPONIN SUBUNITS. P.J. Cachia, W.D. McCubbin, C.M. Kay and R.S. Hodges. Department of Biochemistry and Medical Research Council Group in Protein Structure and Function, University of Alberta, Edmonton, Alberta, T6G 2H7 Canada.

Classical methods for the purification of native troponin and its subunits employ both ion-exchange and gel exclusion chromatography. These purification methods are successful in providing pure forms of the native troponin complex as well as the subunits (TnC, TnI, TnT) from both the rabbit skeletal and bovine cardiac systems. There is a disadvantage, however, in that these methods of purification are time consuming and result in the dispersion of the desired product(s) in large volumes of column effluent. As well, many of the usual methods for purification do not provide sufficient resolution to effect the identification of possible heterogeneity within any one of the subunits. Recently, Gusev and coworkers have isolated isoforms of bovine cardiac troponin T which differ in their M_r values, amino acid content, degree of phosphorylation, and aggregation.

Our laboratory has employed high performance liquid chromatographic (HPLC) techniques to effect the separation of both the rabbit skeletal and bovine cardiac troponin complexes. Using both weak cation and strong anion exchange columns in 8 M urea we have successfully separated both these systems into their pure subunits. Furthermore, these ion exchange columns have demonstrated their ability to resolve the I and T components of both systems into multiple peaks. We present results which show that the speed and resolving power of HPLC makes this technique an important tool for the fast, efficient purification of troponin subunits as well as for the further investigation of heterogeneity within these subunits. (Supported by MRC and AHFMR)

T-Pos142 HYBRIDIZATION OF FAST SKELETAL AND CARDIAC MUSCLE MYOSINS - LIGHT CHAIN EXCHANGE. S. P. Scordilis and M. H. Cole, Dept. Biol. Sci., Smith College, Northampton, MA 01063.

A protocol has been devised which allows for the hybridization of any myosin light chain with another isoform of the heavy chain. The method involves the incubation of column purified myosin (Scordilis and Adelstein, J. Biol. Chem., 253: 9041-9048, 1978) with a 7-10 fold molar excess of purified homologous light chains in a solution of 45% deionized glycerol, 540 mM KCl, 360 mM LiCl, 20 mM EDTA, 10 mM MgATP, 5.4 mM Tris-HCl (pH 7.0) and 0.07 mM dithiothreitol (DTT). This mixture was gently stirred for 3 hrs at 25-30°C. The exchange reaction was terminated by dilution with 9 volumes of 10 mM Tris-HCl (pH 7.4) and 0.5 mM DTT. The insoluble hybridized myosin was pelleted at 45,000 x G for 20 min. The pellet was resuspended in a high ionic strength buffer and chromatographed on Sepharose CL-4B to remove any contaminating light chains. SDS polyacrylamide gel electrophoresis demonstrated that between 51% to 75% of the light chains were exchanged in rabbit fast skeletal muscle myosin with cardiac light chains or in cardiac myosin with fast skeletal light chains. Neither the high ionic strength ATPase values in the presence of EDTA or Ca^{2+} were changed by the exchange in either hybrid nor were the actin-activated low ionic strength V_{max} or K_{app} (actin) altered. In short, exchange of the cardiac (slow) light chains into the fast heavy chain or exchange of the skeletal (fast) light chains into the slow heavy chain did not change the physiologically relevant myosin ATPase activity nor the characteristic high salt values.

This work was supported by grants from the Muscular Dystrophy Association of America and the Blakeslee Fund for Genetics Research at Smith College to SPS.

T-Pos143 CARDIAC MYOSIN SUBFRAGMENT 1. A KINETICALLY HOMOGENEOUS FORM. S. J. Smith and M. A. Cusanovich, Dept. of Biochemistry, University of Arizona, Tucson, AZ 85721.

The kinetics of ATP binding and hydrolysis by bovine cardiac myosin subfragment 1 (S1) have been reinvestigated using protein prepared by a different procedure. More than 90% of the protein binds ATP with an apparent second-order rate constant of $8.1 \times 10^5 \text{ M}^{-1} \text{ s}^{-1}$ (100 mM KCl, 10 mM MgCl_2 , 50 mM bis-tris propane, 20°C). The maximum rate of the fluorescence transient at saturating concentrations of ATP was 138 s^{-1} . Some 10% of the protein binds ATP more slowly with a rate constant of $\sim 1 \text{ s}^{-1}$ which is independent of the ATP concentration. This is in contrast to previous studies where protein and nucleotide dependent S1 aggregation was observed (J. Biol. Chem. 258, 977-983, 1983). Moreover, the observed rate constants are independent of S1 concentration under pseudo first-order conditions for ATP with respect to protein. In addition, the fraction of protein which hydrolyses ATP fast is not a function of the nucleotide or protein concentration and is independent of temperature and ionic strength within the range studied ($I=0.1-0.2 \text{ M}$, 15-20°C, pH 7.0). Cardiac S1 can be prepared, which is, for the purpose of kinetic studies, homogeneous and is thus amenable to detailed kinetic analysis. Supported by NIH Grant HL28906.

T-Pos144 ESSENTIAL LIGHT CHAIN EXCHANGE IN SCALLOP MYOSIN. G. Ashiba & A. G. Szent-Györgyi, Department of Biology, Brandeis University, Waltham, Massachusetts 02254.

The essential light chains (SH-LC) of scallop myosin exchange readily with SH-LCs provided the regulatory light chains of the myosin have been previously removed by EDTA treatment at 23°. Exchange is performed by incubating myosin with excess SH-LCs alkylated with [¹⁴C] labeled iodoacetic acid, unbound light chain is removed from myosin by repeated cycles of reprecipitation. In 0.6M NaCl, pH 7.5, 60-70% of the SH-LCs of desensitized myosin is replaced after 1 hr incubation at 4° with an 8-18 molar excess of [¹⁴C] SH-LC. At low ionic strength, equilibration of the SH-LCs is slow and limited (<15% in 24 hrs at 4° in 40mM NaCl). SH-LC exchange does not require ATP or Mg²⁺. Myosin containing alkylated SH-LC recombines with regulatory light chains and fully regains its calcium sensitivity. The recombined myosin contains a 1:1 molar ratio of regulatory and essential light chains with actin activated Mg²⁺ATPase activities like those of untreated normal myosin preparations. Equilibration of SH-LCs in intact myosin requires ATP (cf. Sivaramakrishnan & Burke, J. Biol. Chem. 256: 2607, 1981), probably as a result of weakening regulatory light chain attachment to myosin. The results are consistent with the findings of Wagner & Stone (J. Biol. Chem. 258: 8876, 1983) which suggest that in rabbit myosin, the DTNB light chains inhibit alkali light chain exchange. (Supported by NIH AM-15963 and MDA grants.)

T-Pos145 PROXIMITY OF THE REGULATORY LIGHT CHAIN IN SCALLOP MYOSIN. P.M.D. Hardwicke and A.G. Szent-Györgyi, Department of Biology, Brandeis University, Waltham, Massachusetts 02254.

We have shown previously using heterobifunctional photo-reagents that part of the N-terminal region of the regulatory light chain (R-LC) lies within 9Å of the essential light chain (SH-LC) in media physiologically producing rigor but is further away under resting conditions; while the C-terminal part of the R-LC is close to both the SH-LC and the heavy chain (HC) in both rigor and rest. Hybrid scallop myofibrils containing equal amounts of native scallop R-LC and foreign R-LC's labelled at different positions with heterobifunctional photo-reagents specific for thiol groups have now been used to determine the proximity of the R-LC's on the two heads of a myosin molecule. Rabbit anti-scallop R-LC IgG, anti-scallop SH-LC IgG, anti-mercenaria R-LC IgG and anti-chicken DTNB-LC IgG were used to detect and identify products cross-linked by photolysis. When the cross-linker was in the N-terminal region of the R-LC, the two R-LC's were cross-linked both under resting and rigor conditions and under rigor condition the R-LC was also cross-linked to the SH-LC. When the cross-linker was in the C-terminal region, no cross-linking of the R-LC's to each other was observed, although R-LC cross-linked to both the SH-LC and the HC in both rigor and rest. If scallop myofibrils hybridized with chicken DTNB-LC, labelled in the C-terminal region with p-azidophenacylbromide, were photolyzed then subsequently digested with papain, the chicken R-LC was cross-linked to the S-1 fragment but not to the rod portion of the myosin. These results suggest that the N-terminus of the R-LC points towards the S1-S2 hinge region. (Supported by NIH AM-15963 and MDA grants.)

T-Pos146 PARAMYOSIN KINASE: A CA⁺⁺ AND cAMP INDEPENDENT MOLLUSCAN PROTEIN KINASE
L.W. Radlick and W.H. Johnson, Dept. of Biology, Rensselaer Polytechnic Institute, Troy, N.Y. 12181 and Dept. of Nutrition and Food Science, University of Arizona, Tucson, Az. 85721.

The regulation of many biological processes involves phosphorylation. In molluscan catch muscles, phosphorylation of paramyosin, a protein found in the thick filaments, may play a role in the regulation of tonic contraction (R.K. Achazi, 1979, Eur. J. Phys. 379, 197.). A protein kinase has been prepared from *Mercenaria mercenaria* which is specific for α-R-paramyosin. This paramyosin kinase is optimally active at 30°C and at high ionic strength (0.6 M). As the ionic strength is lowered to 0.1 M, there is a corresponding decrease in incorporation of phosphate. This protein kinase appears to be most catalytically active in the presence of 10mM EGTA. In the presence of 10⁻⁴ M Ca⁺⁺, there is an observed decrease in phosphate incorporation. If 10⁻⁴ cAMP and 10mM EGTA replace the Ca⁺⁺, no enhancement in incorporation beyond what is obtained in the presence of only 10 mM EGTA is noted.

Paramyosin kinase is highly specific for α-R-paramyosin. As previously reported (L. Radlick and W.H. Johnson, 1982, Biophysics J. 37, 36a.), this protein kinase does not catalyze the phosphorylation of proteins which are substrates for cyclic nucleotide dependent protein kinases; nor is β-paramyosin a substrate for this enzyme. Additionally, paramyosin kinase does not phosphorylate myosin rod, a protein of similar molecular weight and molecular length to α-R-paramyosin.

T-Pos147 MONOCLONAL ANTIBODIES TO LIMULUS PARAMYOSIN. Rhea J.C. Levine, Pat Levitt*, Harriet King* and Vilma Cooper*(Intr. by Dallas Pulliam). Dept. of Anatomy, The Medical College of PA, Philadelphia, PA 19129.

We raised monoclonal antibodies to isolated Limulus paramyosin (LPM) by fusion of immunized BALB/CJ mouse spleen cells with mouse NS-1 myeloma cells. Of 416 fusions, 392 clones produced anti-LPM as assayed by the immunodot method (Hawkes, et al., *Anal. Biochem.* 119:142, '82). We selected 38 clones for further culture, on the basis of strength of the immunodot reaction and apparent health of cells, of which 36 survived. Of eleven clones tested thus far, the supernatants from only two stained the A bands of Limulus myofibrils with a pattern identical to that we previously reported for polyclonal anti-LPM (by the indirect fluorescent antibody technique) (Levine, et al., *J. Cell Biol.* 55:221, '72), although all supernatants continued to react strongly with isolated LPM. Staining was unaffected by absorption of the two supernatants with Limulus myosin (LM) but was abolished by absorption with LPM. It is likely that the non-staining but reactive supernatants contain antibodies against epitopes on LPM that are covered by myosin in intact thick filaments.

Studies are underway to characterize the antibodies further, both with respect to class and subtype as well as to identify the portions of the PM molecule against which they react. We are also engaged in studies to localize the "hidden" epitopes by examining antibody binding to both isolated intact Limulus thick filaments and myosin-stripped filament cores. We hope that the results we obtain will provide information regarding PM-PM and PM-M packing in invertebrate thick filaments.

Supported by USPHS grants NS19606 and HL15835 to The Pennsylvania Muscle Institute.

T-Pos148 PARAMYOSIN AND MYOSIN CONTENT OF THE THICK FILAMENTS OF LIMULUS STRIATED MUSCLE.

B. Gaylinn, and M. M. Dewey. Department of Anatomical Sciences, School of Medicine, State University of New York at Stony Brook, Stony Brook, New York 11794

Limulus muscle homogenate, when examined on discontinuous SDS polyacrylamide gels, contains a group of bands in the 100k dalton region that includes paramyosin. Antibodies to purified Limulus paramyosin have been used to distinguish paramyosin from other muscle homogenate bands of similar mobility by blotting gels to nitrocellulose sheets and staining with peroxidase coupled second antibody. Purified paramyosin bands on Coomassie blue stained SDS gels appear to bind an anomalously large amount of dye when protein loading is quantitated by the Lowry assay. This anomaly may be resolved by UV and dry weight measurements which show the Lowry assay to underestimate paramyosin concentration by a factor of two. This may effect the paramyosin to myosin ratios reported by Levine, Elfvin, Dewey and Walcott, *J. Cell Bio.* 71:273-279, 1976. Calibrated amino acid analysis is underway to more accurately quantify both paramyosin and myosin content on SDS gels. If this paramyosin to myosin ratio is combined with measurements of thick filament mass from STEM, then assuming there are no other major thick filament proteins, we calculate very close to four myosin molecules for each 146Å spaced crown of crossbridges. This is in harmony with X-ray (Wray, Vibert and Cohen, *Nature* 257:561-564, 1975) and optical diffraction (Stewart, Kensler and Levine, *J. Mol. Biol.* 153:781-790, 1981) studies which have shown that the thick filament projections form a four stranded helix.

T-Pos149 REVERSIBLE INHIBITION OF TENSION DEVELOPMENT AND ACTO-MYOSIN ATPASE ACTIVITY IN BARNACLE MUSCLE BY THE Ca^{2+} INDICATOR DYE ANTIPYRYLAZO III. G.R. Dubyak, Dept. Biochemistry & Biophysics, University of Pennsylvania, Philadelphia, PA 19104.

We have investigated the effects of the Ca^{2+} indicator dyes arsenazo III (AS3) and antipyrilazo III (AP3) on: (1) tension development in myofibrillar preparations from barnacle depressor muscle, rabbit psoas muscle, and guinea pig portal vein smooth muscle; and 2) actomyosin ATPase activity in myofibrils/native actomyosin isolated from barnacle muscle and in actomyosin hybrids prepared from pure (unregulated) rabbit F-actin and either pure rabbit myosin or partially purified barnacle myosin. In all solutions, pCa was heavily buffered with suitable [CaEGTA]/[EGTA] and measured with a Ca-electrode so as to offset the appreciable Ca^{2+} -buffering effects of the dyes. AS3 (0.05-1 mM) had no effect on either tension development or ATPase activity in any of the listed preparations. Likewise, AP3 (0.05-1 mM) was without effect on tension development by psoas muscle or smooth muscle, or on the ATPase rate of rabbit myosin hybridized with pure F-actin. Conversely, AP3 produced a concentration-dependent inhibition of both tension development by isolated barnacle myofibrils and Ca-regulated ATPase activity in barnacle myofibrils and native actomyosin. 50% inhibition of both maximal tension (P_{max}) and maximal ATPase rate (both measured at pCa 4) was produced by 80 μM AP3; AP3 (>500 μM) produced >90% inhibition of either P_{max} or ATPase max . These effects were rapid and fully reversible. While AP3 had no effect on the basal ATPase activity (measured at pCa 8) of native barnacle actomyosin, the dye did inhibit the Ca-independent ATPase activity (similar at pCa 8 or 4) of partially purified barnacle myosin hybridized with unregulated F-actin. This latter result suggests that AP3 may affect the interaction of actin with binding sites on barnacle--and perhaps other--invertebrate myosins. Supported by NIH HL-15835.

T-Pos150 INWARD RECTIFICATION IN FROG MUSCLE: FURTHER ANALYSIS OF ITS EFFECT ON RADIAL POTENTIAL SPREAD. J.A. Heiny, F.M. Ashcroft, and J. Vergara. Dept. of Physiology, UCLA School of Medicine, Los Angeles, CA, and Univ. Laboratory of Physiology, Oxford University, UK.

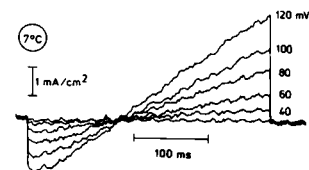
Inward rectifier currents and T-system optical signals were recorded from single voltage-clamped frog fibers. As reported previously (Heiny et al., *Nature* 301:164, 1983) activation of this conductance introduces significant decrements of potential in the T-system. These data were further analyzed using a radial cable model. This conductance has several features which make it ideally suited for quantitative analysis of radial potential spread. 1) It behaves essentially as a voltage-dependent shunt conductance with near perfect rectification. Therefore, after fitting depolarizing control records, hyperpolarizing test records can be fit by adjusting only the specific membrane resistance. 2) It is essentially instantaneously activated, and therefore no kinetic parameters are needed. Assuming literature values for morphometric and passive membrane constants, steady state current and light data were well fit using an equal distribution of inward rectifier conductance over the surface and T-system, and a specific conductance obeying a Boltzmann type voltage dependence. At maximal activation, the effective T-system space constant is reduced by 70-80%. When the measured G-V, and the assumed specific G-V relationships were compared, radial decrements reduce the steepness of the former, without significantly changing the mid point; small progressive conductance increases at large hyperpolarizations are also predicted in part by radial decrements. Attempts to fit the complete time course of current and light transients at early times were reasonably successful, but some discrepancies were consistently found which we are currently investigating.

T-Pos151 DENERVATION PRODUCES ACTION POTENTIALS IN TONIC FIBERS OF RAT EXTRAOCULAR MUSCLES. A.Y. Bondi, D.J. Chiarandini and J. Jacoby (Intr. by J.R. Wiggins) Depts. Ophthalmology and Physiology and Biophysics, New York Univ. Med. Cent., New York, NY 10016

Extraocular muscles of mammals possess various populations of twitch or singly innervated fibers (SIF's) and multiply innervated fibers (MIF's). In response to depolarization SIF's generate action potentials (AP) while one of the populations of MIF's (tonic or global MIF's) produces a small, graded, Na-dependent response or slow peak potential (SPP). After denervation the electrical properties of muscle fibers are changed. Frog tonic fibers which normally lack AP become capable of generating AP (1). The present experiments were carried out to determine whether similar changes occur in global MIF's which have physiological properties similar to frog tonic fibers. Rat inferior rectus muscles were denervated by sectioning the oculomotor nerve. After 6-9 days recordings were made *in vitro* from the global surface. The muscle was superfused with oxygenated saline containing 10 mM Ca. The resting potential (RP) of the fibers ranged from -35 to -63 mV. Records were obtained holding the fibers at -80 mV. For later retrieval cells were labeled with Lucifer yellow and nerve endings were stained for AChE. Fibers were followed in serial sections to ascertain their innervation (2). In denervated global MIF's a modification of the SPP was observed which ranged from an increase in amplitude to a transformation into virtually an AP. Anodal break responses, absent in normal muscles, could be evoked after denervation. The input resistance (R_{in}) and membrane time constant (τ_m) were unchanged. In SIF's the amplitude of the AP was essentially unchanged but maximal dV/dt appeared to be reduced and anodal break responses could be evoked at much less negative membrane potentials. R_{in} and τ_m were increased. Supported by USPHS grants EY01297 and EY00165. (1) Miledi, R., Stefan, E. and Steinbach, A.B., *J. Physiol.* 1971, 217: 737. (2) Bondi, A.Y. and Chiarandini, D.J., *Invest. Ophthalmol.* 1983, 24: 516.

T-Pos152 SLOW INWARD CURRENT IN FROG SKELETAL MUSCLE INDUCED BY THE "Ca²⁺ ENTRY BLOCKER" D-600. S.R. Taylor, F. Zite-Ferenczy*, and R. Rüdell*, Abt. Allg. Physiologie, Universität D-7900 Ulm, FRG.

Slow inward current through a Ca²⁺ channel in frog skeletal muscle becomes apparent when currents carried by other ions are reduced. Results from EGTA-loaded cut fibers (*J. Physiol.* 312:159, 1981) differ from those of intact fibers in hypertonic solution (*J. Physiol.* 338:395, 1983). Both treatments reduce the depolarization-induced rise in myoplasmic Ca²⁺. Hence we used the "loose patch" voltage clamp (*J. Physiol.* 336:261, 1983) on intact fibers from leg muscles of *R. temporaria* in a normal solution at 7 to 24°C. A 2-15 min treatment with D-600 ($\leq 10^{-6}$ M) reversibly reduced or abolished Na⁺ and K⁺ currents. Extended treatment caused slow inward and outward currents, particularly after cooling and re-warming. All effects were strongly use-dependent and slowly reversed in normal solution. Resting potentials were unaffected. Maximum size of the slow inward current was 0.2-0.5 X the size of a normal fast Na⁺ current; time to peak was 10-30 ms in the cold, sometimes much longer in the warm; half-time of decline during maintained depolarization was 40-50 ms and not related to step size (in mV in figure). The size of the slow inward current increased linearly with the size of a hyperpolarizing pre-pulse or with increase in the depolarizing test pulse. The slow inward and outward currents remained in solutions containing only D-600, 83 mM CaCl₂ and 2.5 mM KCl, and were unaffected by TTX. We infer that the slow inward current is carried by Ca²⁺ and is induced, not merely revealed, by D-600.



T-Pos153 CALCIUM ANTAGONISTS MODIFY CONTRACTION OF SKELETAL MUSCLE FIBERS. K.E. Cooper, R.T. McCarthy, R.L. Milton, and R.S. Eisenberg, Physiology Dept, Rush Medical College, Chicago, IL 60612

The tertiary amine D-600 (methoxy-verapamil) has been shown to block excitation contraction coupling in single skeletal muscle fibers of the frog in the cold (5-7°C) after a conditioning contracture in which a fiber contracted and relaxed in response to 190 mM K^+ (J. Physiol. 341:495, 1983). The closely related tertiary amine Verapamil reduces contracture tension; however, the quaternary ammonium derivative (D-890) of D-600 has no effect. The dihydropyridine nifedipine does not produce paralysis. It seems likely that D-600 acts on a nonpolar region of a membrane protein, on the sarcoplasmic side of the T membrane. Its blocking actions on contraction are reminiscent of the actions of local anesthetics (often tertiary amines) on sodium channels, although steep temperature dependence has apparently not been reported in the latter case.

Paralysis by D-600 can be graded: changes in the conditioning procedure produce partially paralyzed and progressively paralyzing fibers. 1) If the conditioning contracture is produced by 25 mM K^+ or reduced in duration by early application of normal Ringer, a partially paralyzed fiber results. In either case repeated exposure to K^+ progressively paralyzes fibers, even in the absence of drug. 2) If a fiber exposed to D-600 is repetitively stimulated at 1 Hz in the cold, fatigue occurs much more quickly than normal, producing a fiber unresponsive to electrical stimulation after some 31 seconds compared to 250 seconds for a normal fiber. Partially paralyzed, and progressively paralyzing fibers may prove useful in correlating phenomena of excitation contraction coupling with underlying molecular mechanisms.

T-Pos154 CONSTANT LEVEL OF INTRACELLULAR FREE MAGNESIUM CONCENTRATION DURING MUSCULAR ACTIVITY AND FATIGUE. J.R. Lopez, L. Alamo, C. Caputo. Centro de Biofísica y Bioquímica, IVIC, Apartado 1827, Caracas, Venezuela.

Mg^{2+} selective microelectrodes have been used to measure the intracellular free magnesium concentration in skeletal muscle fibers immediately after the onset of the spontaneous relaxation that follows K^+ contractures, after electrical stimulation at low frequency, and during muscle fatigue. Microelectrodes with a tip outer diameter of 0.4 μm were filled with Mg^{2+} selective neutral carrier (ETH 1117). The calibration curve of these microelectrodes gave a Nernstian response (29.5 mV per decade) between 1 and 10 mM (physiological range) when no interfering ions were present. However, they showed sub-Nernstian (18-23 mV per decade), but still useful responses in the presence of an ionic environment similar to that of the myoplasm. The microelectrodes were calibrated before and after muscle fiber impalements. As it was reported previously (López et al. Biophys J. 41:129a 1983) the intracellular $[Mg^{2+}]$ found in sartorius muscle at rest was 3.8 ± 0.24 (SEM) mM, $n=48$, at 22-23°C. In depolarized muscle fibers (-22 mV) treated with 100 mM K^+ the myoplasmic $[Mg^{2+}]$ was 3.7 ± 0.36 (SEM) mM, $n=14$, immediately after the spontaneous relaxation of the contracture. Similar determination in muscle fibers during stimulation at low frequency (5Hz), and after fatigue development showed no changes in the concentration of free cytosolic Mg^{2+} . These results point out that $[Mg^{2+}]$ is not modified under these three different experimental conditions (Supported by CONICIT S1-1148).

T-Pos155 DILTIAZEM, A CALCIUM ANTAGONIST, PARADOXICALLY INCREASES MECHANICAL ACTIVITY IN MAMMALIAN SKELETAL MUSCLE. K. B. Walsh, S. H. Bryant and A. Schwartz, Department of Pharmacology and Cell Biophysics, University of Cincinnati College of Medicine, Cincinnati, OH 45267

Recently it was reported that d-cis diltiazem (d-Dtz) potentiates twitch tension in frog skeletal muscle (Gonzales-Serratos et al., NATURE 298:292, 1982). We studied the effects of d-Dtz on twitch tension and mechanical threshold in mouse and rat EDL fibers. For twitch studies 5 to 10 small bundles (0.5 mm Dia.) were dissected from tendon-to-tendon and secured in a 1 ml fast flow chamber. Addition of d-Dtz at 22°C resulted in a concentration-dependent increase in twitch amplitude from 4.5% at 10^{-8} M to a maximal effect of 23.6% at 5×10^{-7} M. The l-cis diltiazem stereo isomer, less effective pharmacologically, was also less effective in potentiating the twitch. Its concentration response curve was shifted 2-fold to the right and the maximal increase of twitch tension was only 16.1%. Effects of d-Dtz on twitch duration were seen only at concentrations of 10^{-5} M with the durations measured at 75%, 50% and 25% of the peak amplitude increasing by 33%, 21% and 19%, respectively. Mechanical threshold was determined by a point voltage clamp for square pulses from 0.1 to 1000 msec duration. At concentrations of 5×10^{-7} M and 10^{-6} M, d-Dtz decreased (i.e., more negative potentials) the rheobase by 10.3 mV and 15.7 mV, respectively. No effects were observed below these concentrations. Tension and mechanical threshold effects occurred 5 to 10 min after addition of d-Dtz. These results strongly suggest that binding of d-Dtz to a specific intracellular site promotes EC-coupling. This action could be related to other specific effects of the drug including inhibition of mitochondrial Na^+/Ca^{++} exchange and/or stimulation of H^3 -nitrendipine binding to the t-tubular membrane. (Supported by NIH grants NS-03178 and HL-07382; K.B.W. is a predoctoral trainee.)

T-Pos156 MEMBRANE POTENTIAL MEASUREMENTS IN TOAD SKELETAL MUSCLES INCUBATED IN TOAD RINGER'S AND PLASMA. Ranjith P.M. Shetty* and Donald D. Macchia. Indiana University School of Medicine, Northwest Center for Medical Education, Gary, Indiana 46408.

Here we report the effects of toad plasma albumin on the resting membrane potential of isolated toad muscles. The membrane potential time transients and the reversible nature of the albumin effects were obtained. Semitendinosus muscles from the toad (*Bufo marinus*) were dissected out and placed in either a toad plasma or Ringer's bath. The mean resting potential, E_m , of muscles incubated in plasma (-90.9 ± 3.0 mV, $n = 7$) was found to be significantly greater than the mean potential of muscles incubated in Ringer's (-81.0 ± 1.5 mV, $n = 34$). Further studies involved making control E_m measurements followed by a single recording which was maintained while the incubation solution was changed. When the E_m of muscles were measured first in plasma followed by a change of incubation solution to Ringer's (while holding a single potential recording) the potential was observed to decrease by approximately 21% over two minute period. When the reverse experiment was performed (incubation solution changed from Ringer's to plasma) very little if any change was noticed. If the muscles were first incubated in Ringer's containing bovine albumin and then the solution changed to Ringer's alone, the potential was observed to decrease by an average 16%. Again when the reverse experiment was performed (Ringer's to Ringer's plus bovine albumin) no significant difference in E_m was observed. Finally when the change of incubation solution is from plasma to Ringer's plus bovine albumin, no change in E_m is observed. These studies would suggest that the effect of plasma on maintaining an elevated E_m in toad semitendinosus muscles is due primarily to plasma albumin. Further, once the muscles are incubated in Ringer's the albumin effect is abolished and the potential cannot be reversed to the increase plasma values. (NIH AM 27148).

T-Pos157 CHLORIDE CONTRACTURES IN SKINNED FROG MUSCLE FIBERS UNDER PROCAINE AND OUABAIN TREATMENTS. M. Yamakawa and B. A. Mobley, Department of Physiology and Biophysics, University of Oklahoma, College of Medicine, Oklahoma City, OK 73190.

Single contractures were initiated in segments of physically skinned frog skeletal muscle fibers by quickly changing the bathing solution from relaxing-loading solutions to various test solutions. The test solutions substituted chloride for the apparently less permeant anions, methanesulfonate and gluconate, in the relaxing-loading solutions. The substitution of chloride for impermeant anions was accomplished by either raising the $[K] \times [Cl]$ product or by keeping the $[K] \times [Cl]$ product constant, i.e. by also substituting choline for potassium. We assumed that the former solution produced a potential change in the sarcoplasmic reticulum (SR) membranes and increased the volume of the SR compartment, while the latter solution produced a potential change only. Procaine treatment, which inhibited the calcium induced calcium release (tested by caffeine contractures), involved placing 25 mM procaine in the rinsing solution that followed loading and in the test solutions. Ouabain treatment, which was designed to eliminate the possibility of SR stimulation by "sealed off" transverse tubules, involving bathing the single fibers in Ringer's solution with 1 mM ouabain and 3 mM Mg for 2.5 - 3 hours at 25°C prior to skinning and bathing the skinned fibers in 1 μ M ouabain. Calcium release was monitored in terms of the maximum force (peak) and time integral (area) of the force transient. In all cases we observed greater contractures upon moving the segments to solutions of increased $[K] \times [Cl]$ product than to solutions of the same $[K] \times [Cl]$ product, and at no time did the procaine or ouabain treatments eliminate either type of contracture. (Supported by USPHS NS16989).

T-Pos158 The Physiology of Single Giant Smooth Muscle Cells Isolated from the Ctenophore Mnemiopsis. P. G. Stein and P. A. V. Anderson, C. V. Whitney Laboratory and Dept. of Physiology, University of Florida.

The ctenophore Mnemiopsis possesses two bundles of giant (15-20 μ m diameter) smooth muscle cells. In large individuals, single cells can be 4-5 cm long. During the isolation procedure these long cells invariably fragment, producing cell segments that range in length from several mm to less than 100 μ m. The membranes of the cell segments anneal at sites of breakage and thereafter the muscles behave electrically like whole cells *in situ* producing a fast, overshooting action potential that is carried by both Ca^{++} and Na^{+} . The Ca^{++} component of the spike can be blocked by D-600, verapamil and various divalent cations. The Na^{+} component is insensitive to both TTX and STX. Repolarization is achieved by a K^{+} efflux through TEA and 4-AP sensitive channels. A component of the K^{+} current is also blocked by Ca^{++} blocking agents implying the presence of Ca^{++} -activated K^{+} channels. By recording electrotonic potentials at various distances from a current source, an analysis of the cable-like properties of these cells was made. Equations for a short cable (Hodgkin and Nakajima, 1972) were applied in determining the length constant (λ). By this method, λ was determined to be 1.7 mm (± 0.33 s.e.m. $N=11$). Further cable analysis produced mean values for R_i (247 Ω cm), R_m (7,546 Ω cm²), τ_m (12.3 msec) and C_m (1.65 μ F cm⁻²). These data, taken together, indicate that Mnemiopsis cells are physiologically conventional smooth muscle cells. Additionally, the length constant and low membrane capacitance allow spatial and temporal control of membrane potential during voltage clamp such that membrane currents can be quantified. Funded by the Whitehall Foundation.

T-Pos159 CALCIUM UPTAKE AND K^+ CONTRACTURES IN PARALYZED AND CONTRACTING MUSCLE FIBERS.

R.S. Eisenberg, B.A. Curtis, and R.T. McCarthy, Departments of Physiology, Rush Medical College, Chicago, IL 60612 and University of Illinois College of Medicine at Peoria, Peoria, IL 61656.

Calcium uptake by isolated frog muscle fibers soaked in 30 μ M D-600 at 3-5°C was measured by counting radioactive disintegrations from the center of the fiber following a period of ^{45}Ca influx (Curtis, 1966, *J. Gen. Physiol.* 50:255). Fibers were equilibrated in ^{45}Ca for 3 minutes before the elevated K^+ (containing ^{45}Ca) was applied for 2 minutes. After one K^+ contracture in D-600, fibers were unable to contract in response to K^+ depolarization despite normal resting potentials, action potentials and caffeine contractures, as previously reported. The uptake of calcium associated with the first, paralyzing contracture was 42 ± 10 pmoles/cm² T membrane (mean \pm SEM, n = 11, diameter 142 μ m). The calcium uptake during a subsequent application of K^+ to the same fiber (which did NOT produce tension) was reduced by 72% (n = 17). After warming to at least 16°C, a K^+ contracture was associated with a calcium uptake of 50 ± 9 pmoles/cm² (n = 7). Caffeine contractures were not accompanied by significant calcium uptake.

The action of D-600 on calcium uptake, nonlinear charge movement, and contraction have a specific "signature": they occur only in the cold, after a prior conditioning contracture, and they are reversed by warming. These actions can be explained if D-600 blocks a gating current for a channel in the T membrane through which messenger calcium flows to activate calcium release from the sarcoplasmic reticulum. Other explanations require that D-600 has several actions, presumably mediated by several receptors, all of which have the same signature of action.

T-Pos160 COMPARATIVE STUDIES OF NILE BLUE A ANALOGUES. M. Block, S. Krasne, and J. Vergara, Dept. of Physiology, Sch. of Med., UCLA, Los Angeles, CA 90024.

Nile Blue A has been used by several researchers to monitor potential changes across the sarcoplasmic reticulum (SR) following stimulation of single muscle fibers. Only one particular dye lot (from Allied Chemical Co.) has been found to be effective in producing these signals, however, without producing significant muscle deterioration. One apparently ineffective dye is Eastman's laser-grade Nile Blue A. We report here that following additional dye purification and removal of the perchlorate anions both the Eastman and Allied dyes give comparable signals. We have determined that these dyes are structural isomers and are ethyl derivatives of Nile Blue A. We have also investigated Nile Blue A from Gurr Chemical Co. which appears to have the correct Nile Blue A structure and which also gives the same types of fluorescence signals in single muscle fibers as the other two dyes. We have examined spectrophotometrically the membrane adsorption and potentiometric signals from these three dyes in large (0.2 μ m), PC and 1:1 PC/PS vesicles and in SR vesicles from rabbit skeletal muscle. For a given type of vesicle, all the dyes appear to have the same partition coefficient (K). The K's for PC and SR vesicles are similar ($K_{PC}=1.5(\pm 2) \times 10^4$; $K_{SR}=1.4(\pm 1.6) \times 10^4$) but those for PC/PS vesicle ($K_{PC/PS}=7.9(\pm 1.2) \times 10^4$) are a factor of 5.3 larger. In any given type of vesicle, all the dyes appear to show the same fluorescence-voltage (F-V) relationship, this relationship depending, however, upon the dye/lipid ratio. At dye/lipid ratios below .05, the dyes' F-V relationships are the same in PC and PC/PS but in SR vesicles. At dye/lipid ratios between 0.1 and 1, the F-V relationships in PC/PS vesicles appear more similar to those in SR than in PC vesicles. Supported by NIH and MDA grants to S.K. and J.V.

T-Pos161 LOCALIZATION OF INTRACELLULAR FREE Ca^{++} DURING CONTRACTIONS OF SINGLE VASCULAR MUSCLE CELLS. Michael Sturek and Kent Hermsmeyer, Department of Pharmacology, The Cardiovascular Center, University of Iowa, Iowa City, Iowa 52242.

Intracellular free Ca^{++} concentration was localized during spontaneous and norepinephrine (NE)-induced contraction of single vascular muscle cells using arsenazo III (AZIII). Cells were cultured from the azygous vein of neonatal rat and AZIII was introduced into the cells (final concentrations up to 300 μ M) via liposomes. The combined use of interference contrast optics, shielded photomultiplier detector, dual wavelength fiber optics illumination, and lock-in amplifier allowed 0.5 μ m resolution with 10,000-fold enhancement of signal/noise ratio. Absorbance changes averaged 0.0008 in the 660 nm signals at the peak of a Ca^{++} signal. Corrections for light scattering during contraction were made by subtraction of simultaneously recorded signals at 580 nm in some experiments. An imaging diaphragm in the focal plane of the final imaging lens, giving a slit equivalent to 0.5 μ m of the cell image was observed in the eyepieces enabling precise positioning for localized measurements. All contracting cells displayed marked inhomogeneity in amplitudes of Ca^{++} signals in adjacent 0.5 μ m strips, and in 7 cells there was greater than 10-fold difference in signal amplitude in adjacent areas (less than 1 μ m apart). Despite the inhomogeneities, no specific area of the cells showed a consistently high signal strength, e.g. the subsarcolemmal area displayed both large and small signals. In 1 nM NE, contraction amplitude increased 1.6-fold and duration increased 1.5-fold, with a return to baseline level after withdrawal of NE. These results suggest that different vasoactive agents may exert their various effects on vascular muscle contraction by actions on multiple intracellular Ca^{++} pools.

T-Pos162 SEQUENCE DEPENDENT THERMODYNAMICS OF NETROPSIN BINDING TO DNA POLYMERS. Luis A. Marky, James Curry, Beth Buono, Kenneth Blumenfeld, and Kenneth J. Breslauer, Department of Chemistry, Rutgers University, New Brunswick, NJ 08903.

Netropsin is a basic oligopeptide that exhibits a wide range of biological activities. Previous studies have shown that it binds strongly to the minor groove of B-DNA duplexes. This binding, which depends on base sequence, increases the thermal stability of the duplex. In fact, the extent of binding can be correlated with the magnitude of the increase in the melting temperature (ΔT_m) of the drug-DNA complex compared with the free DNA duplex. From uv melting experiments we have measured ΔT_m values for netropsin binding to a series of DNA polymers and observed the following sequence-dependent trend: poly dA·polydT=polydAT>polydAC·polydTG>salmon sperm (s.s.) DNA>polydGC. The ΔT_m values range from a high of about 50°C to a low of about 10°C.

To define the nature of the molecular forces that control these sequence binding preferences, isothermal batch calorimetry has been employed. For all of the polymers noted, we measured exothermic netropsin binding enthalpies. However, the magnitude of the binding enthalpy was strongly dependent on base sequence and ranged from a low of -9.2 kcal/drug bound to a high of -2.3 kcal/drug bound. Specifically the exothermicity of netropsin binding decreased in the order: polydAT>polydAC·polydTG>s.s. DNA>polydGC>polydA·polydT.

The significant observation is that the sequence-dependent binding affinities of netropsin (as defined by ΔT_m) are not paralleled by the sequence-dependent binding enthalpies. In fact, polydA·polyT which exhibits the largest stabilization due to netropsin binding also exhibits the least favorable binding enthalpy. These trends will be discussed in terms of possible models for the sequence-dependent interactions of netropsin with B-DNA double helices.

T-Pos163 HISTONES H3 AND H2a ARE HOMOLOGOUS TO THE LAMBDA REPRESSOR AND CRO PROTEINS IN 22 RESIDUE SEGMENTS IMPLICATED IN DNA BINDING. K.A. Magnus and E.E. Lattman, Dept. of Biophysics, Johns Hopkins School of Medicine, Baltimore, MD. 21205

The histones H3 and H2a from calf thymus are homologous to the repressor and cro repressor proteins of bacteriophage lambda in a 22-residue segment that has been implicated by mutational and model-building studies in DNA binding. In the lambda proteins this segment is folded into a helix-turn-helix unit of supersecondary structure, and we propose that the homologous regions in the histones possess the same fold. Homology was quantified with a unified procedure based on criteria of identity of key residues, primary structural homology and similarity of secondary structural potential. It has previously been shown that a set of other prokaryotic DNA-binding proteins have primary structural homology with the two lambda proteins. Homologies detected between the histones H4 and H2b and members of this set suggest that these histones also contain the putative DNA-binding fold. This work was supported by an NSF grant PCM 81-09-755 and by a USPHS National Research Service Award to K.A.M.

T-Pos164 EQUILIBRIUM AND KINETIC BINDING STUDIES OF *E. COLI* SSB PROTEIN WITH SINGLE STRANDED NUCLEIC ACIDS. Timothy M. Lohman and Leslie B. Overman, Department of Biochemistry and Biophysics, Texas A&M University, College Station, TX 77843.

The *E. coli* Single Stranded Binding protein (SSB) is a helix destabilizing protein by virtue of its selective and high binding affinity for single stranded nucleic acids. SSB is necessary for DNA replication, recombination and repair in *E. coli*. We are using the quenching of the intrinsic tryptophan fluorescence of SSB upon binding to single stranded nucleic acids to investigate its equilibrium and kinetic binding properties with a series of synthetic homopolynucleotides and S.S. M13 DNA as a function of solution variables. In stopped-flow studies, in excess nucleic acid, a single exponential decay is observed in an association experiment. The bimolecular rate constant for formation of noncooperative SSB-poly(rU) complexes is $k_1 = 7.5 \times 10^6 \text{ M}^{-1} (\text{nucleotide}) \text{ sec}^{-1}$ at 0.10 M NaCl, pH 8.1, 25.0°C, and is relatively insensitive to [NaCl] over the range of 20 to 100 mM. The apparent rate constant for dissociation of SSB-poly(rU) complexes is extremely salt dependent with $(d \log k_d(\text{app})/d \log [\text{NaCl}]) = 4$ to 5 at pH 8.1, 25.0°C.

(Supported by NJH Grant GM30498 and Robert A. Welch Foundation Grant A-898)

T-Pos165 CHROMATIN CORE PARTICLE STABILITY IS pH DEPENDENT. L. J. Libertini and E. W. Small, Dept. of Biochemistry and Biophysics, Oregon State University, Corvallis, OR 97331.

Chromatin core particles prepared from chicken erythrocytes undergo a reversible transition with changing pH centered near pH 7. The transition can be detected at near physiological ionic strength by tyrosine fluorescence anisotropy measurements and may also be reflected by changes in DNA circular dichroism. However, no corresponding changes in the sedimentation coefficients are observed. The presence of magnesium ion up to 10 mM had no apparent effect.

Previous results (Libertini and Small, *Biochemistry* **21**, 3327 (1982)) on effects of pH on the low salt transition indicated a greater stability of the core particle at pH 6 than at pH 9. Efforts in the present work to relate the observations at low salt to the pH 7 transition have failed to show a direct relationship.

However, we find that high salt dissociation of core particles is also dependent on the pH, but in a manner which correlates with the pH 7 transition. The observed effects indicate that core particle stability in the presence of high salt concentrations (0.3 - 1.0 M KCl) is also enhanced at low pH (6) as compared to higher pH (8). (Supported by NIH Grant GM 25663)

T-Pos166 A QUANTITATIVE MODEL FOR GENE REGULATION IN PHAGE λ PREDICTS PHENOTYPIC EXPRESSION OF MUTATIONS IN DNA CONTROL REGIONS AND REGULATORY PROTEINS. Madeline A. Shea and Gary K. Ackers, Dept. of Biology, The Johns Hopkins University, Baltimore, MD 21218.

A quantitative model of gene regulation has been developed for the O_R/O_L control region of phage lambda where two repressor proteins (cI and cro) modulate the activity of three promoters to control stable lysogenic growth and the induction of lysis (Shea and Ackers, (1984) *J. Mol. Biol.*, in press). The model permits simulations of protein synthesis through calculation of promoter activities as a function of (1) concentrations of active species of regulatory proteins, (2) resolved protein-DNA and protein-protein interaction energies and (3) catalytic effects of protein-protein interactions. Thus it is possible to predict changing levels of cI, cro and N synthesized by wild type and mutant phages during lysogenic and lytic growth.

We have now used this model to explore the expected behavior of mutant phages carrying defective cro or cI proteins, virulent mutations of O_R and O_L , and promoter mutations that affect binding and isomerization of RNA polymerase. The simulated protein levels agreed with known phenotypes in cases that had been characterized genetically or biochemically, thus providing support for the underlying physico-chemical assumptions used in this model.

These calculations provide both quantitative and qualitative criteria for determining the molecular basis of phenomena arising from superficially similar mutations or regulatory mechanisms. They provide quantitative insight into the degree of change in physical properties that may be manifest as changes in cellular physiology. They may also be used to develop screening techniques for phage carrying specific mutations. Supported by a grant from the N.I.H.

T-Pos167 STRUCTURAL ANALYSIS OF HMG 17-NUCLEOSOMES BY SMALL-ANGLE NEUTRON SCATTERING

E.C. Uberbacher, V. Ramakrishnan, and G.J. Bunick (intro. by B.E. Hingerty), University of Tennessee-Oak Ridge Graduate School of Biomedical Sciences, and the National Center for Small-Angle Scattering Research, Oak Ridge National Laboratory, Oak Ridge, TN 37830.

The high mobility group (HMG) 17 protein is one of several nonhistone proteins believed to be involved in the activation of chromatin. In this study, HMG 17 molecules were stoichiometrically bound to nucleosome core particles and the conformation of the resulting 2:1 complex analyzed by small-angle neutron scattering. The use of several ratios of H_2O/D_2O in the buffer (contrast variation) allows examination of the conformation of the protein components and the DNA essentially independently of each other. An extensive modeling analysis was performed which involved the calculation of scattering curves and radial density distribution functions from a large number of possible models. Each model was constructed by applying structural perturbations to a three-dimensional digitized density map of the nucleosome core particle. The results indicate the probable binding sites for the HMG 17 molecules and the conformation of the DNA and histone core. The DNA has a more extended conformation in the HMG-nucleosome complex than in the nucleosome. The extended DNA conformation in the complex is most likely maintained by the additional HMG 17 contacts to the DNA. (Supported by NIH Grant GM 29818, and by the National Science Foundation under grant DMR-77-24458 with the U.S. Department of Energy; under contract W-7405-eng-26 with the Union Carbide Corporation.)

T-Pos168 HIGH RESOLUTION MAP OF THE H1-DNA INTERACTION. J. S. Sevall*, S. L. Berent⁺, and A. Gonzalez*. *Southwest Foundation for Biomedical Research, San Antonio, TX 78284, ⁺Wadley Institute of Molecular Medicine, Dallas, TX

A rat liver H1 high affinity deoxyribonucleic acid (DNA) binding site has been mapped. This binding site is within a 390 base pair (bp) rat DNA fragment. The H1 binding site was initially identified by measuring the specific retention of restricted DNA fragments on nitrocellulose filters. By scanning for sites within the 390 bp fragment that were resistant to endonucleolytic cleavage of their phosphodiester bonds, it was possible to localize the site in the rat DNA fragment. The protein binding site has a neighboring 43 bp sequence composed of adenines and thymidines but devoid of cytosines and guanosines. The localization of the binding site at 270 bp from the initiation site of the rat albumin gene places it between the first and second intron and because of this location suggests a functional role for the H1-DNA interaction. Currently, individual variants of rat liver H1 are under investigation as to their role as essential components for the mechanism of protein affinity toward this binding protein site.

T-Pos169 LASER RAMAN SPECTROSCOPIC STUDY OF CALF THYMUS CHROMATIN AND ITS CONSTITUENTS. R. Savoie and J.-J. Jutier (intr. by F.O. Schanne), Department of Chemistry, Laval University, Quebec, Que. Canada G1K 7P4.

Extensive Raman measurements have been made on calf thymus chromatin and its constituents, and spectra with high signal/noise ratio have been obtained through multiscan experiments. Computerized spectral stripping of the data has allowed a comparison to be established between the spectra of the individual components of polynucleosomes and the corresponding spectral contribution of these same units within the various complexes involved. The results indicate a gradual increase in the α -helical structure content of the inner histones in the hetero complexes that lead to the formation of the nucleosome protein core. However, the secondary structure this histone octameric core is not modified when it binds to DNA in the nucleosome. Only minor changes, at the limit of the experimental error, occur in the spectrum of DNA as it wraps itself around the protein core to form a nucleosome. No specific interaction between the histones and the DNA bases can be inferred from the spectra. The DNA essentially retains its B conformation in polynucleosomes, although slight changes seem to occur in the stacking of the bases and in the conformation of the ribose-phosphate backbone. Our results are consistent with previous Raman measurements using u.v. excitation, which showed that histone H1 interacts with thymine bases in polynucleosomes. In the (H3-H4)₂/DNA complex, the α -helical content of the histone core is much higher than in the isolated tetramer in aqueous solution, and the structure of DNA appears to be considerably more perturbed than by the normal histone octameric core found in nucleosomes.

T-Pos170 COMPLEX OF FD GENE 5 PROTEIN AND DOUBLE-STRANDED RNA. Carla W. Gray, Gregory A. Page, and Donald M. Gray. Program in Molecular Biology (FO3.1), The University of Texas at Dallas, Box 830688, Richardson, TX, 75083-0688.

We report the formation of complexes of the single-stranded DNA binding protein encoded by gene 5 of fd virus, with natural double-stranded RNAs (dsRNAs) from the mycoviruses PcV and PbcV. In the first direct visualization of a complex of the fd gene 5 protein with a double-stranded nucleic acid, we show by electron microscopy that the dsRNA complex has a structure which is distinct from that of complexes with single-stranded DNA and is consistent with uniform coating of the exterior of the dsRNA helix by the protein. The contour lengths of the complexes correspond to the range of lengths of the intact dsRNA genome segments, indicating that there is not significant intercalation of protein aromatic residues into the RNA double helix. Circular dichroism (CD) spectra confirm that the RNA double helix in the complex is undisrupted. Significantly, a strong reduction of the 228-nm CD assigned to protein tyrosines is found to occur in the absence of intercalation of protein aromatic residues with nucleotide bases. A parallel reduction of the 228-nm CD which occurs in complexes of fd gene 5 protein with single-stranded DNA may therefore not arise from tyrosine intercalation with the bases. Our findings emphasize the potential importance of interaction with the sugar-phosphate polynucleotide backbone (accessible on the exterior of a double helix) in the binding of the fd gene 5 protein to nucleic acids.

Supported by NIH grants GM19060, SO7 RR-07133; by grant AT-503 from the Robert A. Welch foundation; and by NSF instrumentation grant PCM-8116109.

T-Pos171 GLUCONEOGENESIS IN ISOLATED, PERFUSED LIVERS OF NORMAL AND MALARIAL MICE: A ^{13}C -NMR STUDY. Geoffrion Y., Deslauriers R., Butler K., Pass M.¹ and I.C.P. Smith. National Research Council, Division of Biological Sciences, Ottawa, Canada K1A 0R6. ¹University of Queensland, Department of Physiology and Pharmacology, Australia.

We have used ^{13}C -NMR to monitor the metabolic changes induced by a 2- ^{13}C pyruvate load (25 mM) in perfused mouse livers isolated from starved (24h) normal animals and from animals in the terminal stages of malarial infection. Under identical perfusion conditions (37°C, 10 mL/min perfusion flow of erythrocyte-free Krebs-Henseleit bicarbonate buffer), the time required for removing 50% of the initial pyruvate 2- ^{13}C resonance was shorter in the case of the normal liver (31 ± 2 min; Mean \pm SE, $n = 3$) than for the moribund malarial liver (42 ± 6 min; $n = 3$). In the last 15 min of the 2h perfusion after the addition of labelled pyruvate, the NMR spectra of normal livers showed that 64% of the ^{13}C resonances could be ascribed to carbons 2,5 (34%) and carbons 1,6 (30%) of glucose, and 13% to carbon 2 of lactate. The malarial liver spectra acquired between 1.75 and 2h after addition of labelled pyruvate showed that 48% of the resonances arose from glucose carbons 2,5 (24%) and 1,6 (24%), while 41% of the ^{13}C resonances was due to carbon 2 of lactate. These results are indicative that pyruvate enters the gluconeogenic pathway directly and via the TCA cycle. With acquisition parameters of the NMR spectra being the same in all experiments, the last spectra ($t = 1.75$ -2h) showed identical absolute intensities in the labelled glucose carbons in both normal and malarial livers. This suggests that malaria does not impair the gluconeogenic function of the isolated liver under our perfusion conditions.

T-Pos172 DETERMINATION OF THE CARBOHYDRATE STRUCTURE OF OVARIAN CYST MUCIN GLYCOPROTEINS BY NMR SPECTROSCOPY. Virendra K. Dua and C. Allen Bush. Dept. of Chemistry., Ill. Inst. of Tech., Chicago, IL. 60616.

At least 15 reduced oligosaccharides have been isolated from alkaline borohydride degradation of ovarian cyst blood group substances. Pure samples, ranging in size from two to eight carbohydrate residues have been fractionated by both reverse phase and normal phase HPLC. All the structures terminate with GalNAc-OL and also contain Gal, GlcNAc and fucose with various linkages and branching. Both carbon and proton nmr spectroscopy were used to assay the purity of the samples, to determine their carbohydrate composition and the anomeric configuration of each linkage. In most cases chemical shifts can be used to identify the positions of linkage substitution. Nuclear Overhauser effects may be used to determine connectivity between the residues due to the proximity of anomeric and linkage protons.

T-Pos173 ANISOTROPIC ROTATIONAL DIFFUSION OF D- β -HYDROXYBUTYRATE DEHYDROGENASE (BDH) SPIN-LABELED WITH [^{15}N]-NITROXIDE AND STUDIED BY SATURATION TRANSFER (ST)-EPR. J. Oliver McIntyre, Bruce H. Robinson* and Sidney Fleischer. Dept. of Molecular Biology, Vanderbilt Univ., Nashville, TN 37235 and *Dept. of Chemistry, Univ. of Washington, Seattle, WA 98195.

BDH is a lipid-requiring enzyme purified from the mitochondrial inner membrane. The enzyme devoid of lipid (apoBDH) is inactive but can be reactivated by insertion into phospholipid vesicles containing lecithin. BDH in the membrane is a tetramer with two sulfhydryls per monomer, one of which is essential for function. BDH, inserted into mitochondrial phospholipid (MPL), was selectively labeled at the essential sulfhydryl using a spin label (SL) [3-maleimido-2,2,6,6-tetramethylpiperidinoxyl]. The SL was both perdeuterated and ^{15}N in the spin-label moiety, to increase sensitivity, enhance resolution and simplify spectral simulation [Beth, A.H. et al. (1981), Proc. Nat. Acad. Sci. USA 78, 967-971]. EPR spectra exhibited sensitivity to motion in the temperature range studied (2-25°C). ST-EPR spectra were best simulated using an anisotropic motional model [Robinson, B.H. and Dalton, L.R. (1980) J. Chem. Phys. 72, 1312-1324]. A simulation of the ST-EPR spectra was obtained with orthogonal magnetic and diffusion tensors ($\theta = 90^\circ$) obtaining correlation times of $\sim 10^{-6}$ sec (τ_{\perp}) and $\sim 5 \times 10^{-8}$ sec (τ_{\parallel}). The two motional components are referable to the anisotropic motion of the protein, the faster (τ_{\parallel}) likely being rotation about an axis normal to the bilayer and the second (τ_{\perp}) being referable to tilting of the protein relative to the plane of the bilayer. This slower motion may also be interpreted in terms of a restoring potential. This study represents the first characterization by ST-EPR of distinct anisotropic components of a membrane protein. [Supported by NIH AM 21987 and NSF PCM 8216762]

T-Pos174 PHOSPHORYLATED G-ACTIN IN SMOOTH AND SKELETAL MUSCLE — A P-31 NMR STUDY. Manfred Brauer and Brian D. Sykes. Department of Biochemistry and MRC Group on Protein Structure and Function, University of Alberta, Edmonton, Alberta, Canada T6G 2H7.

It has recently become appreciated that G-actin can be phosphorylated *in vitro* and that phosphorylated G-actin does exist in various species *in vivo*. The P-31 NMR spectrum of unphosphorylated smooth muscle G-actin was obtained in 1 mM Tris, 0.1 mM CaCl₂, 0.25 mM DTT, pH 7.8, 4°C in 50% D₂O. The spectrum was very similar to that of skeletal muscle G-actin previously studied under the same conditions [Brauer, M. and Sykes, B.D. (1981) Biochem. 20, 6767-6775], indicating that the ATP is bound similarly in the two G-actin forms. Purified catalytic subunit of cyclic-AMP dependent protein kinase was used to phosphorylate smooth muscle G-actin. Two new P-31 resonances, at +4.2 and 4.0 ppm from 85% H₃PO₄ external standard, appeared after kinase treatment. Extensive washing and reconcentration of the sample did not diminish the size of the two new resonances, indicating either very tight non-covalent or covalent binding of phosphate moieties to the smooth muscle G-actin. These results are consistent with the fact that the amino acid sequence of G-actin contains two serine residues, Ser-119 and -337, within the proper amino acid recognition sequence for the binding of the catalytic subunit of cyclic-AMP dependent protein kinase [Krebs, E.G. and Beavo, J.A. (1979) Annu. Rev. Biochem. 48, 923-959]. P-31 NMR spectra of extracts of the Straub acetone powders of both skeletal and smooth muscle show a P-31 resonance at +4.0 ppm, indicating that at least one of these serine residues is phosphorylated *in vivo*. The physiological role of phosphorylated G-actin remains unknown. (Supported by the Medical Research Council of Canada and the Alberta Heritage Fund for Medical Research).

T-Pos175 SPIN RELAXATION DATA ON Mb BELOW 1 K: POSITIVE IDENTIFICATION OF A PHONON BOTTLENECK. J. T. COLVIN, P. J. MUENCH, T. R. ASKEW, AND H. J. STAPLETON, Dept. of Physics and Materials Research Laboratory, University of Illinois, Urbana, IL 61801.

Identification of the dominant low temperature electron spin relaxation mechanism in paramagnetic proteins is essential to an accurate determination of the net contribution from the more interesting, higher order Raman or Orbach processes. The temperature dependence of the Orbach or Raman rates yield energy levels of excited electronic states or the fractal dimension (1,2) of the entire biopolymer, respectively. It is generally assumed that low temperature relaxation rates which appear to follow a T² dependence are indicative of a phonon-limited rate for which a (coth(hv/2kT))² dependence is predicted. In some materials, such as amorphous silicon, relaxation rates are known to vary as simple Tⁿ power laws (3), with n ≈ 2 even under conditions for which hv/2kT is about unity and a T² approximation to (coth(hv/2kT))² is not valid. Relaxation models exist which can explain such a temperature dependence and do not involve a phonon bottleneck. Measurements on high spin Fe³⁺ in myoglobin at 16.5 GHz and at temperatures as low as 0.4 K confirm a (coth(hv/2kT))² dependence predicted of a true phonon limited relaxation process. Supported in part by NIH Grant GM24488 and the DOE, Division of Materials Sciences, under contract DE-AC02-76ER01198.

- (1) H. J. Stapleton, et al., Phys. Rev. Lett. 45, 1456 (1980).
- (2) J. P. Allen, et al., Biophys. J. 38, 299 (1982).
- (3) T. R. Askew, et al., Solid State Communications, to be published.

T-Pos176 NUCLEAR MAGNETIC RESONANCE STUDY OF MUSCLE REGULATION: TROPOMYOSIN-TROPONIN COMPLEX. J.-R. Brisson, B.D. Sykes, K. Golosinska and L.B. Smillie, Department of Biochemistry, University of Alberta.

¹H nuclear magnetic resonance has been used to study the nature of the interaction between tropomyosin (TM) and troponin (Tn) to delineate the molecular mechanism by which these two protein complexes participate in the actin-linked calcium regulatory systems of skeletal and cardiac muscle. Using fragments of both TM and Tn prepared by limited proteolytic or chemical degradation, we are probing the nature of the head-to-tail polymerization of TM molecules and the effects of TM-binding domains on Tn-T on this phenomenon. Resonances corresponding to the histidine residues in each of the fragments can be resolved and assigned in the high resolution ¹H NMR spectrum. Changes in the pH titration profiles of these resonances when the various fragments are mixed provide probes of the titration sites between the proteins. Thus, the resonance corresponding to the histidine (residue 276) located in the COOH-terminal region of the TM molecule is perturbed upon head-to-tail binding of TM fragments. Changes in the pH titration of a histidine present in the T1 fragment (residues 1-158) of Tn-T when mixed with Cyl fragment (residues 1-189) of TM indicate an interaction between the NH₂-terminal regions of these proteins. This change was much reduced when fragment T1 of Tn-T and fragment Cn1A (residues 11-127) of TM were mixed indicating the importance of TM residues 1-11 in this phenomenon. This is the first direct evidence for such interactions and supports a model in which Tn-T overlaps contiguous TM molecules at their molecular ends.

T-Pos177 CALCIUM-BINDING PROTEINS: INVESTIGATIONS OF THE ROLE OF THE F-HELIX IN THE EF DOMAIN OF PARVALBUMIN. David C. Corson, Thomas C. Williams, and Brian D. Sykes. Department of Biochemistry and the MRC Group on Protein Structure and Function, University of Alberta, Edmonton, Alberta, Canada T6G 2H7.

Calmodulins, Tn-C's, myosin light chains, and parvalbumins chelate calcium ions in elegantly structured loops of acidic amino acid ligands, frequently referred to as "EF hands": in all cases, a 2- to 3-turn α -helix extends from each end of the chelating loop. Although the role of the chelating loop may seem obvious, the function(s) of the accompanying helices is (are) not. To investigate this question, we have enzymatically (via carboxypeptidases A and B) shortened the F-helix of the EF calcium-binding domain of carp parvalbumin (pI 4.25). As judged by their ^1H NMR-monitored lanthanide-exchange behaviors, the N-1 and N-2 forms of parvalbumin (i.e., the cleaved proteins which lack the C-terminal ALA-108 and ALA-108/LYS-107 residues, respectively) are very similar to the native form. Not only do Lu(III) and Yb(III) maintain high affinities for the modified-EF sites but Yb(III) also causes nearly identical paramagnetic shifts in the three forms, indicating that the conformation within 10Å of the metal ion has undergone little change.

T-Pos178 FLOW BEHAVIOR OF RED CELLS IN THE PRESENCE OF CELL-CELL INTERACTION. K. KON and H. KON, Laboratory of Chemical Physics, NIADDK, National Institutes of Health, Bethesda, MD 20205.

The red cell deformation in shear flow plays a significant role in blood circulation. In most methods for assessing the deformation of red cells, observations are made under the condition of a low hematocrit value, and the deformation is determined by the shear stress of the flowing extracellular medium. Previously, we have devised a method for evaluating the degree of deformation and orientation of cells using the ESR. By this method, we can assess the flow behavior of cells under the conditions in the presence of the cell-cell interaction. (1) To investigate the effect of varying the hematocrit on the deformation/orientation behavior of red cells in shear flow, the cells were spin labeled with 5-doxyl stearic acid. The relative ESR spectral change due to flow, measured as a function of the hematocrit, shows that there is an upper limit of the deformation/orientation for a given hematocrit. (2) The effect of the hardened cells on the deformation/orientation of the intact cells was studied in a mixture of the intact and the glutaraldehyde (or diamide) treated cells. Only the intact cells were labeled with 5-doxyl phosphatidylcholine. With this spin label, there is no transfer of the labels from the intact to the hardened cells, enabling observation of the flow behavior of only the intact cells. The results show decrease in the degree of deformation/orientation in the presence of the hardened cells. This is explained on the basis of the disturbance of the laminar flow by the hardened cells, thereby causing the decrease in the effective shear stress, to which the intact cells are subjected. Thus, the actual deformation/orientation of the cells in flow is determined not only by the single cell deformability but also by the way cells interact with each other under a given fluid dynamic condition.

T-Pos179 PROTON NUCLEAR MAGNETIC RESONANCE STUDIES OF SPECTRIN FROM HUMAN ERYTHROCYTES Paul D. Sima*, M.E. Johnson⁺ and L.W.-M. Fung*, *Department of Chemistry, Loyola University of Chicago, Chicago, Illinois 60626, ⁺Department of Medicinal Chemistry, University of Illinois Medical Center, Chicago, Illinois 60680.

The peripheral protein network of erythrocyte membrane is essential for the maintenance of the erythrocyte shape, reversible deformability and membrane structural integrity; it also controls the lateral mobility of integral membrane proteins. Spectrin is the principal structural protein of this network, and is a heterodimer composed of two chemically distinct polypeptides with molecular weight of above 220,000 and 240,000. The association of heterodimers give tetramers and probably oligomers. We have extracted the spectrin network from human erythrocyte membrane by the low ionic strength - 37°C incubation procedure and have further purified it by column chromatography at 4°C. High resolution nuclear magnetic resonance (NMR) spectroscopy has been used to study the purified spectrin at different concentrations, temperatures and pH values in D₂O buffer. Lyophilized samples suspended in D₂O buffer have also been used. Several sharp resonances are observed for the lyophilized samples. Some of these resonances are selectively suppressed in the more native systems. The functional significance of this spectral behavior will be discussed.

(This research was supported by NIH grants HL-23697 (MEJ) and HL-31145 (LWMF). MEJ is an Established Investigator of American Heart Association and LWMF is a Research Career Development Awardee from NIH (HL-011901).)

T-Pos180 MAGNETIC RESONANCE STUDIES OF HUMAN ERYTHROCYTE MEMBRANE-DRUG (CETIEDIL) INTERACTION
C. Narasimhan and L.W.-M. Fung, Department of Chemistry, Loyola University of Chicago, Chicago, Illinois 60626.

Cetiedil, (2-hexahydro-1H-azepin-1-yl)ethyl α -cyclohexyl-3-thiophenacetate-2-hydroxy-1,2,3-propanetricarboxylate hydrate, has been used as a vasodilator for chronic cardiovascular disease in Europe. More recently, cetiedil's potential usefulness has been recognized in sickle cell disease. It acts as an antisickling agent, presumably by interacting with the erythrocyte membrane to produce changes in ion and water movements across cell membranes, resulting in reduced intracellular hemoglobin concentration. The detailed molecular mechanism of the cetiedil-membrane interaction is not clear.

We have used electron paramagnetic resonance (EPR) spectroscopy to study the cetiedil-membrane interaction. With a protein spin label on membrane, we observe a substantial decrease in a spectral parameter, W/S, in membrane in the presence of cetiedil. With a fatty acid spin label we detect a large decrease in hyperfine splitting when cetiedil is added to the membrane. These studies indicate that both proteins and lipids in membranes are affected upon binding of cetiedil to membrane.

We have further used C-13 nuclear magnetic resonance (NMR) spectroscopy to study cetiedil molecules in solutions of various polarities as well as in membrane samples. A working model for cetiedil-membrane interaction has been proposed and will be discussed. (This research was supported by NIH grants HL-31145 and HL-16008, a Wayne State University Comprehensive Sickle Cell Center grant; LWMF is a Research Career Development Awardee from NIH (HL-011901).)

T-Pos181 THE VARIATION OF K_{eq} , $K_{forward}$, and $K_{reverse}$ OF THE CREATINE PHOSPHOKINASE (CPK) REACTION WITH pH. EVIDENCE FOR CRITICAL DAMPING AT PHYSIOLOGICAL INTRACELLULAR pH.

R.L. Coulson, Physiology and Joel Gober, Molecular Science, Southern Illinois University-Carbondale P.A. Mole, and John Caton, Physical Education, University of California-Davis CA 95616.

Using a Nicolet 200 MHz, 20 mm bore FT-NMR spectrometer and Sigma CPK, Phosphocreatine, and ADP parameters of the reaction $Cr + (ATP \rightleftharpoons Iz) \quad (PCr \rightleftharpoons Sz) + ADP$ were measured using a combination of non-selective and selective inversion recovery experiments at pH 8.46, 8.05, and 7.57. Using all "hard" pulse experiments the following results were obtained:

pH	ρI s ⁻¹	ρS s ⁻¹	σ s ⁻¹	KI	KS	K	K_{eq}	ATP ∞ molar	ADP ∞ molar
8.46	.594	.254	.014	.133	.504	.265	.070	.119	.031
8.05	.635	.278	.013	.108	.568	.191	.036	.126	.024
7.57	.741	.302	.019	.079	.630	.126	.016	.133	.017

by applying the modified Bloch equations. $\lambda \pm$ were both real and negative, approaching coincidence with declining pH. The reaction would appear, by extrapolation, to be critically damped at pH 7.

T-Pos182 AN UNBIASED METHOD OF REMOVING PHASING ERRORS FROM MAGNETIZATION ESTIMATES OBTAINED FROM PEAK-HIGHT MEASUREMENTS IN NMR INVERSION RECOVERY EXPERIMENTS. R.L. Coulson, Department of Physiology and Joel Gober, Molecular Science, Southern Illinois University, Carbondale IL 62901.

In any inversion recovery experiment in which the degree of magnetization is estimated from NMR spectrum peak heights there is error potential in the failure to achieve perfect phasing of the real spectrum before the measurements are made. For example, in the typical T_1 experiment where data are analysed after the form: $I_z = I_\infty - 2 I_\infty \exp(-t/T_1)$ [1] the errors due to mis-phasing in the greater than zero order phase corrections can be avoided by using the modulus spectrum which maintains correct amplitudes while abolishing phase information. In this approach the data form: $I_z^2 = I_\infty^2 - 4 I_\infty^2 \exp(-t/T_1) + 4 I_\infty^2 \exp(-t/(2 T_1))$ [2] may be used. Since there are no more unknowns in equation two than in equation one the former is as easily solved as the latter. Advantage of the inherent phase-independent accuracy of the modulus spectrum amplitude may be taken. Examples from ³¹P FT-NMR spectra will be presented.

T-Pos183 ³¹P NMR DETECTION OF CHANGES IN INTRACELLULAR FREE Mg(II) and MgATP DURING BLOOD STORAGE. Jay L. Bock, Barry Wenz*, & Raj K. Gupta, Departments of Laboratory Medicine, and Physiology and Biophysics, Albert Einstein College of Medicine, Bronx, NY 10461.

Human blood for transfusion is stored in preservation media containing citrate, a chelator of divalent cations. Little is known concerning changes in erythrocyte divalent cations during blood storage. Intracellular free Mg(II) modulates the oxygen carrying function of the red cell, since phosphorylated compounds and their Mg(II) complexes have different metabolic effects. To investigate changes in the extent of Mg(II)-complexation of ATP and intracellular free Mg(II) during storage at 4°, we measured ³¹P NMR spectra of aliquots of blood collected from a single donor in ACD and in CPDA-1. Measurements were made at various times over a 5-week storage period. The same donor's blood stored in sodium heparin was also analyzed over a 1-week period. The extent of Mg(II)-complexation of ATP and the concentration of free Mg(II) were measured from the Mg(II)-dependent chemical shift difference at 25° between the αP and βP resonances of intracellular ATP. The differences changed from 725 and 720 Hz on the day of collection, in ACD and CPDA-1, respectively, to 745 and 740 Hz after 1 week, and to 780 and 750 Hz after 3 weeks of storage. Small changes in intracellular pH (<0.3 unit) were detected from shifts in the P_i resonance over the entire storage period. These data indicate a sizable change in the extent of Mg(II)-complexation of ATP and a 65% decrease in free Mg(II) during the shelf life of stored blood in ACD and CPDA-1 media. In contrast, blood stored in heparin exhibited a 50% increase in intracellular free Mg(II), which may reflect release of Mg(II) upon decomposition of ATP. The observed decrease of free Mg(II) in citrate media may be explained by entry of citrate into the cells and may be related to the storage lesion of banked blood.

T-Pos184 SPIN-LATTICE RELAXATION RATES: CORRELATION BETWEEN EPR AND MÖSSBAUER RESULTS. C. Schulz, Physics Dept., Knox College, Galesburg, IL 61401 and P. G. Debrunner, Physics Dept., University of Illinois, Urbana, IL 61801.

The Mössbauer spectra of paramagnetic compounds depend on the electronic eigenstates of the paramagnetic ion, typically described by a spin Hamiltonian \mathcal{H}_S , and on the transition rates between these states. We recently developed a model that allows the simulation of Mössbauer spectra for arbitrary transition rates W_{ij} between the states $|i\rangle$ and $|j\rangle$ of \mathcal{H}_S (1). The rates W_{ij} include terms describing one and two phonon processes, and the Mössbauer spectra are calculated using a Liouville operator technique (2). We now show how the transition rates W_{ij} relate to the spin lattice relaxation rates measured in EPR. The eigenvectors of the non-Hermitian matrix W correspond to certain populations of the electronic levels, and the respective eigenvalues are the decay rates of the eigenvectors towards thermal equilibrium. A superposition of eigenvectors with their proper rates will describe the approach to equilibrium of any given population. The EPR intensity in a saturation recovery experiment can be similarly expressed as a superposition of terms decaying with the eigenvalues of W ; typically a single term dominates whose decay rate can be identified with the experimental spin lattice relaxation rate. We apply this model to the heme protein horseradish peroxidase and show that the rates W_{ij} obtained by fitting the Mössbauer spectra are consistent with the EPR data (3). Supported in part by GM-16406.

1) C. Schulz and P. G. Debrunner, *Biophys. J.* **41**, 267a (1983).

2) H. Winkler, C. Schulz and P. G. Debrunner, *Physics Lett.* **69A**, 360-363 (1979).

3) J. T. Colvin, R. Rutter, H. J. Stapleton and L. P. Hager, *Biophys. J.* **41**, 105-108 (1983).

T-Pos185 LOCALIZATION OF HYDROXYL RADICAL PRODUCTION IN STIMULATED PMN USING EPR.

F. W. Kleinhaus, S. T. Barefoot, and D. A. Hawley, Dept. of Medical Research, Methodist Hospital of Indiana, Indianapolis, IN 46202 and IUPUI, P.O. Box 647, Indianapolis, IN 46223.

Hydroxyl radical production by stimulated polymorphonuclear leukocytes (PMN) can be assayed using EPR spin trapping techniques. DMPO (5,5-dimethyl-1-pyrroline-N-oxide) is used to trap the OH• forming a spin adduct detectable via electron paramagnetic resonance (EPR). Work by Okolow-Zubkowska and Hill (1980) using latex IgG as a stimulant indicates that the trapped OH• is produced in the extra-cellular medium, however their examination of lysed, pelleted cells does not adequately exclude an intracellular component. Work by Berg and Nesbitt (1979) suggested to us the use of potassium trioxalochromate as an extracellular signal broadening agent which would not disrupt or enter the PMN (as NiCl₂ does). We found that 50 mM chromium oxalate yields a 99.3% reduction in signal amplitude of (DMPO/OH)• adduct produced via Fenton's reaction in aqueous phase. Exposure of PMN to this same concentration of chromium oxalate for 10 minutes did not affect cell viability as measured via trypan blue exclusion. To look for intracellular (DMPH/OH)• adduct the following experiment and control were performed. 188 μl of human PMN at 5 x 10⁷ cells/ml in PBSG buffer, 150 mM DMPO, with 10.5 mg/ml opsonized zymosan as a stimulant were monitored by EPR at 37°C for 10 minutes and the peak (DMPO/OH)• amplitude measured. Repeating the experiment in the presence of 50 mM chromium oxalate yielded no detectable signal and a noise level of 1% of the peak EPR signal measured without chromium oxalate. The estimated intracellular volume at 5 x 10⁷ cells/ml is 5% indicating that the intracellular spin adduct concentration is less than 20% of the extracellular concentration.

T-Pos186 NMR ASSIGNMENT AND EXCHANGE KINETICS OF TYR-35 SIDE CHAIN OH PROTON IN BPTI. S. Ramaprasad and Clare Woodward (Intr. by L. Ellis) Dept. of Biochemistry, Univ. of Minnesota, St. Paul, MN 55108.

A new exchangeable resonance in the ^1H NMR spectrum of bovine pancreatic trypsin inhibitor (BPTI) in water has been identified at 9.9 ppm. The protein sample was predeuterated to eliminate the slower exchanging NH's from the spectra, which were obtained using the Redfield technique. Saturation of the 9.9 ppm resonance gives a clear negative NOE with ^1H of Try35 at 6.95 ppm, indicating that it arises from the Tyr35 OH proton. The exchange rate constant obtained by the saturation transfer technique, in combination with T_1 relaxation studies, yields a value of 62 min^{-1} (+15%) at pH 2.5, about two orders of magnitude slower than model compound OH rate constants (M. Nakanishi and M. Tsuboi, J.A.C.S., 100 1273-75, 1978). The rate constants as a function of pH have been determined. There are four tyrosine residues in BPTI at positions 10, 21, 23 and 35, but only the Tyr35 OH exchanges slowly enough to be observed in these experiments. This is not explained by H-bonding, since only the side chain OH of Tyr23 is H-bonded in the crystal structure. The significantly lower dynamic accessibility of Try35 OH in the solution structure is consistent with, but not explained by, the observations that the ring rotation rate for Tyr35 is significantly slower than for the other three tyrosine side chains, and that the susceptibility to nitration is lowest for Tyr35 and Tyr23 (Snyder *et al.*, Biochemistry, 14, 3765-77, 1975).

T-Pos187 ^{31}P NMR MEASUREMENT OF INTRACELLULAR FREE Mg(II) IN AMPHIBIAN OOCYTES. R.K. Gupta, A.B. Kostellow, & G.A. Morrill. Dept. Physiol. & Biophys., Albert Einstein Coll. Med., Bronx, NY 10461

Noninvasive measurement of the concentration of free Mg(II) in excitable cells is of considerable physiological interest. Because of their large size, easy availability, and physiological stability when superfused in the NMR tube, *Rana* oocytes constitute a particularly favorable model system. We have used NMR to determine the fraction of the ATP complexed to Mg(II) , which in turn allows calculation of intracellular free Mg(II) . The chemical shift difference between αP and βP resonances of intracellular ATP in prophase oocytes was $704 \pm 2 \text{ Hz}$ [23°C , 81 MHz, Ringer's solution with 0.8 mM Mg(II)]. A comparison of this value with differences of 685 ± 1 and 870 ± 2 for noncellular MgATP and ATP , respectively, revealed that 90% of the total intracellular ATP is complexed to Mg(II) . A K_D of $50 \pm 10 \text{ }\mu\text{M}$ has been determined for MgATP using a combination of ^{31}P NMR and optical absorbance spectroscopy. Using this K_D we obtain a value of $0.45 \pm 0.05 \text{ mM}$ for intracellular Mg(II) in the prophase oocyte. The free Mg(II) level remained unchanged for at least 2-3 h following insulin-induced resumption of the meiotic divisions. The total Mg concentration of the prophase oocyte is $30 \pm 2 \text{ mmols/liter}$ cell water. Thus, only a very small fraction (1.5%) of the total oocyte Mg(II) is in a free or kinetically active form. These observations are in agreement with the Mg(II) equilibrium studies of Ling *et al.* (J. Cell Physiol. 101:261, 1979). Knowledge of free Mg(II) permits an accurate estimation of the phosphorylation potential and the cellular energy charge of the oocyte. The observation of only a single set of $\text{ATP } ^{31}\text{P}$ resonances in oocytes suggests 3 possibilities: (1) free Mg(II) is the same in all cell compartments, (2) ATP exchanges rapidly among compartments, and/or (3) only cytosolic ATP is observed by NMR. (Supported by NIH AM32030 & HD10463).

T-Pos188 EFFECTS OF ESTROGEN STATUS ON NMR RELAXATION TIMES IN TISSUES OF FEMALE ANIMALS. P. T. Beall and L. K. Misra, Department of Physiology, Baylor College of Medicine, Houston, Texas 77030.

Alterations in water content or macromolecular organization in cells may cause changes in water proton relaxation times, which will be indicative of their physiological state. One example would be the effects of estrogens and analogs on responsive tissues in females. This study reports changes in T_1 of the breast (B), uterus (U), liver (L), heart (H), and skeletal muscle (M) of rats and mice in variable estrogen status. Young (3 m) and old (12 m) Sprague-Dawley rats and mature BALB/C mice were given hormones and the T_1 of tissues was measured by a $180^\circ - \tau - 90^\circ$ sequence, at 25°C and 30 MHz. Ovariectomy or total estrogen deprivation resulted in physiological changes similar to those seen in postmenopausal older women. Significant changes were seen in uterine tissue T_1 ($575 \pm 69 \text{ ms}$ vs. $640 \pm 35 \text{ ms}$) and water content (78.6 ± 4.0 vs. 80.3 ± 0.8). A possible effect was seen on heart ventricle ($T_1 = 716 \pm 64$ vs. control of $T_1 = 660 \pm 17$). Supplementation with the estrogen analog clomiphene citrate (20 mg/kg/week) restored T_1 of the tissues to normal values. A single dose of estradiol ($100 \text{ }\mu\text{g}$) in rats did not elevate T_1 in B, U, H, or M. A slight elevation of T_1 was seen in liver. A single injection of clomiphene greatly elevated both T_1 (275 ± 46 vs. 800 ± 44) and water content (27% vs. 72%) of the virgin mouse breast. Pregnancy in mice also elevated breast T_1 to $373 \pm 9 \text{ ms}$. These findings have special significance for the NMR imaging of the human female population who may be on birth control pills, in various stages of their menstrual cycle or pregnancy, in the post-menopausal period, or on prolonged hormone supplementation. (This work supported by ONR N00014-K-82-0167 and USPHS RP-05424.)

T-Pos189 ^1H NMR STUDIES OF MYOCARDIAL METABOLISM. K. Ugurbil, M. Petein, R. Maidan, A. From, J. Cohn, S. Michurski. Dept. of Biochemistry and Gray Freshwater Biological Institute, (KU and SM) and Cardiovascular Division (MP, RM, AF, JC), University of Minnesota.

^1H NMR studies of perfused rat hearts were conducted at 361 MHz. Selective presaturation and Hahn spin-echo pulse sequence was used to eliminate the H_2O resonance and resonances from short- T_2 protons. Several resonances including acylglycerides, creatine, phosphocreatine, lactate, glutamate succinate, acetate, carnitine and taurine have been identified in the spectra of intact hearts and of acid extracts prepared from freeze-clamped hearts. Accumulation of lactate and succinate was monitored in the ^1H spectra upon going from normoxia to ischemia; three prominent, as yet unidentified resonances appeared upon transition from normoxic to hypoxic conditions. Acylglyceride resonances were drastically affected upon starvation of animals prior to measurements indicating that they arise from metabolically mobilizable fatty acid pools. Results demonstrate that ^1H NMR can be used to monitor aspects of myocardial metabolism which are complementary to the ^{31}P NMR measurements.

T-Pos190 PARTIAL UNFOLDING OF THE BIOLUMINESCENT PROTEIN AEQUORIN SUBSEQUENT TO LIGHT EMISSION

B. D. Ray, M. D. Kemple, B. D. Nageswara Rao, Department of Physics, IUPUI, P.O. Box 647, Indpls., IN 46223, and F. G. Prendergast, Pharmacology Dept., Mayo Medical School, Rochester, MN 55901.

Aequorin, one of two proteins responsible for the bioluminescence of jellyfish (*Aequorea forskalea*), emits blue light at 469nm upon binding Ca^{2+} . Light emission of $\sim 10^{-6}$ of that in the presence of Ca^{2+} occurs independent of Ca^{2+} and is suppressed by the presence of Mg^{2+} , an inhibitor of aequorin. A tightly bound chromophore is oxidized to cause light emission. The oxidized chromophore does not appear to be as tightly bound as the unreacted chromophore and can be removed by dialysis, or sephadex chromatography. Proton NMR spectra of aequorin, and aequorin with a 50 fold excess of Mg^{2+} were acquired during the course of Ca^{2+} -independent discharge, and the spectra were correlated with protein activity. In addition, spectra of Ca^{2+} -discharged aequorin were acquired over time and compared with the Ca^{2+} -independent discharged aequorin spectra. In every case, a pattern of line narrowing emerged indicating side chain mobility, which begins with release of the oxidized chromophore and progressively increases with time to what appears to be a final conformation in which specific regions of the protein are partially unfolded. In all cases, there seems to be an immobilized core of amino acid residues as suggested by a comparison of the areas of the aromatic and aliphatic regions of the spectra with areas predicted from the protein amino acid content. (Supported by NSF PCM 80-22075, NIH GM 30178, RR 01077, and PRF (ACS).)

T-Pos191 ELECTRON PARAMAGNETIC RESONANCE OF VO^{2+} BOUND TO AEQUORIN, M. D. Kemple, B. D. Ray, B. D. Nageswara Rao, Physics Dept., IUPUI, P.O. Box 647, Indpls., IN 46223 and F. G. Prendergast, Pharmacology Dept., Mayo Medical School, Rochester, MN 55901.

Aequorin is a bioluminescent protein (M.W. 20,000) from the jellyfish *Aequorea forskalea*. Upon the binding of Ca^{2+} *in vitro*, aequorin emits blue light at 469nm with no requirement for exogenous oxygen or energy. Lanthanide ions are substituent, highly efficient activators of aequorin, and Mn^{2+} is a weak activator. Aequorin contains a relatively small, tightly bound chromophore which is oxidized upon binding of activating metal ions. The blue light is emitted from an excited state of the oxidized chromophore. We have found that the paramagnetic vanadyl ion, VO^{2+} , activates the bioluminescence of aequorin with an efficiency nearly as great as that of Ca^{2+} and considerably greater than that of Mn^{2+} , and we have observed the electron paramagnetic resonance (EPR) spectrum of VO^{2+} bound to aequorin. In pH 8.0 Hepes buffer, free VO^{2+} forms diamagnetic hydroxide complexes and gives a negligible EPR signal at room temperature. Thus for aequorin with VO^{2+} in Hepes buffer, the only EPR signals detected are those from VO^{2+} bound to aequorin. It has been shown by Chasteen and coworkers that measurement of the parameters of the VO^{2+} EPR spectrum, most notably the hyperfine interaction parameters ($I = 7/2$ for ^{51}V), can lead to identification of the ligands of the VO^{2+} . The implication of EPR studies of aequorin with regard to the ligands of the VO^{2+} , the VO^{2+} stoichiometry, and the competition of various metal ions for the VO^{2+} sites will be presented. (Supported by NSF PCM 80-22075, NIH GM 30178, and a Petroleum Research Fund Grant administered by ACS.)

T-Pos192 NUCLEAR MAGNETIC RESONANCE STUDIES OF COWPEA MOSAIC VIRUS PARTICLES. DETECTION OF POLYAMINE AND ITS DISPLACEMENT BY CESIUM CHLORIDE. R. Virudachalam*, Melissa Harrington†, John E. Johnson†, and John L. Markley*. Departments of Chemistry* and Biological Sciences†, Purdue University, W. Lafayette, IN 47907.

Cowpea mosaic virus (CpMV) is a T=1 icosahedral particle with a divided genome. Particles which contain the 1.4×10^6 -Da RNA form the middle (M) component on a CsCl density gradient and those with the 2.5×10^6 -Da RNA form the bottom (B) component. The empty shells (devoid of RNA) form the top (T) component on the gradient. The B component splits into two bands, the bottom upper (B_U) and bottom lower (B_L), when the pH of the gradient is above 7.0. 470 MHz proton nuclear magnetic resonance spectra of the four different components (T, M, B_U , B_L) and 50 MHz ^{13}C spectra of the T and M components obtained at pH 7.0 showed the presence of polyamine only in the M and B_U components. After dialysis of the B_L component against spermidine, the presence of polyamine in the virion gave rise to NMR peaks very similar to those assigned to polyamine in the B_U or M components. The polyamine peak in the NMR spectrum of the middle component disappeared when the virion was dialyzed against 3 M CsCl above neutral pH. Our NMR results conclusively demonstrate that polyamine can penetrate the protein shell of CpMV and is exchangeable for cesium ion. It also provides experimental support for the hypothesis that the B_L component is formed from B_U through the displacement of polyamine by CsCl. No sharp peaks attributable to mobile amino acid side chains were seen in the spectra of the intact virus particles or empty shells. This result contrasts with similar studies of belladonna mottle virus which indicated that some protein side chains become mobile (give sharp ^1H and ^{13}C NMR peaks) when the RNA is removed from intact virus particles to yield empty capsids. (Supported by NIH grants RR01077 and GM19907.)

T-Pos193 COMPARISON OF NORMAL AND DEUTERATED PROTEINS: STRUCTURE STABILITY AND SOLVENT ISOTOPE EFFECT, Chang-Hwei Chen, Fred Tow and Donald S. Berns, Center for Laboratories and Research, New York State Department of Health, Albany, New York 12201

Differential scanning microcalorimetry was used to investigate the enthalpy (ΔH_d) and the temperature (t_d) of thermal denaturation of normal (H-PC) and deuterated (D-PC) phycocyanins isolated from two blue-green algae, *Plectonema calothricoides* and *Phormidium luridum*. In both H_2O and D_2O solvents, values of t_d in D-PC are about 5-7°C lower than those in H-PC. The magnitudes of ΔH_d in D-PC are 64-82% and 21-23% of those in H-PC in H_2O and D_2O solvents, respectively. The heat capacity change (ΔC_p) in protein unfolding is essentially the same for D-PC and H-PC in H_2O solvent. While, in D_2O solvent, the magnitude of ΔC_p in D-PC is lower than that in H-PC.

Circular dichroism was employed to study the secondary structure and urea denaturation of proteins. These proteins have about the same α -helix content in both H_2O and D_2O media. D-PC is less resistant to the denaturant urea than is H-PC. The denaturant concentration at the midpoint of the denaturation curve, $(C_u)_1$, is lower in D-PC. In general, the apparent free energy of unfolding at zero denaturant concentration (ΔG_{app}^{sol}) is higher in D-PC than in H-PC.

Solvent isotope effect essentially does not change the α -helix content in H-PC and D-PC. However, D-PC or H-PC has a higher random coil content in its secondary structure in D_2O than in H_2O . Substitution of H_2O with D_2O as the solvent increases t_d in both D-PC and H-PC, lowers ΔH_d in H-PC, and greatly lowers ΔH_d in D-PC. Deuterium solvent isotope effect does not change ΔC_p in H-PC but lowers ΔC_p in D-PC. In the urea denaturation, the magnitudes of $(C_u)_1$ in H-PC and D-PC are not affected by such a solvent effect, however, those of ΔG_{app}^{sol} are greatly increased.

T-Pos194 INTRACELLULAR GLASS FORMATION AS A METHOD OF NATURAL CRYOPROTECTION IN SUPERHARDY *POPULUS BALSAMIFERA* V. *VIRGINIANA*. A. Hirsh*, R.J. Williams*, E. Erbe**, R. Steere**, and H.T. Meryman*. (Intr. by H.T. Meryman). *Cryobiology and Tissue Banking Laboratory, American Red Cross, Bethesda, MD; **Plant Virology Laboratory, United States Department of Agriculture, Beltsville, MD.

Using differential scanning calorimetry (DSC) and freeze-fracture freeze-etch electron microscopy we have found that the intracellular fluids of superhardy *Populus balsamifera* v. *Virginiana* go through several glass transitions as they are cooled below -20°C. Specifically, we present evidence of: (1) equilibrium glass transitions upon slow cooling between -20°C and -30°C, and -40°C and -50°C and -80°C and -90°C; (2) evidence that if *Populus* tissue is quench cooled in liquid nitrogen (LN_2) from temperatures $\leq -20^\circ C$, these intracellular glasses are resistant to devitrification (cold crystallization) upon warming; (3) evidence that if quench cooling in LN_2 commences at temperatures $\geq -15^\circ C$, the moiety with an equilibrium glass transition near -80°C becomes unstable and devitrifies upon warming, introducing ice into the cell interior and thereby causing significant further ice formation at temperatures above -60°C, and consequent cellular death.

This is the first time that natural glass formation as a strategy for the avoidance of osmotic stress and intracellular ice formation has been reported.

T-Pos195 MOLECULAR PACKING OF QUARTERNARY STRUCTURE OF GLOBULAR PROTEINS

M. Prabhakaran (Intr. by James A. Schafer) Department of Biochemistry, University of Alabama in Birmingham, Birmingham, AL 35294

The molecular packing arrangement of the quaternary structure of some globular proteins has been investigated as continuation of our analysis on the shape of globular proteins. Solvent accessibility method (Lee B. and Richards F.M. (1971) J. Mol. Biol. 55, 379-400) and Vornoi Polyhedron method (Finney, F.L., (1975) J. Mol. Biol. 96, 721-732) have been adopted for this analysis. The investigation, carried out on the quaternary structure of proteins, whose three dimensional coordinates are known, reveals the following features:

- Molecular packing arrangement of the monomers in the quaternary structure and its interpretation in terms of function;
- The difference in the packing arrangement of the monomers and between the monomers in an oligomer;
- hydrophobic contribution for packing;
- the structural stability of the quaternary structures.

T-Pos196 GUANIDINE HYDROCHLORIDE AS A PROBE FOR DOMAIN INTERACTIONS IN RHODANESE

Paul Horowitz and Nick Criscimagna, Biochem. Dept., UT Hlth. Sci. Ctr., San Antonio, Texas 78284.

The conformation of the sulfur free-form of the enzyme rhodanese (E) was followed after addition of GuHCl (0-5M). CD shows loss of organized 2° structure in a broad transition extending from 0.5 to 1.6M GuHCl. Low [GuHCl] induces protein aggregates that dissolve at higher [GuHCl]. The maximum aggregation occurs at 1.5M GuHCl and depends on noncovalent forces as shown by GuHCl chromatography. The fluorescence of the apolar probe 2,8 ANS bound to E shows the same biphasic character as the turbidity. The activity of E can completely recover after dilution from up to 1M GuHCl. This recoverability is completely lost at 1.5M GuHCl. In the presence of iodoacetamide which is sterically excluded from reacting with the active site SH in native E, the recoverability begins to fall at 0.2M GuHCl and is gone at 1M, where only 25% of the final CD change is reached. Protein fluorescence shows GuHCl effects the E conformation without significant CD change, correlating with IAM reaction with the active site. These results show that the active site becomes accessible at lower [GuHCl] than needed for complete denaturation and are interpreted using a model in which the inter-domain interactions in the x-ray structure of rhodanese are significantly weaker than the intra-domain interactions. This effect would contribute to observed catalytically linked conformational changes that effect the active site which is in the interdomain region. (This research was supported by grants GM25177 from NIH and AQ723 from the Robert A. Welch Foundation).

T-Pos197 ULTRACENTRIFUGAL ANALYSIS OF THE ASSOCIATION OF RICIN A AND B CHAINS. Marc S. Lewis and Richard J. Youle, National Institutes of Health, Bethesda, MD. 20205.

Ricin, an extremely toxic protein from the castor bean, *Ricinus communis*, has two dissimilar, disulfide linked chains. A variety of data suggests a non-covalent interaction between these chains when the disulfide bonds are reduced. Since intact ricin and isolated ricin A and B chains are obtainable in a pure state, analytical ultracentrifugation is a very effective technique for determining values for the thermodynamic parameters describing this association.

Ricin and the isolated A and B chains were homogeneous by SDS gel electrophoresis. The ultracentrifugal data was analyzed by non-linear least-squares curve-fitting of concentration as a function of radial position in the centrifuge cell to appropriate mathematical models. Intact ricin and the isolated A and B chains exhibit no self-association. Equimolar mixtures of ricin A and B chains were obtained by reduction of intact ricin with β -mercaptoethanol, were dialyzed against a DTT-containing buffer and centrifuged with DTT present to prevent the reformation of disulfide bonds. The absence of disulfide bond reformation was verified by SDS gel electrophoresis. Data from different initial concentration loadings were analyzed by simultaneous curve-fitting where the only parameters were the equilibrium constant common to all cells at a given temperature, the A and B chain concentrations and the scanner error terms unique to each cell. The molar equilibrium constant for the association was then calculated from the optical density equilibrium constant using the molar extinction coefficients of intact ricin and the A and B chains. The values of ΔG° as a function of temperature were then calculated and used to obtain the values of $\Delta H^\circ = -22 \text{ kcal mol}^{-1}$ and $\Delta S^\circ = -49 \text{ cal mol}^{-1} \text{ deg}^{-1}$ for the initial series of experiments.

T-Pos198 FUNCTIONAL LABELING IN CYTOCHROME C BY 2D NMR. A.J. Wand. Dept. of Biochemistry and Biophysics. University of Pennsylvania, Philadelphia, PA 19104

Cytochrome c from horse heart is being examined by 1H 2D NMR techniques to study redox-linked changes in the protein. The intention is to meld the "functional labeling" method with high resolution NMR methods in order to study the individual amide protons that change their hydrogen exchange rates with the redox state of the protein. In this way we hope to: 1) identify the parts of the protein that are sensitive to the redox state (and which therefore help to set the redox potential) 2) measure the energetic contributions of each involved segment 3) illuminate state-sensitive changes in internal structure dynamics. Assignment of amide protons in cytochrome c from standard COSY and NOESY spectra is difficult. To identify spin systems we are using phase sensitive detection, and multiple quantum and relayed coherence techniques at 500 and 360 MHz. These techniques have helped resolve many ambiguities that arise when tracing out spin system connectivities using standard absolute value spectra. NOESY spectra in water reveal several amide-amide NOE patterns expected of alpha helices. One of these, which displays redox sensitive hydrogen exchange, can be identified by virtue of several known residues therein. (Supported by NIH AM 11295 to S.W. Englander)

T-Pos199 ELECTROSTATIC EFFECTS IN AN ALIPHATIC SERIES OF SEMISYNTHETIC AMINO TERMINAL VARIANTS OF SPERM WHALE MYOGLOBIN. M. R. Busch, D. G. Maskalick, G. W. Neireiter, D. E. Harris, and F. R. N. Gurd, Department of Chemistry, Indiana University, Bloomington, Indiana 47405.

Semisynthetic variants of sperm whale myoglobin with an aliphatic series of amino acids replacing the amino terminal side chain have been prepared. The effects of stepwise variations in the amino terminal side chain have been examined by extensive characterization of the semisynthetic proteins including potentiometric titrations, acid denaturation behavior, and ^{13}C NMR of enriched variants. Enriched isoleucine, valine, alanine, and glycine have been substituted for the native valine. ^{13}C NMR experiments on the isotopically enriched proteins have included determination of the amino terminal pK and examination of the pH dependence of motions of the enriched residue by relaxation phenomena. The pK of the amino terminal is shown to be markedly affected by the aliphatic side chain, varying from 7.6 for [Gly¹]myoglobin to 7.1 for [Ile¹]myoglobin. The T_1 's and NOE's of the enriched protonated carbons have been analyzed using the model free approach of Lipari and Szabo (JACS 1982, 104, 4546) and then interpreted using various models of molecular motion. For example, the range of α -carbon motion as described by conical diffusion in semiangle θ increases with pH for [Gly¹]myoglobin and [Ala¹]myoglobin but is not clearly pH dependent in [Ile¹]myoglobin. In addition, when amino terminal motions in [Ile¹]myoglobin are compared with five assigned internal isoleucines using the restricted diffusion model, similar restrictions about the C β -C γ^1 bond are seen when additional mobility of the terminal α -carbon is accounted for. Substantial restriction ($< \pm 20^\circ$) of the C α -C β bond rotation is demonstrated in the uniformly enriched terminal isoleucine. (Supported by US Public Health Service Research Grants HL-05556 and HL-14680.)

T-Pos200 OXYGEN EQUILIBRIA OF OCTOPUS DOFLEINI HEMOCYANIN. Karen I. Miller, Joan C. Sias and K. E. van Holde, Department of Biochemistry and Biophysics, Oregon State University, Corvallis, Oregon 97331.

We have examined oxygen binding by *Octopus dofleini* hemocyanin under carefully controlled conditions of temperature, pH, and ionic composition. There was no effect of temperature on affinity at pH 7.7 (.1 M HEPES in physiological saline), but cooperativity increased from $n_H = 1.8$ to $n_H = 3.2$ when temperature dropped from 25° to 10°. The Bohr effect is identical at 10° and 20° over the pH range 6.0 to 8.3. The linear portion of both curves was between pH 7.0 and pH 8.0 with a slope of $\Delta \log p_{50}/\Delta \text{pH} = -1.7$. The Hill plots approach very closely the high and low affinity states of the molecule. The maximum Hill coefficient occurs close to physiological pH at 10°, but at 20° it shifts to pH 7.0. The hemocyanin was 100% saturated in pure oxygen down to pH 7.0 at 20°. Below this pH the ability of the molecule to become fully saturated was reduced. At pH 6.6 it achieved only 68% saturation, and further lowering of the pH produced no alteration of oxygen carrying capacity or binding curve shape. The Root effect thus demonstrated appears to result from the allosteric behavior of the molecule. The 51S whole molecule normally dissociates upon removal of divalent cations, but adding .4 M NaCl stabilizes the 51S form in the absence of Mg^{2+} . This allowed examination of the effect of both Mg^{2+} and NaCl on oxygen binding independent of their effect upon subunit structure. In both cases lowering cation concentration lowers affinity, but cooperativity is unaffected. These results allow us to consider the mechanism of oxygen binding in light of the several models of allosteric behavior of proteins. This work was supported by Grant No. PCM 82-12347 from the National Science Foundation.

T-Pos201 ASSOCIATION-DISSOCIATION REACTIONS OF OCTOPUS DOFLEINI HEMOCYANIN. K. E. van Holde and Karen I. Miller, Department of Biochemistry and Biophysics, Oregon State University, Corvallis, OR 97331.

Octopus hemocyanin exists *in vivo* as a 51S decamer of 11S subunits. The subunits are single polypeptide chains of molecular weight $\sim 350,000$. Complete dissociation into subunits is obtained at low salt concentrations, in the absence of divalent cations, pH 8.0. Addition of 10 mM CaCl_2 or MgCl_2 , or 400 mM NaCl to dissociated oxyhemocyanin results in quantitative reassociation to decamers. At lower ion concentrations, an equilibrium exists between monomer and decamer. Such mixtures obey the mass-action law. The variation of the equilibrium constant with divalent ion concentration shows that about 25 Mg^{2+} or Ca^{2+} ions are bound upon formation of each mole of decamer, Ca^{2+} binding somewhat more weakly than Mg^{2+} . The equilibrium between monomer and decamer is also sensitive to oxygenation of the protein, with deoxyhemocyanin being more labile under all conditions examined. Preliminary studies of the kinetics of decamer formation indicate a process second order in monomer concentration. We postulate then that formation of a rapidly-consumed dimeric species may be the rate-limiting step in association. Supported by Grant No. PCM 82-12347 from the National Science Foundation.

T-Pos202 Heterogeneous Association of *Pagurus pollicaris* Hemocyanin. David G. Rhodes and David A. Yphantis, Univ. Connecticut, BSG, Biochemistry and Biophysics Section, Storrs, CT 06268.

The association behavior of the hemocyanin of the hermit crab, *Pagurus pollicaris*, was investigated under a variety of conditions with specific attention to the detection of heterogeneity. At least three distinct monomer types are distinguishable by gel electrophoresis under dissociating, non-denaturing conditions. At pH 8.0 in the presence of EDTA, the protein is approximately 60% hexamer and 40% monomer. Heterogeneity of the monomer/hexamer association was demonstrated by equilibrium ultracentrifugation. Under these buffer conditions the protein may be separated by gel exclusion chromatography into two fractions, the association constants of which differ markedly, so that over a large concentration range one is fully associated to hexamer, while the other is completely dissociated. Electrophoresis of the two fractions under dissociating conditions shows that the dissociated fraction is depleted of two electrophoretically distinguishable subunits. In the presence of 10 mM Ca^{++} at pH 8, the protein exists as hexamer and dodecamer but the extent of association does not depend on protein concentration over the range tested. Gel exclusion chromatography of this material results in two fractions with very different association constants. By electrophoretic analysis under dissociating conditions, the monomer composition of the two fractions appears to be identical. However, when dissociated to monomers and then reassociated, each of these fractions retains the specific association behavior observed for that fraction. Therefore, the basis of the association heterogeneity in the higher aggregates is due to some difference at the monomer level which is transparent to the electrophoretic analysis. (Supported in part by NSF Grants PCM 76-21847 and PCM 81-11484.)

T-Pos203 THE EFFECTS OF 2,3-DPG ON THE OXYGENATION-LINKED SUBUNIT INTERACTIONS OF HUMAN HEMOGLOBIN. Benjamin W. Turner and Gary K. Ackers, Biology Dept., The Johns Hopkins University, Baltimore, Maryland 21218.

The mutual thermodynamic coupling between the binding of oxygen, the binding of 2,3-diphosphoglycerate (2,3-DPG), and the dimer-tetramer assembly has been studied in human hemoglobin A_0 as a function of 2,3-DPG concentration (0-4 mM 2,3-DPG, pH 7.4, 0.1M Tris, 0.1M NaCl, 1.0 mM Na_2EDTA , 21.5°C). At each DPG concentration, oxygen binding isotherms were measured at a series of hemoglobin concentrations. The data were analyzed simultaneously by nonlinear least squares methods according to a model-independent thermodynamic treatment. The analysis allowed binding of 2,3-DPG by hemoglobin dimers and tetramers in all ligation states. The data set included over 40 oxygenation curves comprising approximately 7500 data points. Independent estimates of several equilibrium constants were incorporated. The principal results are as follows: (a) The total free energy of regulation of tetramer oxygen binding resulting from saturation with 2,3-DPG is approximately 2 kcal. (b) Approximately half of this energy of regulation is utilized in the first 3 binding steps, while the remaining 1 kcal is manifested in the last step. Thus, the corresponding Adair constant, k_4 , is significantly dependent upon the 2,3-DPG concentration. (c) The analysis shows a significant level of 2,3-DPG binding to fully liganded dimers and tetramers. These findings have required the resolution provided by simultaneous analysis of data covering wide ranges of the experimental variables. Supported by a grant from the National Science Foundation.

T-Pos204 TWO HALVES OF THE REGULATORY INTERFACE IN THE HEMOGLOBIN MOLECULE ACT INDEPENDENTLY. Francine R. Smith and Gary K. Ackers, Dept. of Biology, The Johns Hopkins University, Baltimore, MD 21218.

Regulation of oxygen binding affinity in human hemoglobin (cooperativity) is due to free energy changes which arise from interactions at the $\alpha^1\beta^2$ interface, including the intersubunit contacts $\alpha^1\alpha^2$, $\alpha^1\beta^2$, and $\alpha^2\beta^1$ (Pettigrew et al. (1982) *Proc. Natl. Acad. Sci. U.S.A.* 79, 1849). A central issue then is the energetic contribution made by each of these three contacts in the regulation of binding affinity. We have investigated this issue by studying hybrids of normal, mutant, and chemically-modified hemoglobins. We have been able to resolve and quantitatively analyze the energetic properties of hybrid molecules in equilibrium with their parent species. The results imply that the $\alpha^1\beta^2$ and $\alpha^2\beta^1$ intersubunit contacts act independently of each other, whereas significant coupling of local effects is present within each contact. This conclusion is independent of the nature and location of the structural perturbation within the hybrid molecule. Independence of regulatory switching in the two halves of the interface is incompatible with a strictly two state (MWC) mechanism for the cooperative binding of oxygen. Supported by grants from the NSF and NIH.

T-Pos205 CONTRIBUTION OF ELECTROSTATIC INTERACTIONS TO THE ENTHALPY OF THE ALKALINE BOHR EFFECT IN HUMAN HEMOGLOBIN. M.A. Flanagan, NIADDK, National Institutes of Health, Bethesda, MD 20205, G.K. Ackers, Department of Biology, Johns Hopkins Univ., Baltimore, MD 21218, and F.R.N. Gurd, Chemistry Dept., Indiana Univ., Bloomington, IN 47405.

The release of Bohr protons upon ligation of human hemoglobin has been shown to be the major source of cooperative energy in hemoglobin (Chu et al. (1983) *Biochemistry*, in press). In this study, the portion of the enthalpy of the Bohr effect due solely to the quaternary structural change is estimated. This is done using the electrostatic interaction model of hemoglobin which estimates the portion of the alkaline Bohr effect due only to the quaternary transition (Matthew et al. (1979) *Biochemistry* 18, 1919, 1928). This model is used to predict the alkaline Bohr effect as a function of temperature and to calculate individual site enthalpies for all titrating residues. The dependence on temperature of the pH maximum of the alkaline Bohr effect predicted in this way is in quantitative agreement with the experimental determination (Antonini et al. (1965) *J. Biol. Chem.* 240, 1096). The difference between the enthalpy for the alkaline Bohr effect calculated by this model, 9 kcal/mol, and the experimentally determined value, 11 kcal/mol, is postulated to be the result of thermodynamic linkage of the quaternary structural change to the release of Bohr protons. Contributions to the Bohr effect by tertiary structural changes may also be a minor factor. Together with other evidence, these results indicate that the release of Bohr protons due solely to the quaternary transition is the major source of cooperative energy in hemoglobin. (Supported by PHS HL-05556.)

T-Pos206 BINDING OF THE ENZYMES OF FATTY ACID β -OXIDATION AND SOME SELECTED ENZYMES TO THE INNER MITOCHONDRIAL MEMBRANE. Balazs Sumegi and Paul A. Srere. (Intr. by J.B. Robinson, Jr.). From the Pre-Clinical Science Unit, Veterans Administration Medical Center, Dallas, TX 75216 and the Dept. of Biochemistry, University of Texas Health Science Center, Dallas, TX 75235.

The enzymes of an individual metabolic pathway may interact (quinary interaction) to form higher order metabolic complexes. We and others have provided evidence for interactions between sequential TCA cycle enzymes. This laboratory has also shown that TCA cycle enzymes can bind specifically to the inner surface of the mitochondrial inner membrane. We have become interested in the possible organization of the enzymes of β -oxidation. An interaction among the enzymes of β -oxidation has already been assumed but no evidence has been presented until now. The binding of enoyl CoA hydratase, β -hydroxyacyl CoA dehydrogenase, β -ketothiolase, succinyl CoA transferase and carnitine acetyl transferase to inner mitochondrial membranes, erythrocyte membranes and liposomes was studied. The succinyl CoA transferase does not bind to any of these membranes. On the other hand, carnitine acetyl transferase binds to all of these membranes. The enoyl-CoA hydratase, β -hydroxyacyl CoA dehydrogenase, and β -ketothiolase binds to inner mitochondrial membranes, but not to liposomes. The binding shows a moderate dependence on ionic strength (2-200 mM) and pH (6.9-8). These data indicate the possibility of an organization of the enzymes of β -oxidation on the inner mitochondrial membrane, but does not support the idea of an organization of the enzymes of ketone body catabolism. (Supported by the VA, NIH, and a Welch Grant).

T-Pos207 INHIBITION OF CARBONIC ANHYDRASE (CA) WITH CYANOGEN, Jane Ann Willett, Richard A. Day, Intr. by George Kreishman, Dept. of Chemistry, University of Cincinnati, Cincinnati, Ohio 45221

Carbonic anhydrase catalyzes the physiologically significant reversible conversion of carbon dioxide to the bicarbonate ion. It will also catalyze a variety of other hydrolysis reactions. The bovine carbonic anhydrase (BCA) B has 75% homology with human carbonic anhydrase C. Both enzymes express the highest activity of the carbonic anhydrases with a $k_{cat} = 1 \times 10^6 \text{ sec}^{-1}$.

Incubation of BCA with a solution of the toxic gas cyanogen irreversibly modifies the enzyme. This modification results in a loss of 80% of the enzyme's activity toward the hydrolysis of p-nitrophenyl acetate to the alcohol in tris-sulfate buffer pH-7.55 at 25°C. There is no apparent loss of the enzyme's carbon dioxide activity as assayed by the time of hydration of carbon dioxide in veronal buffer at 0°C.

This modification reaction proceeds with one hundred to one mole to mole excess of cyanogen to CA but evidence suggests that a lower stoichiometry may be sufficient. Cyanogen has the same linear geometry as carbon dioxide with a C-N bond distance of 1.16 Å in comparison with a C-O bond distance of 1.156 Å. The results of the inhibition studies suggest that cyanogen may enter the active site in the same manner as the p-nitrophenyl acetate, which is purported to be an analog of carbon dioxide. The data indicate that the hydration of the carbon dioxide and the hydrolysis of p-nitrophenyl acetate may proceed by different pathways.

T-Pos208 IDENTIFICATION OF AN ACTIVE SITE PEPTIDE OF THE GASTRIC ATPase. Saccomani, G., Jackson, R.J. and Mukidjam, E. Lab. of Membrane Biology, Univ. of Alabama Birmingham, Birmingham, AL 35294

We have isolated and partially characterized a soluble 28,000 daltons peptide fragment obtained by limited papain digestion of the highly purified, membrane-bound (H^+K^+)ATPase. This peptide has been identified in the supernatant obtained after centrifugation at $100,000 \times g$ for 1 hr of the papain-treated enzyme suspension by HPLC, with a linear gradient system consisting of 12.5 mM Na_2HPO_4 (solvent A) and CH_3CN (solvent B) and by SDS-gel electrophoresis. Amino acid analysis showed that 34% of the total amino acid residues are charged with an overall 65% being polar residues, while carbohydrate analysis revealed a 10% monosaccharides content. Upon papain treatment of specifically FITC-labeled gastric ATPase [Jackson, R. et. al (1983), BBA 731, 9-15], the fluorescein originally bound to the 96,000 daltons intact polypeptide appeared sequentially in a 77,000 daltons membrane-embedded fragment and then released into the medium and localized on the 28,000 daltons soluble peptide as followed by illumination of unstained SDS-gels with UV light. The 77,000 daltons fragment, like the original 96,000 daltons polypeptide, can be phosphorylated by [γ - ^{32}P]ATP. In addition, preliminary experiments have shown that the 28,000 daltons fragment is also phosphorylated. Thus, the amino acids that make up the ATP binding domain (i.e. the FITC-reactive site) and the aspartate group that accepts the terminal phosphate of ATP may reside on the same peptide fragment, obtained from the native folded structure of the (H^+K^+) ATPase and in contact with the aqueous phase at the membrane surface. (NIH Support).

T-Pos209 RENIN CLEAVAGE OF A HUMAN KIDNEY RENIN SUBSTRATE HOMOLOGOUS TO HUMAN ANGIOTENSINOGEN, by Martin Poe, Department of Biophysics, Merck Institute for Therapeutic Research, Merck Sharp and Dohme Research Laboratories, P.O. Box 2000, Rahway, NJ 07065.

A synthetic tetradecapeptide, H-Asp-Arg-Val-Tyr-Ile-His-Pro-Phe-His-Leu-Val-Ile-His-Ser-OH, which corresponds to the thirteen amino terminal residues of human angiotensinogen plus a carboxy terminal serine to replace a suggested site of carbohydrate attachment, has been shown to be a good substrate for human kidney renin. At pH 7.2 and 37°C, the Michaelis constant was $8.4 \pm 2.9 \mu M$ and the velocity at infinite substrate concentration was $11.3 \pm 2.4 \mu$ Moles substrate cleaved per hr per mg pure human kidney renin. An HPLC method was used to demonstrate that the scissile bond was the Leu-Val bond, yielding human angiotensin I and H-Val-Ile-His-Ser-OH. This renin substrate was highly resistant to cleavage by mouse submaxillary gland renin. Human kidney renin had a catalytic efficiency, defined as maximal velocity at infinite substrate concentration divided by Michaelis constant, about 2.5-fold higher with this substrate than with the synthetic tetradecapeptide renin substrate, H-Asp-Arg-Val-Tyr-Ile-His-Pro-Phe-His-Leu-Leu-Val-Tyr-Ser-OH, which is homologous to horse angiotensinogen.

T-Pos210 NMR STUDIES OF FRUCTOSE 1,6 BISPHTHOSPHATE ALDOLASE FROM *E. COLI*, B. Szwergold, K. Ugurbil and T.R. Brown, Dept. of Biochemistry, Columbia University (BS), Dept. of Biochemistry and Gray Freshwater Biological Institute, University of Minnesota (KU), and Fox-Chase Cancer Institute (TB).

Fructose 1,6 bisphosphate (FBP) aldolase from *E. coli* is a dimeric Zn^{++} metalloenzyme with a M.W. of 80,000 catalyzing the cleavage of FBP to dihydroxyacetone phosphate (DHAP) and glyceraldehyde phosphate (GAP). We have isolated and purified this enzyme in gram quantities and have synthesized FBP labelled with ^{13}C at the 2 and 5 carbons. Using saturation and inversion transfer measurements we have been able to make the following observations on *E. coli* aldolase: 1) this enzyme does not catalyze the anomerization of FBP, or hydration-dehydration of DHAP, 2) DHAP is utilized only in its keto (unhydrated) form, and 3) FBP is utilized by the enzyme exclusively in its keto form. We were also able to detect ^{13}C resonances from the enzyme bound intermediates derived from the ^{13}C labelled substrates. These intermediates have chemical shifts expected for enol (and/or enolate) forms of FBP and/or DHAP. The presence of these enol/enolate forms on the enzyme require the presence of Zn^{++} . Substitution of Zn^{++} with $^{113}Cd^{++}$ results in a substantial chemical shift of the keto FBP resonance. Depending on the growth carbon source used, this enzyme contains a covalently bound phosphorylated (non-substrate) moiety, which might be of some functional significance. Further studies are continuing to elucidate the identity of the metal ligands in the protein, the metal-substrate coordination geometry, the reaction sequence (FBP to those phosphates), and the identity of the phosphorylated enzyme-bound compound.

T-Pos211 COMPLEXES OF UROHEMIN I WITH THE ANTIMALARIA DRUGS CHLOROQUINE AND QUININE. By Ioannis Constantinidis and James D. Satterlee, Department of Chemistry, University of New Mexico, Albuquerque, New Mexico 87131.

The mechanism of action of antimalarial drugs such as chloroquine diphosphate and quinine-HCl remains obscure. In recent years it has been proposed that such drugs will bind to free heme groups forming a heme-drug complex inside the red blood cells. Urohemine I was chosen as the model for free heme, due to its infinite H₂O solubility and due to our full comprehension of its aggregation properties. Binding studies were performed on monomeric urohemine I at pH 6.0 in deionized H₂O. UV-Vis data were analyzed by the Hill equation. The results indicated that chloroquine exhibits a 1:1 complex formation with an association equilibrium constant of $3.6 \pm 0.2 \times 10^4 \text{ M}^{-1}$. On the other hand, quinine-HCl performs differently and the reaction proceeds as a 2:1 complex formation with overall association equilibrium constant G_{2A} equal to $1.5 \pm 0.15 \times 10^8 \text{ M}^{-2}$.

Further analysis of the system continues in our laboratory with the main goal of elucidating thermodynamic parameters of the system.

T-Pos212 CO-OPERATIVE INTERACTIONS IN EUKARYOTIC POLYPEPTIDE CHAIN INITIATION--THE TERNARY SYSTEM: INITIATION FACTOR 2, NUCLEOTIDE EXCHANGE FACTOR, AND GDP. Dixie J. Goss and Lawrence J. Parkhurst, Dept. of Chemistry, U. of Nebraska, Lincoln, NE 68588-0304 and Harsh Mehta, Charles L. Woodley, and Albert J. Wahba, Dept. of Biochemistry, U. of Mississippi Medical Center, Jackson, MS 39216.

Eucaryotic initiation factor 2 (eIF-2) from both rabbit reticulocytes and *Artemia* embryos has been labelled with the fluorescent probe DANSYL. The association of eIF-2 and nucleotide exchange factor (RF) has been monitored directly by changes in fluorescence anisotropy. Equilibrium constants in the (absence) and presence of GDP were: (0.05) and 0.15 nM for reticulocyte RF-eIF-2; (0.31) and 0.5 nM for eIF-2(α -P)-RF. For *Artemia* RF-eIF-2 and RF-eIF-2(α -P) the equilibrium constants were 0.6 and 0.15 nM, respectively. The reticulocyte eIF-2-GDP-RF system shows an anti-cooperative interaction of GDP and RF with eIF-2, with $\Delta G^\circ = 0.5 \text{ kcal/mol}$. Phosphorylation of the alpha subunit of eIF-2 inhibits protein synthesis in reticulocyte lysate but not *Artemia*, however, this phosphorylation does not greatly affect the affinity for RF. The addition of GTP (10 μM) to the eIF-2-RF complex causes a decrease in fluorescence anisotropy, presumably due to dissociation of eIF-2 and RF. The effect of phosphorylation of eIF-2 in the two systems is very different: For *Artemia*, the eIF-2(α -P)-RF complex is readily dissociated by GTP; for the reticulocyte system, high concentrations of GTP are required. Further interactions of eIF-2-GTP with Met-tRNA_f were also detected by changes in fluorescence anisotropy. Grant Support: NIH HL 15,284 and GM 25451; NSF PCM 8003655, and Research Council, U. of Nebraska.

T-Pos213 SURFACE-CHARGE MODEL FOR CALCULATING DIELECTRIC BEHAVIOUR. R.J. Zauhar, R.S. Morgan, P.B. Shaw, Departments of Biochemistry, Microbiology, Molecular and Cell Biology and Physics, The Pennsylvania State University, University Park, PA.

Dielectric effects are generally computed using the molecular dipole moment μ and the dipole moment per unit volume, P . An alternative approach can use molecular partial charge q and induced surface charge density, σ . Consider the average electric field strength over a cylindrical Gaussian surface which intersects the plate of a condenser containing a polar liquid. The orientation of the molecules of the liquid (found from Langevin's formula) introduces charge within the Gaussian surface. At the limit for field strengths, the dielectric constant found from this heuristic model is $1 + (4\pi r q^2 / 3kT)(\rho N / MW)^{2/3} 10^{-16}$, where r is the separation between the centers of net negative and positive molecular partial charge in Angstroms, q is the magnitude of these charges in electrons, ρ is the density in grams/cc, N is Avogadro's number. The graph shows the results of this calculation for a series of compounds containing a single hydroxyl group: 1) water, 2) methanol, 3) ethanol, 4) 1-propanol, 5) 1-butanol. Despite the simplicity of this model, the results for alcohols compare favorably with the more complex calculations of Oster & Kirkwood (J.Chem.Phys. 11:175, 1943). We hope that a theory developed by this approach and concentrating on the details of surface structure will be applicable to the study of electric fields in and near macromolecules.

